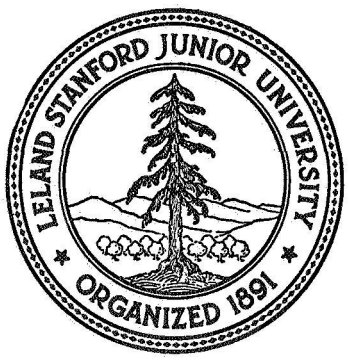

A THEORETICAL INVESTIGATION OF CRACKS IN TWO-PHASE SOLIDS

By

Tsu-Wei Chou

May, 1969

SU DMS Report No. 69-T-51

Department of MATERIALS SCIENCE
STANFORD UNIVERSITY

A THEORETICAL INVESTIGATION OF CRACKS IN TWO-PHASE SOLIDS

by

Tsu-Wei Chou

Department of Materials Science

Stanford University

Stanford, California

May, 1969

Technical Report No. 7

Prepared for the

National Aeronautics and Space Administration

Under NASA Contract NSG-622

ABSTRACT

In composite materials, the presence of inhomogeneities alters the types of stress singularities at tips of cracks and slip bands. The plastic strain concentrated at the crack tip in a notch-tough matrix is essential in determining the critical fracture load of composite materials.

The concept of continuously distributed dislocations is used in the present investigation. A unified description of both cracks and slip bands is reached by using the dislocation model.

The elastic-plastic medium under consideration is made of two half-planes perfectly bonded at the interface. External stresses are uniformly applied at the boundary far from the dislocation arrays. It is found that the effective stresses on dislocations are uniform in the vicinity of the interface. The magnitude of these effective stresses depends on the elastic constants of the constituent phases. The effect of inhomogeneity also causes stresses to be induced at the phase boundary. These stresses decay exponentially with the distances from the interface and can be the primary cause of splitting at interfaces.

For Mode III cracks of finite length, L, lying perpendicular to the phase boundary, the crack tip stress singularity in the neighboring phase is of the type $\left(\frac{L}{\rho}\right)^a$. ρ denotes the distance from crack tips and

$$a = \frac{2}{\pi} \sin^{-1}\sqrt{\frac{1-k}{2}}$$

$$k = \frac{G_2 - G_1}{G_2 + G_1} .$$

The intensity of the resultant stress is smaller than that of a semi-infinite crack by the factor $(1 - a)$. This finding is also valid for the case where screw dislocations pile up against the interface. For Modes I and II cracks, the crack tip stress singularity can be found by employing numerical procedures.

For a Mode III crack crossing a phase boundary, the stress singularities at the crack tips behave as if the crack tip were imbeded in a homogeneous medium. The stress intensity at the crack tip in the comparatively harder phase is higher than that in the softer phase.

The above crack model can be modified to discuss elastic-plastic cracks of composite materials. The static extension of the plastic zone ahead of a crack in the soft matrix and the crack tip opening displacement can be minimized by increasing the shear modulus and the yield strength of the matrix phase. The relationships between the applied load and the crack opening displacement have been found for various bi-material systems. By experimentally determining the fracture toughness of the matrix material, the critical fracture load can be found using the present analysis.

The dislocation model of an elastic-plastic crack has been extended to study the case where the second phase is of finite dimension. Approximate methods of analysis are outlined to discuss the cracking of a hard surface film or a lamina of finite width and having plastic deformation in the neighboring phase.

ACKNOWLEDGMENTS

The author wishes to express his sincere appreciation to:

Professor A. S. Tetelman, his thesis advisor, not only for his constant support throughout the course of this research but also for his encouragement and efforts in introducing the author to this new area of scientific endeavor;

Professor J. P. Hirth, to whom the author is very grateful for his invaluable advice which have stimulated critical thinking;

Professor W. D. Nix, who, throughout the course of the work, so freely and generously gave his time and ideas to the development of this investigation:

Professor C. C. Chao, for his interest and effort spent in reading this manuscript. Professor A. Leonard and Dr. A. G. Gibbs, with whom the author enjoyed many helpful discussions;

His confreres in the Fracture Laboratory, especially Dr. D. M. Barnett and Dr. D. O. Harris, from whom he has learned a great deal of various aspects in the field;

The Ford Foundation, whose fellowship the author held during the first year of his graduate study at Stanford, and the National Aeronautics and Space Administration for supporting this investigation under Contract NASA-NSG-622, and the Advanced Research Projects Agency through the Center for Materials Research at Stanford University for support during the final stage of this study.

His wife, Mei-sheng, for her understanding and encouragement together with her assistance in preparing this manuscript.

Special gratitude is reserved for his parents. It is only through their self-sacrifice that made this education possible. Their constant encouragement is indispensable over the years of study in this country.

TABLE OF CONTENTS

PAGE

LIST OF TABLES

LIST OF ILLUSTRATIONS

LIST OF ILLUSTRATIONS (Cont)

LIST OF ILLUSTRATIONS (Cont)

CHAPTER I

INTRODUCTION AND REVIEW

1. Purpose of the Investigation

Appreciable attention has been given in recent years to the development of composite materials. Dispersed second phase particles and fibers in soft matrices provide important technological advantages. The presence of dispersed phases plays an important role in determining the strength and ductility of the composite.

With the increasing need for ultra high-strength materials in modern technology, it becomes necessary to obtain a better understanding of the properties of composite materials and of the theoretical background underlying these properties. For crystalline materials in particular, a study of the behavior of cracks and dislocation arrays and their interactions with various heterogeneous elements in these materials is evidently of basic importance.

The purpose of the present investigation is to explore certain essential features concerning the propagation of slip bands and elastic-plastic cracks in composite materials. Stress singularities at the tip of cracks and slip bands are first studied. The extension of elastic-plastic cracks under external loading is then examined. Finally, by employing the appropriate fracture criteria, the critical fracture load can be determined as a function of material parameters.

In the following sections, the Dugdale model of an elastic-plastic crack is first introduced (Section I.3). By combining this model with the concept of continuously distributed dislocations (Section I.4), Bilby,

Cottrell and Swinden were able to develop a dislocation model of an elastic-plastic crack. This dislocation model is employed in the present analysis to study the fracture of composite materials. An outline of the mathematical procedure involved and the underlying physical significance of this model are given in Section I.5.

In the dislocation model, stresses arising from three different kinds of sources are essential for determining the equilibrium configuration of dislocations representing the crack. The first kind is the dislocation stress σ_d at a point due to all the dislocations in the array. The effect of inhomogeneity on the elastic field of dislocations has been taken into account in σ_d. The second kind of stress, σ_o, is the resistence stress to the motion of dislocations exerted by the lattice. Stress σ_o is considered to be identified with the lower yield stress of the material. This is because the lower yield stress is the stress at which Lüders bands spread. The third kind is the stress on dislocations due to externally applied loadings. A critical examination of this effective stress due to an uniformly applied stress, σ_a, is given in Chapter II. Stresses on dislocations arise from internal and external sources other than those mentioned above can readily be included in the stress terms σ_o and σ_a respectively.

In Chapters III and IV attention is focused on the behavior of elastic cracks and dislocation arrays in two-phase systems. The medium under consideration is made up of two half-planes with different elastic constants and welded together at the interface. The types of stress singularities at the tip of cracks and dislocation pileups are of primary interest.

Experiences gained in these investigations are essential in extending the results to the examination of elastic-plastic cracks. A study of the static extension of elastic-plastic cracks under external stresses and the determination of fracture load are presented in Chapter V.

Finally, attempts are made to take into consideration the effect of dimension of the constituent phases on the fracture behavior. The second phases considered are in the forms of a surface film and a lamina embeded in the matrix phase.

A flow diagram showing the systematic formulation of the present investigation is presented in Fig. I-1.

2. Modes of Fracture

The redistribution of stresses in bodies caused by the introduction of a crack is one of the essential features in fracture mechanics. The stress fields near crack tips are closely associated with the local mode of deformation which can be divided into three types as illustrated in Fig. I-2 [1].

Mode I, the opening mode, is characterized by local displacements in which the crack surfaces move directly apart (symmetric with respect to the x-y and x-z planes).

Mode II, the edge sliding mode, is associated with displacement in which the crack surfaces slide over one another perpendicular to the leading edge of the crack (symmetric with respect to the x-y plane and skew-symmetric with respect to the x-z plane).

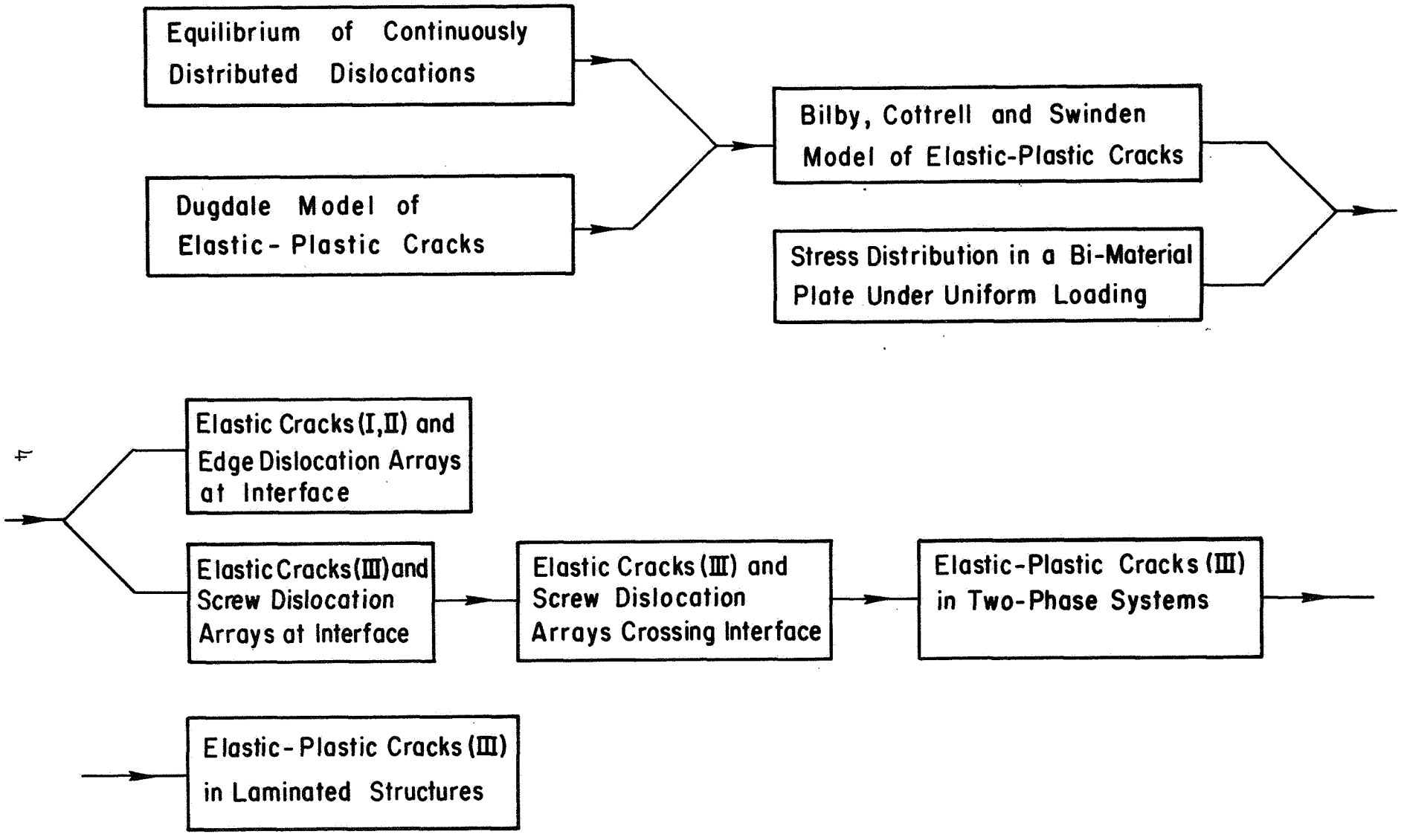

Fig. I-1. FLOW DIAGRAM OF THE PRESENT INVESTIGATION.

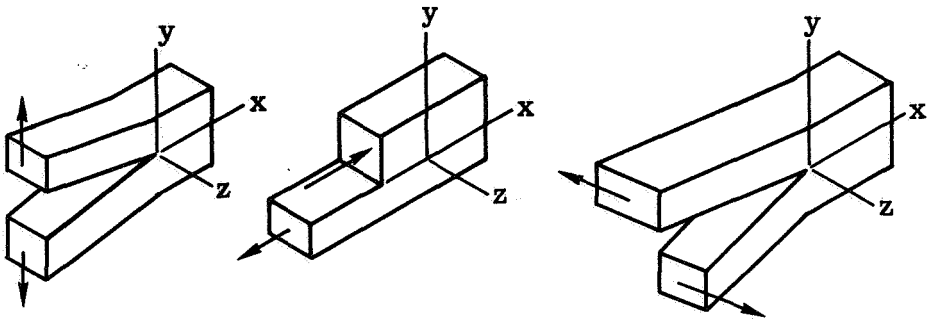

MODE I MODE II MODE III

Fig. I-2. THE BASIC MODES OF CRACK SURFACE DISPLACEMENTS [1].

Mode III, the tearing mode, the crack surfaces undergo anti-plane shear and slide with respect to one another parallel to the leading edge (skew-symmetric with respect to the x-y and x-z plane).

3. Dugdale Model of a Crack

In an investigation of static yielding at the ends of existing slits in stretched plates, Dugdale observed yield zones confined to a very narrow band lying along the line of the slit [2].

Dugdale further provided an analysis of this problem which is based upon the following three hypotheses:

a. The material in the yielded zone is under a uniform tensile yield stress Y.

b. The thickness of the yielded zone is so small that the elastic region outside may be regarded as bounded internally by a flattened ellipse of length $2(c+s)$, where c is the half-length of the slit, and s the length of the plastic extension.

c. The yielded zone is of such a length that the stress at the end of it is finite.

Under these hypotheses the stress distribution for the crack and its associated plastic zone as shown in Fig. I-3 may be determined by superposition of the three stress states shown in Fig. I-4. The combination of states 1 and 2 leads to free crack surfaces. Then the state 3 is needed to impose the yield stress on the plastic zones. The problem of a straight cut loaded over part of its edge has been examined by Muskhelishvili [3]. His stress functions were used by Dugdale in the analysis.

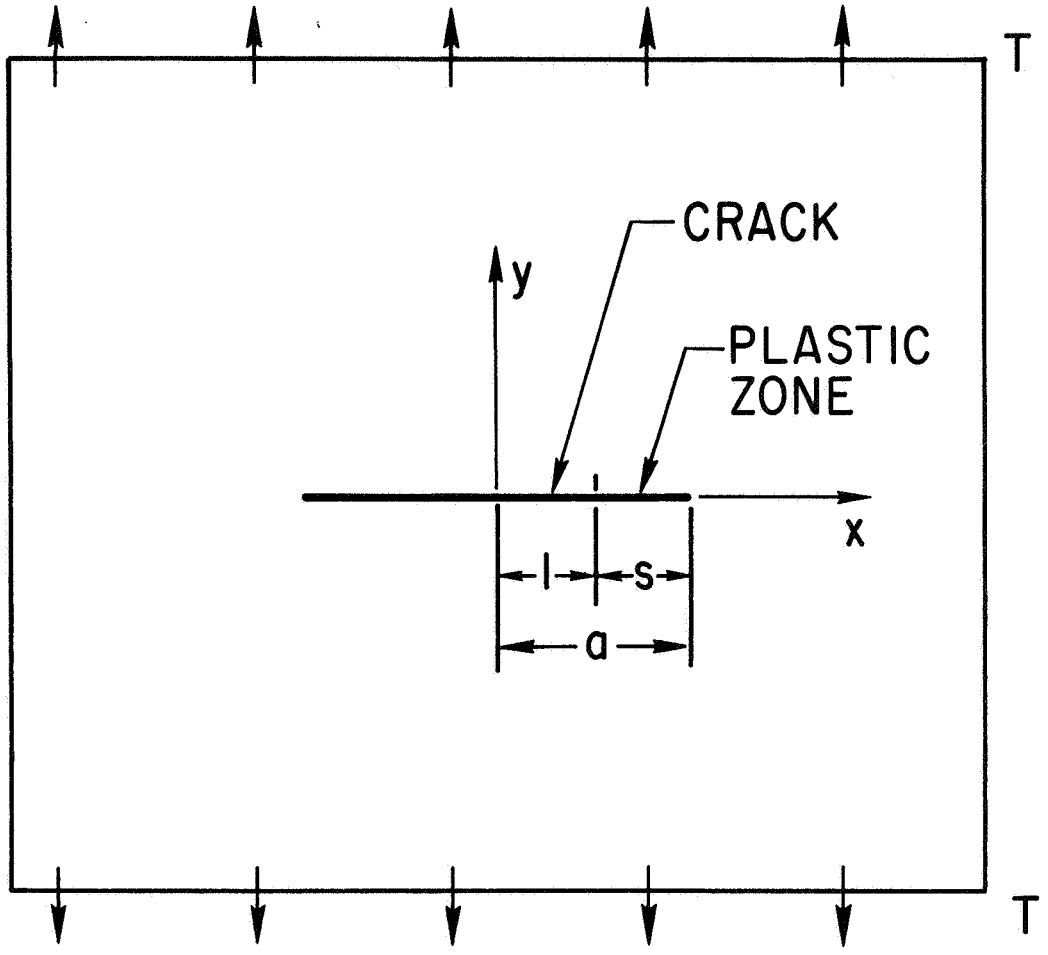

Fig. I-3. DUGDALE CRACK [4].

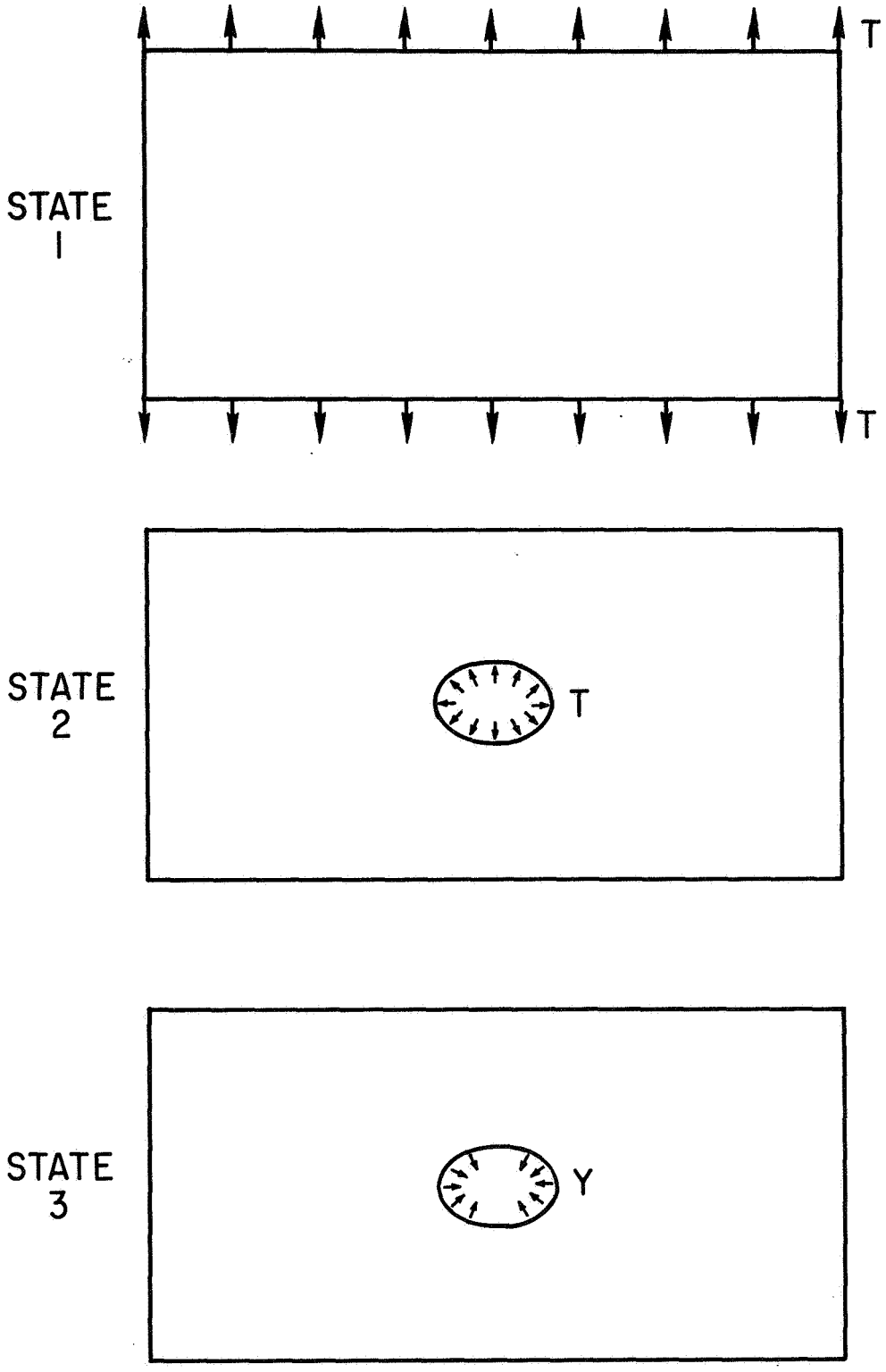

Fig. I-4. COMPONENT STRESS STATES FOR DUGDALE CRACK [4].

By observing that the stress should be finite at the tip of the plastic zone, Dugdale obtained a relation between the applied load and the length of plastic zones as:

$$\frac{s}{a} = 2 \sin^2 \left(\frac{\pi T}{4Y}\right) . \qquad \text{(I.3-1)}$$

It was further pointed out by Goodier and Field [4] that the imposition of the finiteness condition does insure the stress component σ_{yy} at the tip of the plastic enclave to be not greater than the yield stress and the stress along the line of crack is everywhere within the yield condition.

Dugdale's model of crack has a reasonable physical basis and agrees well with his experimental results as shown in Fig. I-5.

4. The Equilibrium of Continuously Distributed Dislocations

To circumvent the difficulties inherent in the discrete dislocation formulations as usually encountered in dislocation pile up problems, the concept of continuous dislocations was introduced [10,11]. In this method of calculation, discrete dislocations with finite Burgers vectors are replaced by continuously distributed dislocations with infinitesimal Burgers vectors. The total Burgers vector of the continuous distribution is the same as that of the discrete configuration. This technique is valid provided the separation distances between dislocations are comparable to the width of dislocations.

Suppose there are n discrete dislocations on a slip plane in the domain D, each having Burgers vector of magnitude b. To replace these

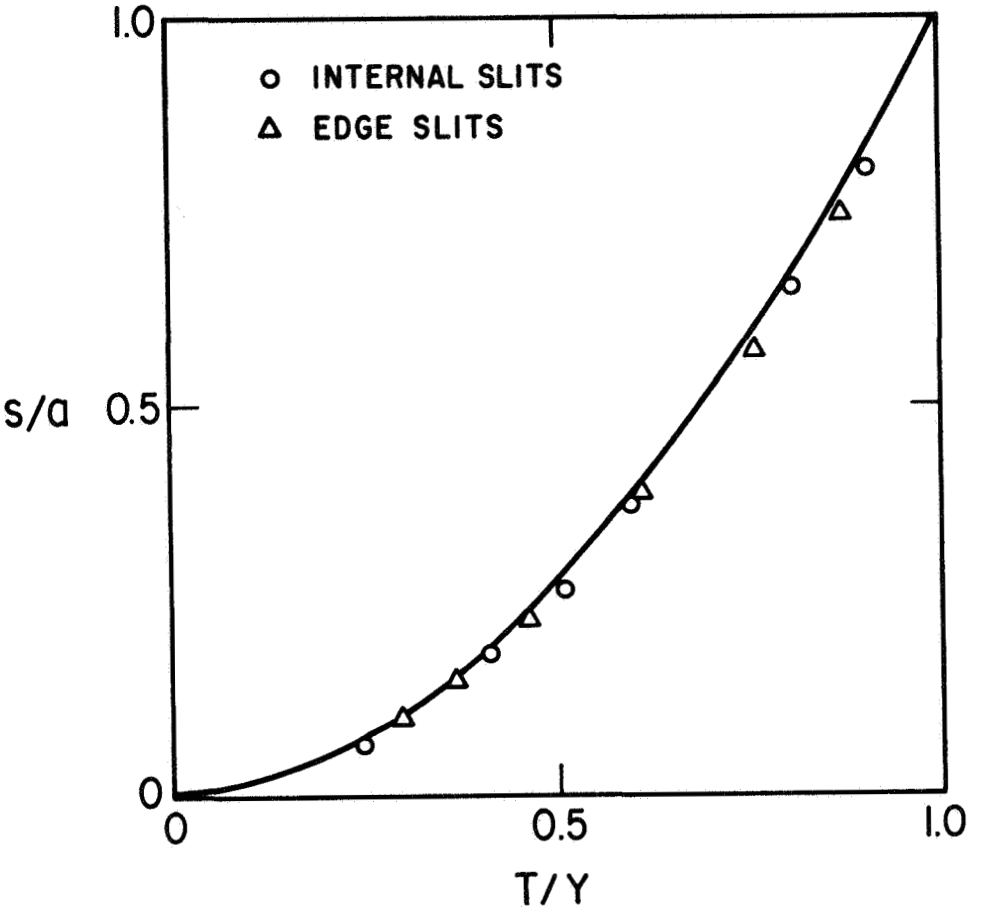

Fig. I-5. PLASTIC ZONE LENGTH-APPLIED LOAD RELATIONS [2].

by an infinite number of dislocations with infinitesimally small Burgers vector, we can define a distribution function $f(x)$ such that $f(x)dx$ is equal to the sum of the Burgers vectors of all the infinitesimal dislocations that lie on the slip plane between the positions x and $x+dx$.

To find the static equilibrium configuration of dislocations at $(x,0)$ in the domain L, we need to take into consideration all the stresses acting on each dislocation. These can be the stress $\sigma_d(x,t)$ due to a dislocation at $x=t$ and the stress $\sigma(x)$ due to sources other than dislocations in the domain L. Consequently, at equilibrium, it requires

$$\int_L \sigma_d(x,t)\, f(t)\, dt + \sigma(x) = 0 \,. \qquad \text{(I.4-1)}$$

The above equation usually has the form of a singular integral equation. A method of solving $f(t)$, the equilibrium configuration of the continuously distributed dislocations, is outlined in Appendix A.

5. Bilby, Cottrell and Swinden Model of an Elastic-Plastic Crack

Dislocations are as useful for discussing fracture as for plastic deformation [5]. In both slip planes and cracks the stress between corresponding points on opposite faces is less than Hooke's law predicts, for the given displacements between these points. Dislocations provide a natural means for including such regions within the framework of linear elasticity.

By means of Volterra-Somigliana dislocations a unified description can be given of various types of cracks in elastic and elastic-plastic

solids. These dislocations need not be crystallographic and can exist in any elastic body, whether crystalline or not. Let such a dislocation lie along the z axis as in Fig. I-6, and take a circuit M to N around it. The Burgers vector $\bar{b}$ of the dislocation is defined by the line integral of the gradient of elastic displacement along this contour, i.e.

$$\bar{b} = \oint \frac{\partial \bar{u}}{\partial s} \, ds \ . \qquad \text{(I.5-1)}$$

When $\bar{b}$ is parallel to the z axis, the dislocation is of screw type; when perpendicular, it is of edge type.

Fracture is a form of nonlinear mechanical behavior. The deviation from Hooke's law may come from rupture of atomic bonds between crack faces, as in simple brittle fracture, or from plastic yielding at the end of the crack, as in ductile substances. Hooke's law is obeyed well outside this region at low applied stresses.

In view of the similarity of associated displacements between dislocations and cracks, the elastic field of the three modes of cracks can be represented by appropriate distributions of dislocations. This is depicted in Fig. I-7. Consequently, we can use linear elasticity everywhere by representing the nonlinear region as a packet of dislocations.

To take into account the unstable growth of cracks and the plastic deformation associated with cracks in ductile materials, Cottrell [6] postulated the following modes of deformation.

In a "cumulative" mode of fracture, for a constant law of force between separating faces, the primary group of dislocations is geometrically

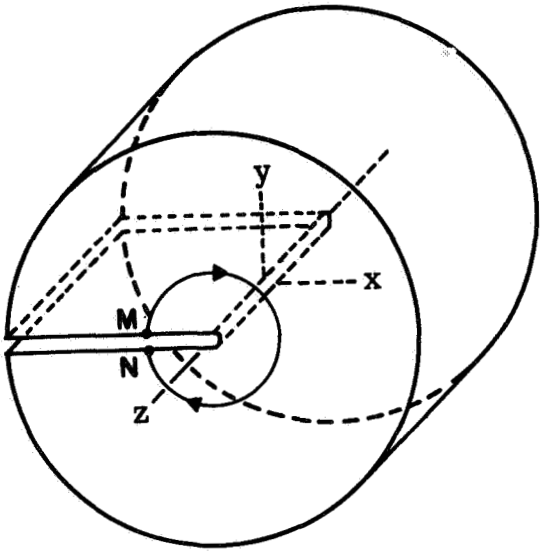

Fig. I-6. DEFINITION OF A DISLOCATION [5].

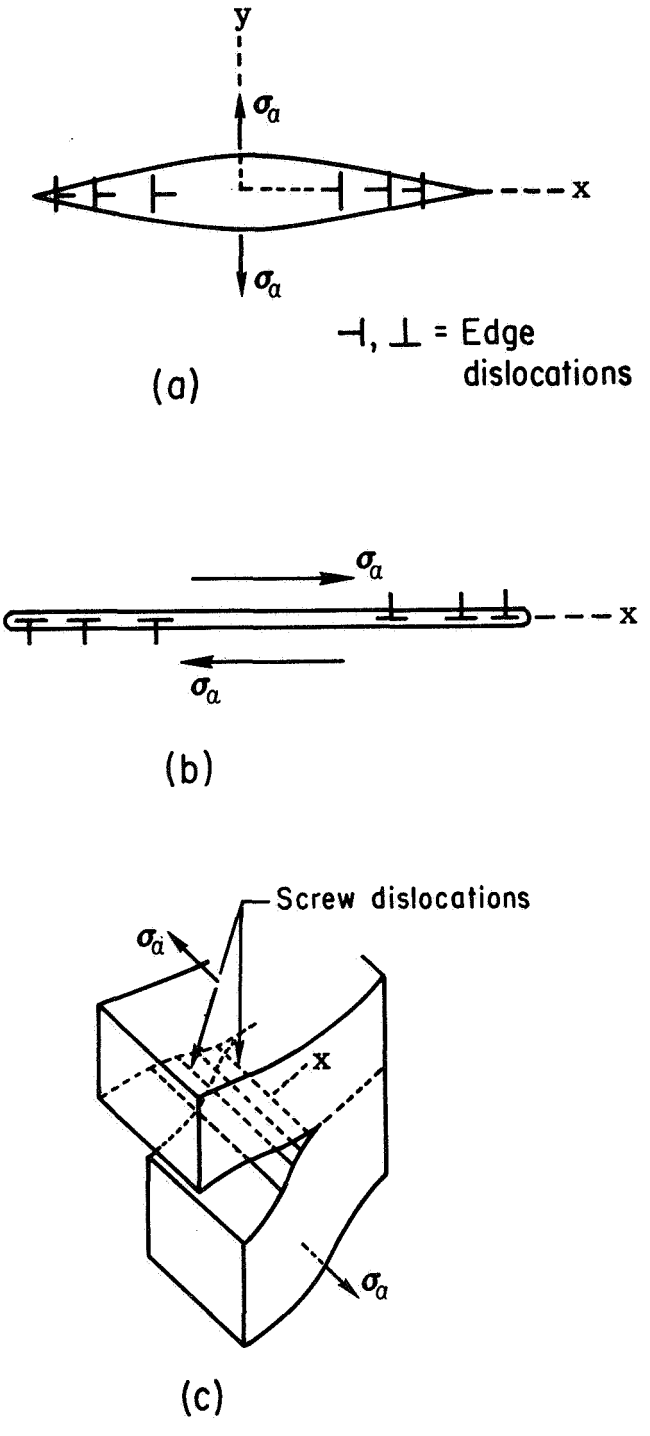

Fig. I-7. TENSILE (a) AND SHEAR (b AND c) CRACKS REGARDED AS GROUPS OF EDGE (a AND b) AND SCREW (c) DISLOCATIONS [5].

sufficient of itself to complete the total fracture, merely by running to the far end of its plane. This is an unstable mode of fracture, i.e., the applied stress needed to keep the dislocations moving diminishes as the dislocations move and multiply.

In a "noncumulative" mode of fracture, each incremental growth of the plastic zone requires the injection of more dislocations into the slip lines and thus push the existing dislocations further across the section. Meanwhile, the applied stress has to be increased correspondingly, reaching the general yield stress when the plastic zone crosses the whole load bearing section, so becoming general-yield.

By combining the above idea with the Dugdale model of a crack, Bilby, Cottrell, and Swinden were able to solve the problem of the spread of plastic yield from a notch [7,8,9]. They considered an infinite isotropic elastic medium with shear modulus G subjected to uniform shear stress $\sigma_{yz} = \sigma_a$ at infinity and containing a distribution of long straight dislocation lines lying parallel to the z axis in the x-y plane. The resistance stress to the motion of dislocations is taken to be $\sigma_o (< \sigma_a)$ in the region $|x| < c$ and $\sigma_1 (> \sigma_a)$ in $-a < x < -c$ and $c < x < a$. When $\sigma_o = 0$ the region $|x| < c$ represents a freely slipping crack and the dislocations beyond $\pm c$ represent plastic slip at the ends of such a crack.

The problem in the theory of continuous distribution of dislocations is most easily solved by setting up the integral equation which expresses the requirement that the resultant shear stress on any dislocation in the distribution is zero when the system is in equilibrium [10,11].

Let $f(t)$ be the distribution function of dislocations at $x=t$. Using the concept of infinitesimal dislocations introduced in Section I.4, the shear stress at $(x,0)$ due to the dislocation at $(t,0)$ is

$$\sigma_{yz}(x) = \frac{Af(t)\,dt}{x-t} \qquad \text{(I.5-2)}$$

where $A=Gb/2\pi$ and b is the magnitude of Burgers vector of dislocations. Hence, at equilibrium, it requires

$$\int_{-a}^{a} \frac{f(t)}{x-t}\,dt + \frac{\sigma(x)}{A} = 0 \qquad \text{(I.5-3)}$$

where $\sigma(x) = \sigma_a - \sigma_o$ for $|x| < c$, and $\sigma(x) = \sigma_a - \sigma_1$ for $c < |x| < a$.

By applying the technique outlined in Appendix A, the above singular integral equation can be inverted and the solution is found to be:

$$f(x) = \frac{\sigma_1 - \sigma_o}{\pi^2 A}\left[\cosh^{-1}\left|\frac{m}{c-x} + n\right| - \cosh^{-1}\left|\frac{m}{c+x} + n\right|\right] \qquad \text{(I.5-4)}$$

where $m = (a^2 - c^2)/a$ and $n = c/a$. Figure I-8 shows the quantity $\pi^2 Af(x)/(\sigma_1-\sigma_o)$ as a function of x for $a = 2c$. It is assumed in this model that plastic relaxation at crack tips is caused only by injection of dislocations into the plastic zone. The form of this distribution function agrees with qualitative expectations. The same analysis holds for in plane shear mode of crack where edge dislocations are used.

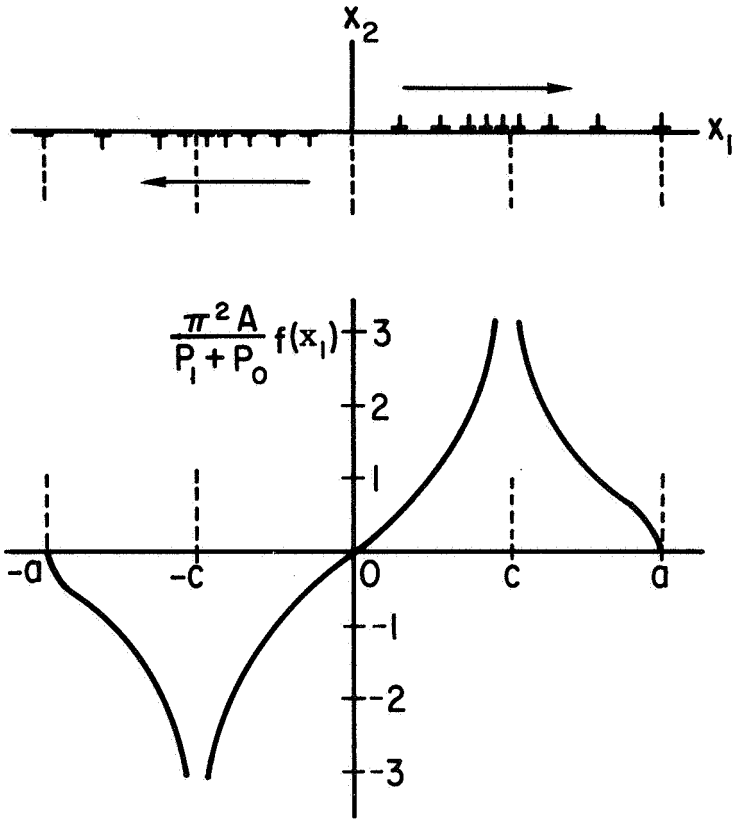

Fig. I-8. DISTRIBUTION OF DISLOCATIONS ALONG A SHEARED SLIT ($|x|<c$) AND ITS ASSOCIATED YIELD ZONES ($c<|x|<a$) [8].

The necessary condition [12] for the existence of solution of the integral Eq. (I.5-3) leads to the relation between the applied stress and the extension of plastic zone:

$$\frac{c}{a} = \sin\left[\frac{\pi(\sigma_1 - \sigma_a)}{2(\sigma_1 - \sigma_o)}\right] \qquad \text{(I.5-5)}$$

This condition is equivalent to Eq. (I.3-1) which was based upon the finiteness of stress at the tip of plastic zones.

Using the theory of a perfect plastic solid, Hult and McClintock [14] have considered the plastic relaxation at the tip of a sharp notch of depth c in a semi-infinite medium $x \geq 0$ subjected to simple shear in anti-plane strain. A comparison of lengths of yield zones as deduced from the dislocation theory and from Hult and McClintock's work is shown in Fig. I-9. The numerical results from the two cases are in good agreement, with a difference of less than five percent. The plastic zone considered by Hult and McClintock is a circular region at the crack tip. Since this is very different from the thin plastic zone considered in the dislocation model, it would appear that the length of the plastic zone is insensitive to the shape.

The dislocation model of the elastic-plastic slit thus agrees in its prediction of the length of plastic zone as a function of stress both with the experiment on thin sheets and with a treatment by classical plasticity theory.

The relative displacement $\Phi(x)$ of the positive side of the slip plane with respect to the negative can be obtained by integration of the distribution function (I.5-4). Thus

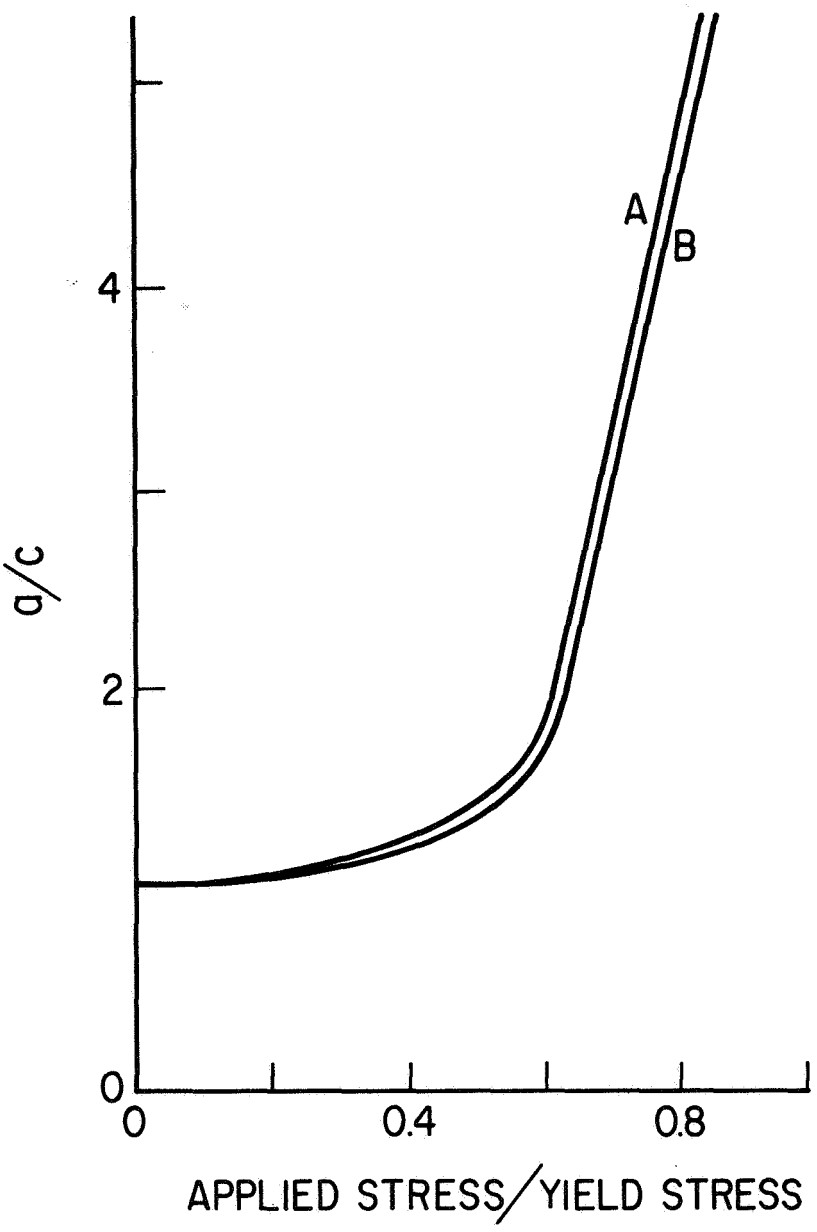

Fig. I-9. COMPARISON OF LENGTHS OF YIELD ZONES AS DEDUCED FROM THE DISLOCATION THEORY (A) AND FROM HULT AND McCLINTOCK'S THEORY (B) [8].

$$\frac{\pi^2 A\Phi(x)}{b(\sigma_1-\sigma_o)} = (x+c)\cosh^{-1}\left|\frac{m}{x+c}+n\right| - (x-c)\cosh^{-1}\left|\frac{m}{c-x}+n\right| . \tag{I.5-6}$$

A plot of the function $\pi^2 A\Phi(x)/b(\sigma_1-\sigma_o)c$ is shown in Fig. I-10 for $a = 2c$. Finally, let $x=c$ in (I.5-6) we have the relative displacement at the tip of a freely slipping crack,

$$\frac{\pi^2 A\Phi(c)}{2cb(\sigma_1 - \sigma_o)} = \ell n\ (\frac{a}{c}) \quad . \tag{I.5-7}$$

Equations (I.5-5) and (I.5-7) relate the important parameters of the problem, namely, the applied stress, the crack opening displacement, the crack length and the extension of plastic zone. To achieve a maximum crack opening displacement for a region of local yielding of given size, the critical crack length can be determined from these two equations.

It is also noted that at low applied stress Eq. (I.5-7) reduces to the familiar form of Orowan [15] and Irwin [16] equation of fracture stress:

$$\sigma_F = \sqrt{\frac{2E\gamma_p}{\pi c}}$$

The plastic work dissipated in propagating the crack is found to be

$$\gamma_p = \sigma_1\Phi(c) . \tag{I.5-8}$$

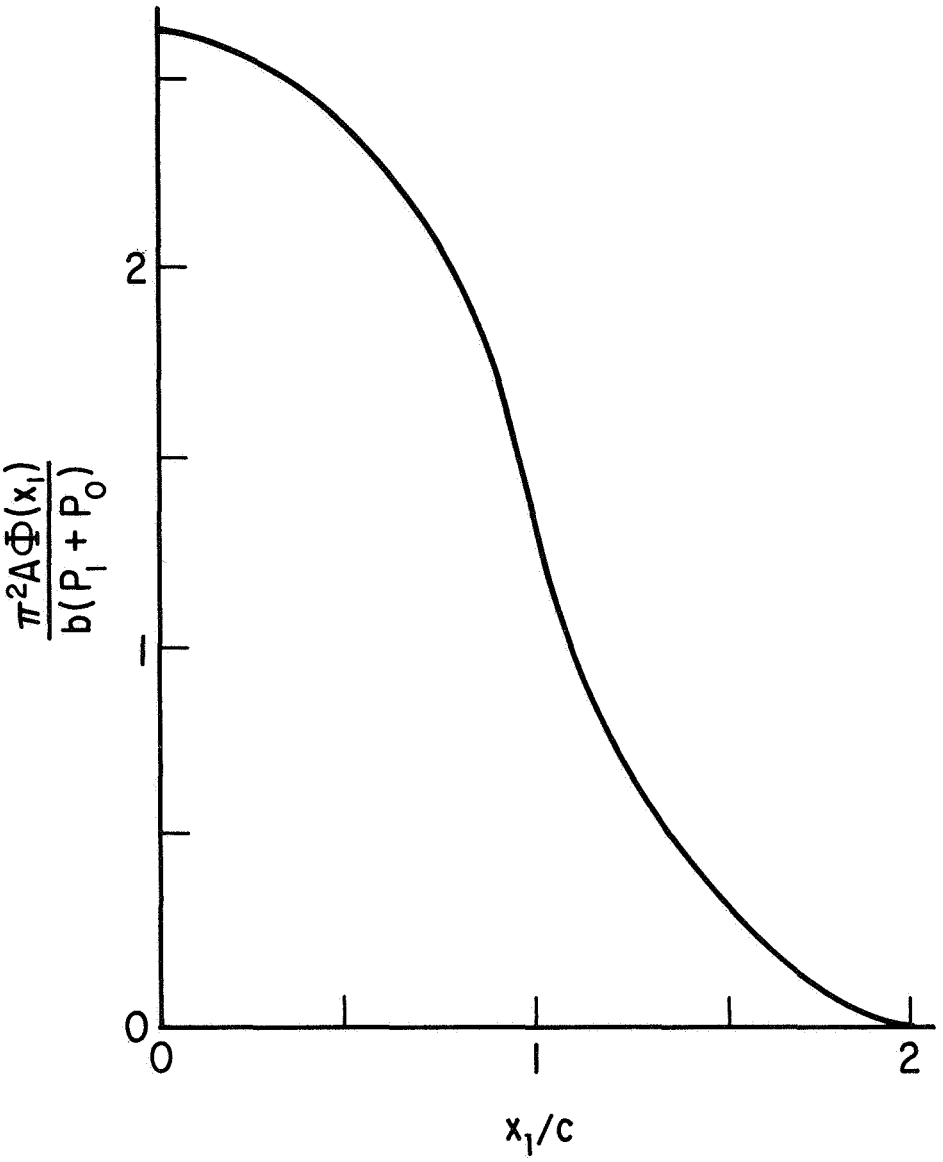

Fig. I-10. SHEAR DISPLACEMENT ALONG THE SLIT AND YIELD ZONE [8].

CHAPTER II

STRESS DISTRIBUTION IN TWO-PHASE SYSTEMS SUBJECTED TO UNIFORM EXTERNAL LOADINGS

1. Introduction

The study of the behavior of cracks and dislocation arrays and their interactions with various heterogeneous elements in materials is of basic importance to the understanding of composite materials. Among the problems examined, particular emphasis has been given to the interaction between screw dislocations and phase boundaries in a composite solid formed by two elastic half-planes having different shear moduli [17,18,19,20].

In a recent paper [21], it was pointed out by Smith that the above results cannot be used to describe the behavior of a bimetallic complex subjected to a uniform anti-plane shear stress at infinity. Owing to the necessity of satisfying the compatibility conditions at the interface, the author claimed that a realistic discussion of these types of problems is achieved only when one of the materials is completely surrounded by the other. However, this is not necessarily true.

On the other hand, the problem of bicrystals subjected to tensile and compressive stress or strain on the surfaces is of interest to the study of interaction of slip systems in two phases [22,23]. The solution of such a problem also simulates the elastic field in a material with one-dimensional fluctuation of composition. The strain energy induced in such a case is of considerable importance to a critical study of the free energy change associated with the process of a spinodal decomposition [24]. Furthermore, the elastic field at the interface has to be considered for a

meaningful discussion of the problems involving cracks and dislocation arrays at phase boundaries.

The aim of this chapter is to examine in detail the effect of inhomogeneity on stress distribution under various loading conditions.

2. Stress Distribution in a Bi-material Plate Under Uniform Anti-plane Shear Stress or Strain

a. Analysis

Consider a bi-material plate of thickness 2h (Fig. II-1), composed of two elastic media welded together at x=0. The shear modulus is G_1 for $x > 0$ and G_2 for $x < 0$. A uniform shear stress $\sigma_{yz}=\sigma_a$ is applied at the upper and lower surfaces of the plate. Assuming perfect bonding at the weld, so that σ_{xz} and the z-component of the displacement have to be continuous at the interface.

Let W_1 and W_2 be the z-component of displacements in regions $x > 0$ and $x < 0$ respectively. The equilibrium of stresses requires that W_1 and W_2 satisfy the Laplace equation. A boundary value problem is then set up for the upper half of the plate (Fig. II-2). By making the substitution

$$\left.\begin{aligned} \Phi_1 &= W_1 - \frac{\sigma_a}{G_1} y \\ \Phi_2 &= W_2 - \frac{\sigma_a}{G_2} y \end{aligned}\right\} \qquad \text{(II.2-1)}$$

the problem can be rewritten with homogeneous boundary conditions.

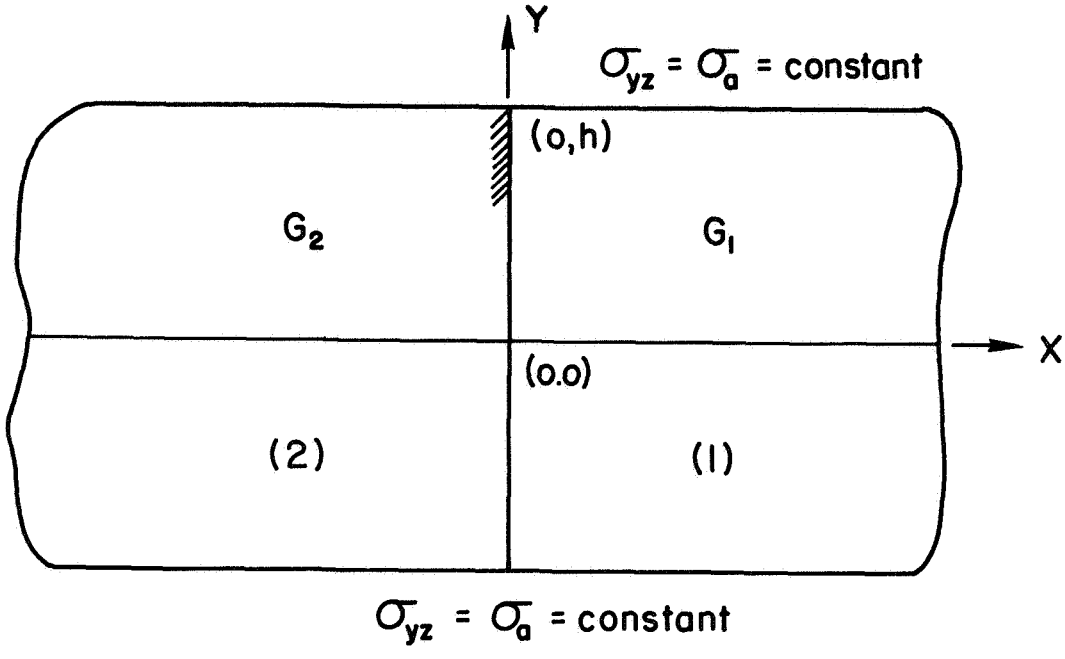

Fig. II-1. THE COORDINATE SYSTEM OF A BI-MATERIAL PLATE UNDER UNIFORM ANTI-PLANE SHEAR STRESS.

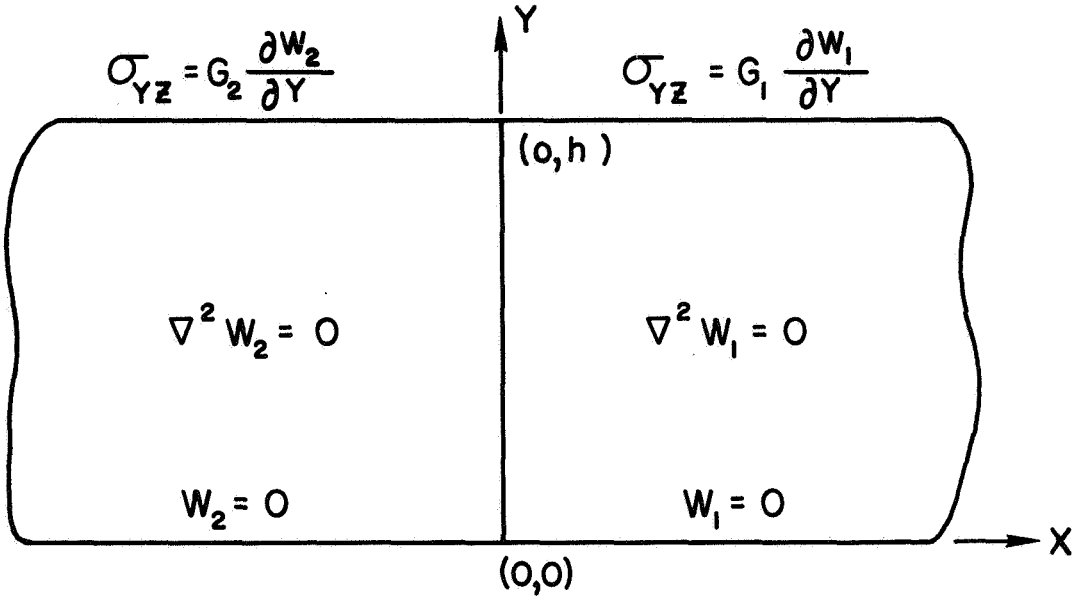

Fig. II-2. THE BOUNDARY VALUE PROBLEM OF THE UPPER HALF OF THE PLATE.

The functions Φ_1 and Φ_2 are assumed in the form of Fourier series with unknown coefficients. By employing the continuity conditions at the interface, these coefficients can be found. The resulting expressions for displacements are obtained as following:

$$\left.\begin{aligned} W_1 &= \sum_{n=0}^{\infty} \frac{-2\sigma_a k \sin\left(n+\frac{1}{2}\right)\pi}{G_1 h \lambda_n^2} \sin\frac{\left(n+\frac{1}{2}\right)\pi y}{h} e^{-\lambda_n x} + \frac{\sigma_a}{G_1} y \quad (x>0) \\ W_2 &= \sum_{n=0}^{\infty} \frac{2\sigma_a k \sin\left(n+\frac{1}{2}\right)\pi}{G_2 h \lambda_n^2} \sin\frac{\left(n+\frac{1}{2}\right)\pi y}{h} e^{\lambda_n x} + \frac{\sigma_a}{G_2} y \quad (x<0) \end{aligned}\right\} \quad \text{(II.2-2)}$$

where

$$k = \frac{G_2 - G_1}{G_2 + G_1}$$

and

$$\lambda_n = \left(n+\frac{1}{2}\right)\pi/h \quad .$$

The expressions for stresses can readily be obtained by differentiation of the above equations

$$\sigma_{yz} = \begin{cases} \displaystyle\sum_{n=0}^{\infty} \frac{-2\sigma_a k \sin\left(n+\frac{1}{2}\right)\pi}{\left(n+\frac{1}{2}\right)\pi} \cos\frac{\left(n+\frac{1}{2}\right)\pi y}{h} e^{-\lambda_n x} + \sigma_a & (x>0) \\ \displaystyle\sum_{n=0}^{\infty} \frac{2\sigma_a k \sin\left(n+\frac{1}{2}\right)\pi}{\left(n+\frac{1}{2}\right)\pi} \cos\frac{\left(n+\frac{1}{2}\right)\pi y}{h} e^{\lambda_n x} + \sigma_a & (x<0) \end{cases} \quad \text{(II.2-3)}$$

and

$$\sigma_{xz} = \begin{cases} \sum_{n=0}^{\infty} \frac{2\sigma_a k \sin\left(n+\frac{1}{2}\right)\pi}{\left(n+\frac{1}{2}\right)\pi} \sin\frac{\left(n+\frac{1}{2}\right)\pi y}{h} e^{-\lambda_n x} & (x > 0) \\ \sum_{n=0}^{\infty} \frac{2\sigma_a k \sin\left(n+\frac{1}{2}\right)\pi}{\left(n+\frac{1}{2}\right)\pi} \sin\frac{\left(n+\frac{1}{2}\right)\pi y}{h} e^{\lambda_n x} & (x < 0) \end{cases} \qquad \text{(II.2-4)}$$

Stress contours of both σ_{xz} and σ_{yz} in a plate of 2 cm thick under unit applied shear stress are shown in Fig. II-3 and II-4 respectively for $k = -.4$.

σ_{xz} is induced at the interface purely due to the inhomogeneity of the medium and fall off exponentially with the distance from the interface. An examination of these contour lines shows that high concentration of the component σ_{xz} occurs at both ends of the interface. This can also be deduced from Eq. (II.2-4) by setting $x=0$ and the stress can be expressed in closed form as:

$$\frac{\sigma_{xz}}{\sigma_a} = \frac{2k}{\pi} \ell n\left[\sec\left(\frac{\pi y}{2h}\right) + \tan\left(\frac{\pi y}{2h}\right)\right] . \qquad \text{(II.2-5)}$$

The variation of σ_{xz} with y at the interface is shown in Fig. II-5. The highly concentrated σ_{xz} near the surfaces of the plate can be the primary cause of splitting of the interface.

As to the component σ_{yz}, it is noted that stress concentration takes place in the harder phase and around the center of the

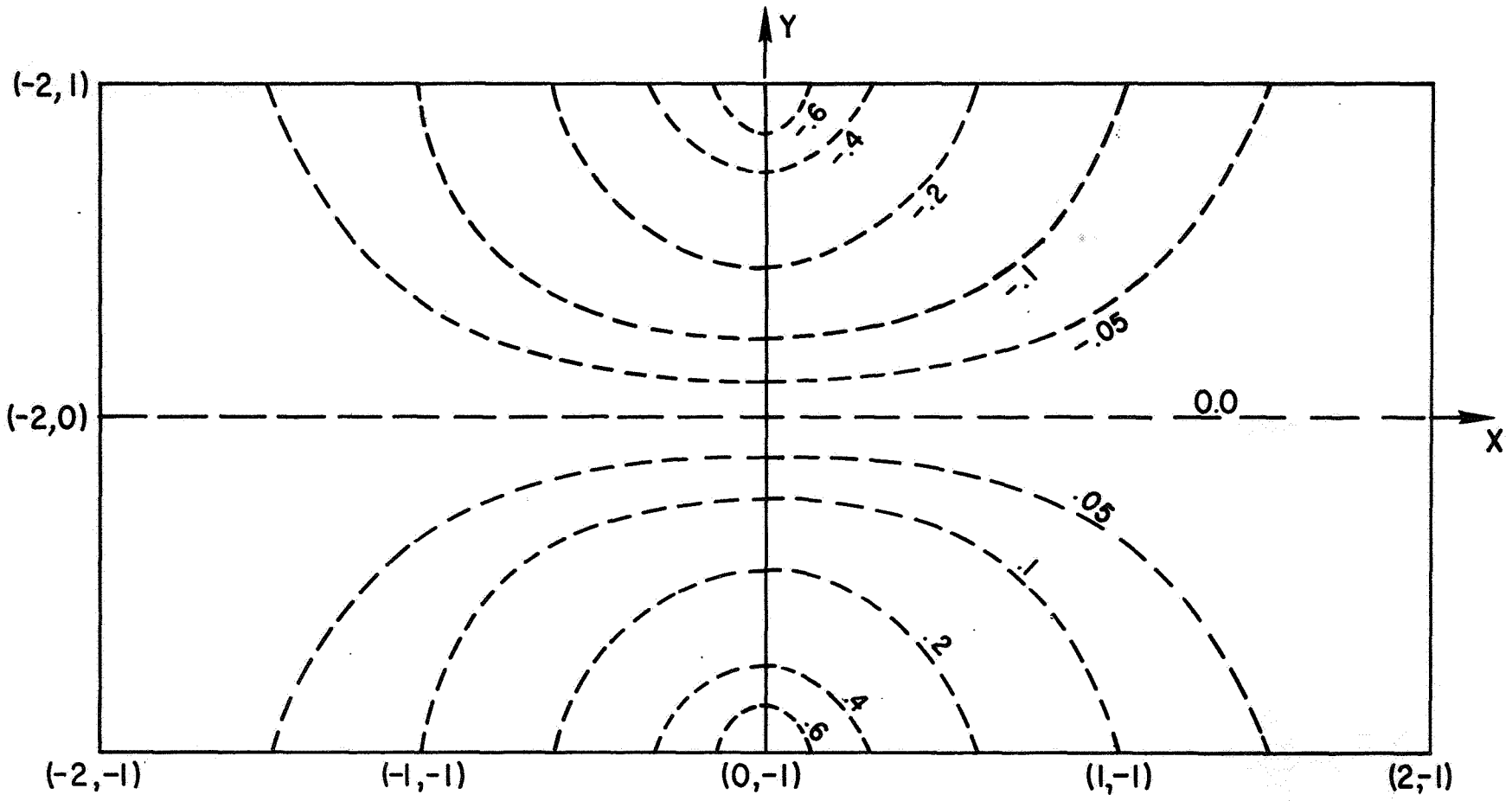

Fig. II-3. CONTOUR LINES OF CONSTANT σ_{xz} IN A BI-MATERIAL PLATE OF k=-.4, UNDER UNIT APPLIED STRESS.

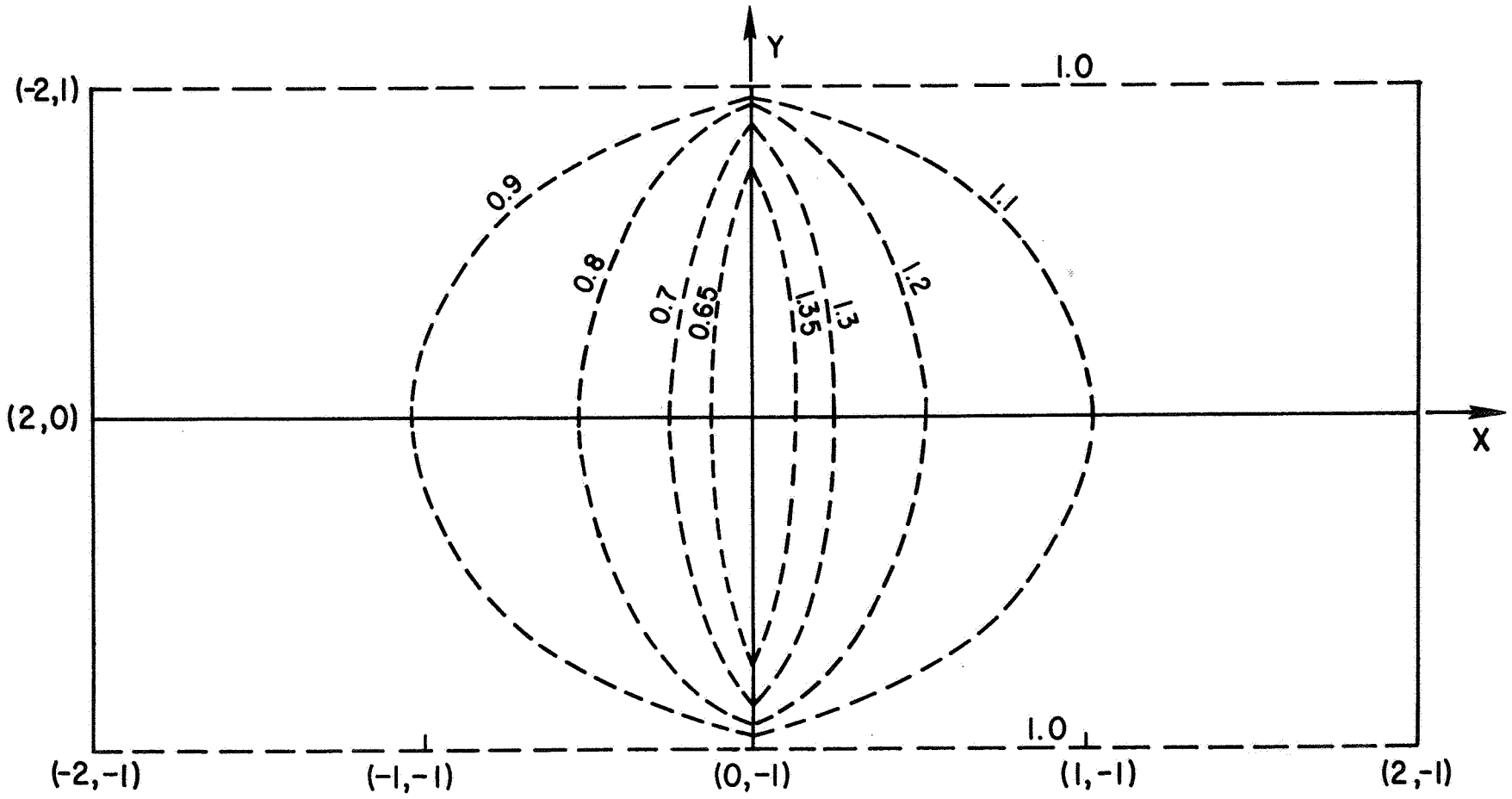

Fig. II-4. CONTOUR LINES OF CONSTANT σ_{yz} IN A BI-MATERIAL PLATE OF k=-.4, UNDER UNIT APPLIED STRESS.

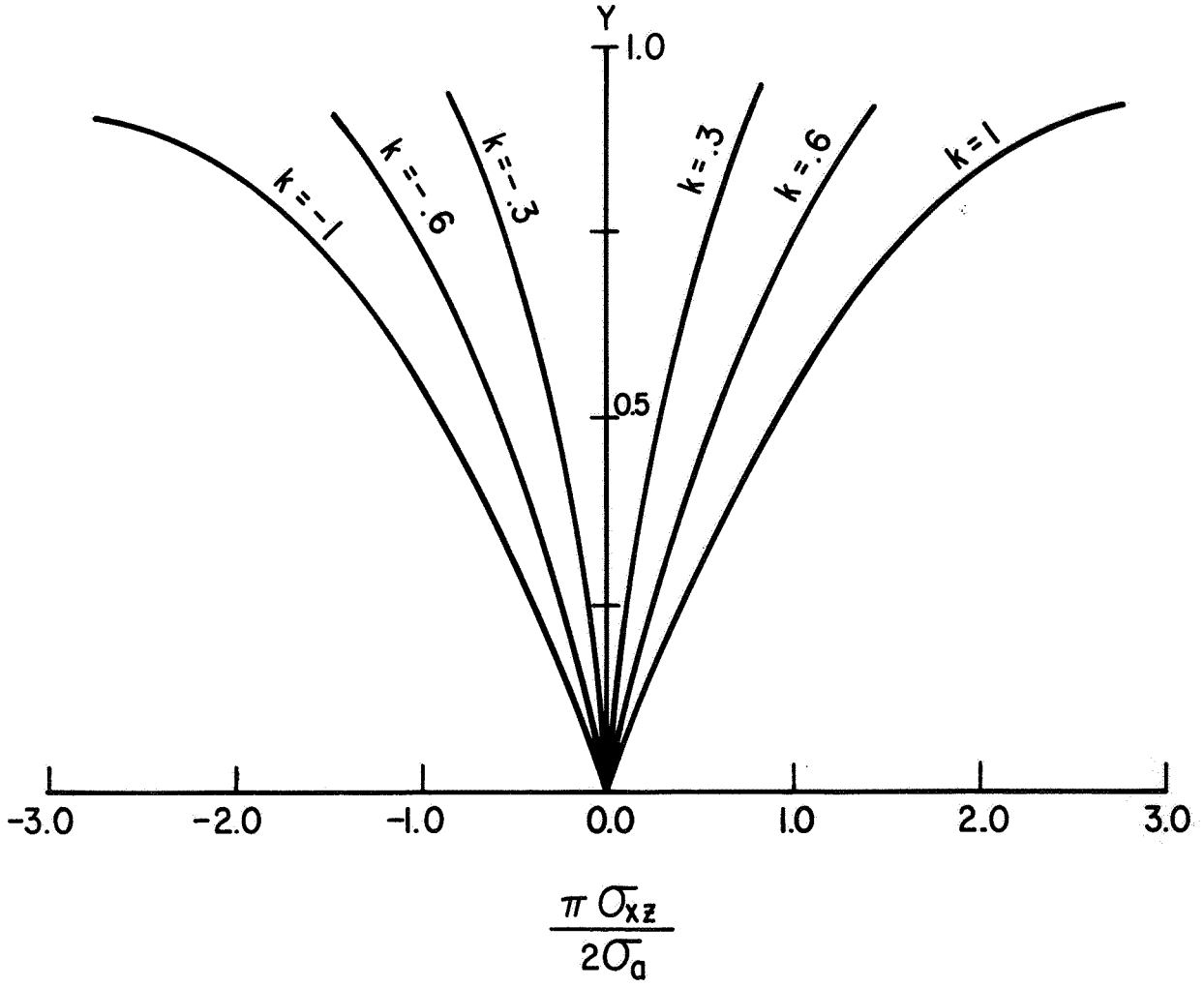

Fig. II-5. VARIATION OF σ_{xz} WITH y AT THE INTERFACE.

the interface. Unlike σ_{xz}, this stress component is discontinuous across the interface. At a distance equal to the thickness of the plate from the interface σ_{yz} tends to become uniform and approaches the value of the externally applied stress.

Also of interest is σ_{yz} on the middle plane of the plate. By setting $y=0$ in Eq. (II.2-3), we obtain in closed form:

$$\sigma_{yz} = \begin{cases} 1 - \frac{4k}{\pi} \tan^{-1}\left(e^{\frac{-\pi x}{2h}}\right) & (x > 0) \\ 1 + \frac{4k}{\pi} \tan^{-1}\left(e^{\frac{\pi x}{2h}}\right) & (x < 0)\,. \end{cases} \qquad \text{(II.2-6)}$$

b. Conclusion

Several interesting features concerning the interaction of screw dislocations and phase boundary can be deduced from the stress configurations:

(1) Consider the case where $k < 0$. The directions of component forces acting on a left-hand screw dislocation are shown in Fig. II-6. The combined effect of σ_{xz} and σ_{yz} in phase 1 for $\sigma_a = \sigma_{yz} > 0$ tends to move left-hand screw dislocations toward the phase boundary and onto the plane $y=0$ provided cross slip is possible. Meanwhile, left-hand screw dislocations in phase 2 are likely to be nucleated at both ends of the interface where there are high stress concentrations. These dislocations will be driven to the plane $y=0$ and further toward the left end. As a result of these motions, left-hand screw dislocations tend to pile up against the phase boundary near the center of the plate

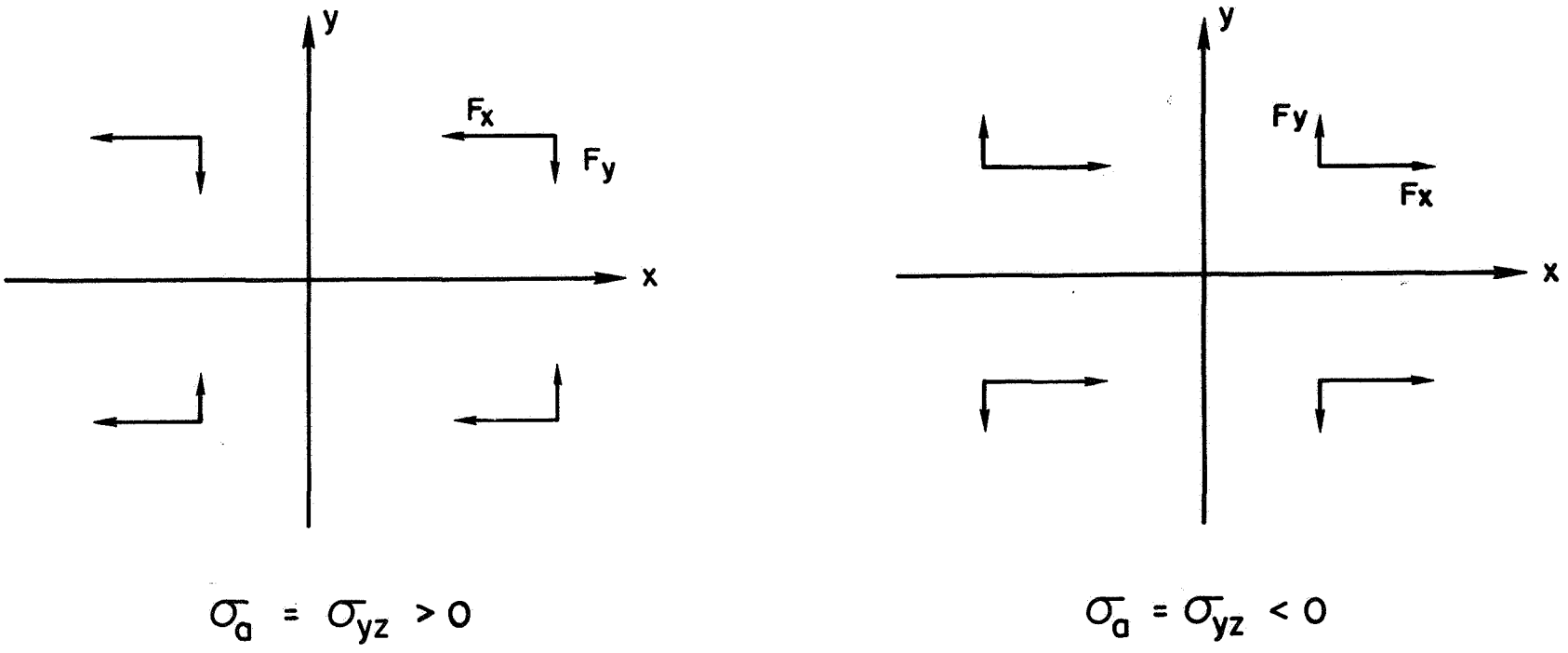

Fig. II-6. THE DIRECTIONS OF COMPONENT FORCES ACTING ON A LEFT-HAND SCREW DISLOCATION.

in the hard phase where crack nucleation is likely to occur. On the other hand, left-hand screw dislocations gliding toward the left end in phase 2 will not form pileups.

By repeating the above investigation for opposite sense of loading and Burgers vector of dislocations, it is found that right-hand screw dislocations can pile up at the phase boundary also only in the hard phase. The image effects on screw dislocations are not considered here.

(2) It is also noted that the stress σ_{yz} on the plane $y=0$ near the interface tends to become uniform as the plate thickness increases (Fig. II-7). Equation (II.2-6) indicates that for a thick plate σ_{yz} near the interface attends the constant values of $\sigma_a(1-k)$ and $\sigma_a(1+k)$ in phases 1 and 2 respectively. This leads to the important conclusion that for lengths of cracks and dislocation arrays much smaller than the physical entities in consideration such as the thickness of a bicrystal and the dimension of a grain, constant stress on dislocations can be achieved by uniformly applied external stresses. This result indicates that the conclusion reached by Smith is not quite right. The magnitude of this stress is effected considerably by the rigidities of the constituents. This finding is especially significant in the later discussion of problems involving crack crossing a phase boundary.

The stress field on the middle plane of the plate is of considerable importance because it simulates the stress field far from the boundary when the plate becomes very thick.

(3) σ_{yz} in phase 1 on the plane $y=0$ decreases as the rigidity of the phase increases. There is virtually no stress on this middle plane when $k=1$. Consequently, uniformly applied shear stress

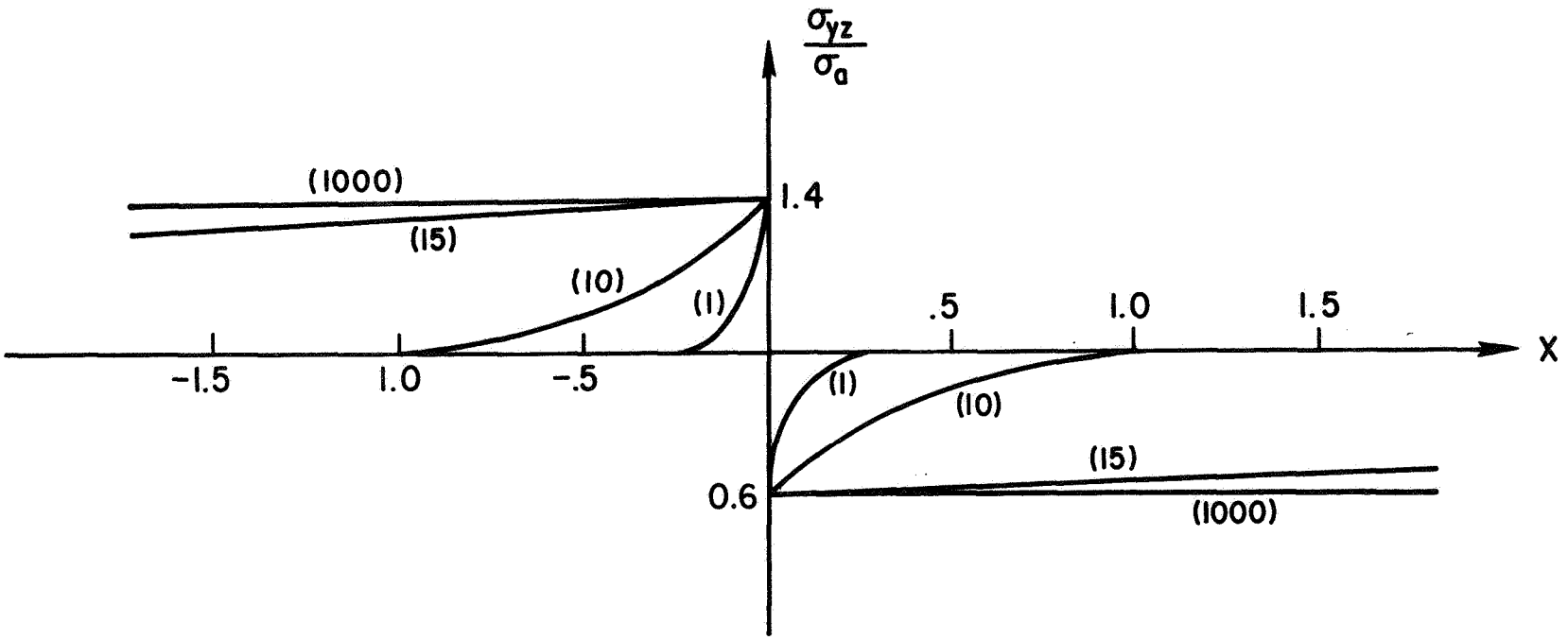

Fig. II-7. THE VARIATION OF σ_{yz} WITH PLATE THICKNESS ON THE PLANE y=0. (The numbers in the parentheses indicate the thickness of the plates.)

can not cause screw dislocations to pile up in phase I against a rigid second phase.

(4) In case a uniform shear strain $\epsilon_{yz} = \epsilon_a$ is applied at the surfaces of the plate, the elastic solution is trivial. The z-component of displacement is uniform and $W = \epsilon_a y$. The only stress component of displacement will be $\sigma_{yz} = G_1\epsilon_a$ for $x > 0$ and $\sigma_{yz} = G_2\epsilon_a$ for $x < 0$.

(5) Now consider the case where a uniform strain $\epsilon_{yz} = \epsilon_a$ is applied at the surfaces of a plate composed of two anisotropic media. The elastic solution of this case is believed to lie within the two extreme cases, namely, a bi-material plate under uniform strain and stress.

3. Stress Distribution in a Bi-material Plate Under Uniform Compressive Stress

a. Analysis

The elastic solution for a bi-material plate (Fig. II-8) under uniform compressive stress is characterized by the complications due to the presence of Poisson's ratio effect. For a welded interface the continuity condition requires that the stress components σ_{xx}, σ_{xy} and displacement components U_1, U_2 and V_1, V_2 in the x and y directions respectively, be continuous across the plane x=0. The subscripts 1 and 2 denote regions for which $x > 0$ and $x < 0$ respectively.

Stress functions for general loadings on a semi-infinite strip under plane stress condition have been discussed by Iyengar and Alwar [25, 26]. This technique is employed in the following analysis. The boundary conditions for both regions are:

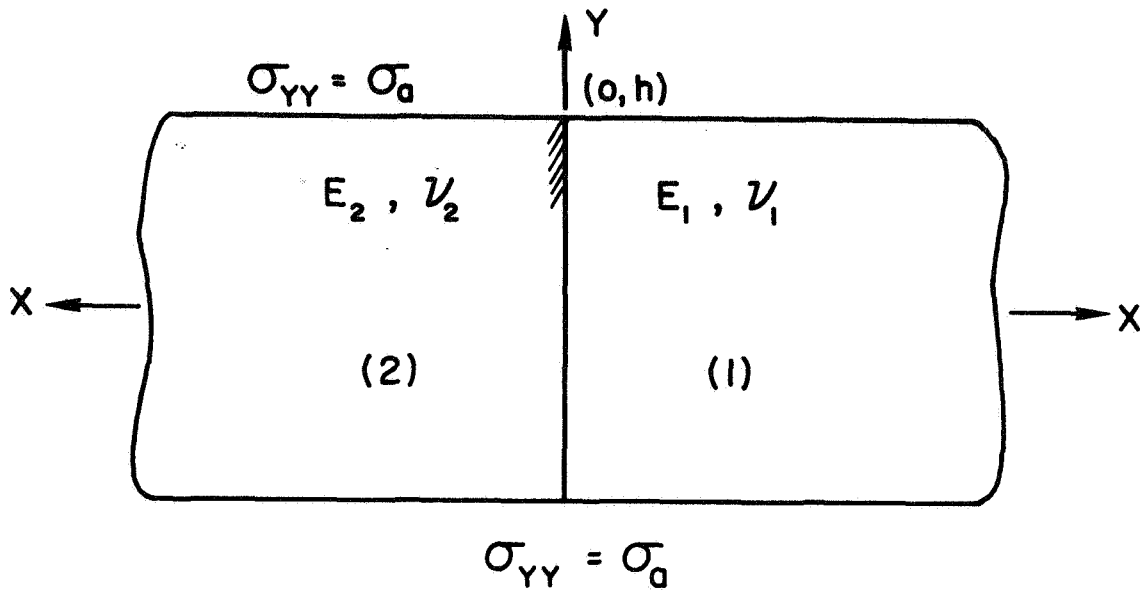

Fig. II-8. THE COORDINATE SYSTEM OF A BI-MATERIAL PLATE UNDER UNIFORM COMPRESSIVE STRESS.

at $x = 0$

$$\left.\begin{aligned} \sigma_{xx})_1 &= \sigma_{xx})_2 = \sum_{m=1,2}^{\infty} K_m \cos \frac{m\pi y}{h} \\ \sigma_{xy})_1 &= -\sigma_{xy})_2 = \sum_{m=1,2}^{\infty} L_m \sin \frac{m\pi y}{h} \\ U_1 &= -U_2 \\ V_1 &= V_2 \ , \end{aligned}\right\} \qquad \text{(II.3-1)}$$

at $y = \pm h$

$$\left.\begin{aligned} \sigma_{yy})_1 &= \sigma_{yy})_2 = \sigma_a \\ \sigma_{xy})_1 &= \sigma_{xy})_2 = 0 \ . \end{aligned}\right\} \qquad \text{(II.3-2)}$$

The unknown normal and shear stresses at the interface are assumed in the form of Fourier series with unknown coefficients to be determined from the continuity conditions.

Let Φ_1 and Φ_2 be the Airy stress functions in regions $x > 0$ and $x < 0$ respectively. All well known theorem for constructing biharmonic function is that for given functions $f(x,y,z)$ and $g(x,y,z)$ harmonic in a simply connected region, then $\Phi = fx + g$ is biharmonic in the same region [27]. By taking into consideration the symmetry property of the stress components of the plate, the following stress function is constructed:

$$\Phi_1 = \frac{\sigma_a x^2}{2} + \sum_{m=1,2}^{\infty} \frac{1}{\alpha_m^2} [A_m(1 + \alpha_m x) + L_m \alpha_m x] e^{-\alpha_m x} \cos \alpha_m y$$

$$+ \int_0^{\infty} \frac{C_1(\alpha) \cos \alpha x}{\alpha^2 \cosh \alpha h} [\alpha y \sinh \alpha y - (1+\alpha h \coth \alpha h) \cosh \alpha y] \, d\alpha$$

(II.3-3)

where A_m, L_m and C_1 are unknown coefficients and $\alpha_m = m\pi/h$.

It can be shown that $\nabla^4 \Phi_1 = 0$ is satisfied. Since the plate has finite thickness and is infinitely extended in the x direction both discrete and continuous eigenvalues occur in the above expression.

The stress components in the region $x > 0$ can readily be obtained by differentiation of Φ_1:

$$\sigma_{xx} = - \sum_{m=1,2}^{\infty} [A_m(1+\alpha_m x) + L_m \alpha_m x] e^{-\alpha_m x} \cos \alpha_m y$$

$$+ \int_0^{\infty} \frac{C_1(\alpha) \cos \alpha x}{\cosh \alpha h} [\alpha y \sinh \alpha y + (1-\alpha h \coth \alpha h) \cosh \alpha y] \, d\alpha$$

(II.3-4)

$$\sigma_{yy} = \sigma_a + \sum_{m=1,2}^{\infty} [L_m(\alpha_m x - 2) + A_m(\alpha_m x - 1)] e^{-\alpha_m x} \cos \alpha_m y$$

$$- \int_0^{\infty} \frac{C_1(\alpha) \cos \alpha x}{\cosh \alpha h} [\alpha y \sinh \alpha y - (1+\alpha h \coth \alpha h) \cosh \alpha y] \, d\alpha$$

(II.3-5)

$$\sigma_{xy} = \sum_{m=1,2}^{\infty} [L_m(1-\alpha_m x) - A_m \alpha_m x]\, e^{-\alpha_m x} \sin \alpha_m y$$

$$+ \int_0^{\infty} \frac{C_1(\alpha) \sin \alpha x}{\cosh \alpha h} [\alpha y \cosh \alpha y - \alpha h \coth \alpha h \sinh \alpha y]\, d\alpha \ . \qquad \text{(II.3-6)}$$

Φ_2 is similar to Φ_1 except that A_m, L_m and C_1 are changed to B_m, $-L_m$ and C_2 respectively.

By considering the stress boundary conditions in both phases, we obtain the following relations

$$A_m = -K_m + 16m^2\pi^2 \sum_{r=1,2}^{\infty} (-1)^{m+r} A_r rM(r,m)$$

$$+ \ 8m^2\pi^2 \sum_{r=1,2}^{\infty} (-1)^{m+r} L_r rN(r,m) \qquad \text{(II.3-7)}$$

$$B_m = -K_m + 16m^2\pi^2 \sum_{r=1,2}^{\infty} (-1)^{m+r} B_r rM(r,m)$$

$$- \ 8m^2\pi^2 \sum_{r=1,2}^{\infty} (-1)^{m+r} L_r rN(r,m) \qquad \text{(II.3-8)}$$

where

$$M(r,m) = \int_0^\infty \frac{x^3 \tanh x \, dx}{\left(1 + \frac{2x}{\sinh 2x}\right)(x^2 + m^2\pi^2)^2 (x^2 + r^2\pi^2)^2} \qquad \text{(II.3-9)}$$

$$N(r,m) = 3M(r,m) + \int_0^\infty \frac{r^2\pi^2 x \tanh x \, dx}{(x^2 + m^2\pi^2)^2 (x^2 + r^2\pi^2)^2 \left(1 + \frac{2x}{\sinh 2x}\right)} \cdot \qquad \text{(II.3-10)}$$

The details of the derivation are too tedious to be shown here. The displacement components can be derived from the stress functions by the method of Coker and Filon [28]. The compatibility of displacements at the interface requires

$$\frac{2A_m}{E_1} + \frac{2B_m}{E_2} + L_m\left(\frac{1-\nu_1}{E_1} + \frac{\nu_2-1}{E_2}\right) = 0 \qquad \text{(II.3-11)}$$

$$\left(\frac{2A_m}{E_1} - \frac{2B_m}{E_2}\right) + K_m\left(\frac{1+\nu_1}{E_1} - \frac{1+\nu_2}{E_2}\right) + 2L_m\left(\frac{1}{E_1} + \frac{1}{E_2}\right)$$

$$- 16m^2\pi^2 \sum_{r=1,2}^{\infty} B_r(-1)^{m+r}\, r\, \frac{Q(r,m)}{E_2}$$

$$+ 16m^2\pi^2 \sum_{r=1,2}^{\infty} A_r(-1)^{m+r}\, r\, \frac{Q(r,m)}{E_1}$$

$$+ 8m^2\pi^2 \sum_{r=1,2}^{\infty} L_r(-1)^{m+r}\, r\, R(r,m)\left[\frac{1}{E_1} + \frac{1}{E_2}\right]$$

$$= (-1)^{m+1}\, 2\sigma_a\left[\frac{1}{E_1} - \frac{1}{E_2}\right] \qquad \text{(II.3-12)}$$

where

$$Q(r,m) = \int_0^{\infty} \frac{x \tanh x\, dx}{\left(1 + \frac{2x}{\sinh 2x}\right)(x^2 + m^2\pi^2)(x^2 + r^2\pi^2)^2} \qquad \text{(II.3-13)}$$

$$R(r,m) = 3Q(r,m) + \int_0^{\infty} \frac{r^2\pi^2 \tanh x}{\left(1 + \frac{2x}{\sinh 2x}\right) x(x^2 + m^2\pi^2)(x^2 + r^2\pi^2)^2} \cdot$$

(II.3-14)

Equations (II.3-7), (II.3-8), (II.3-11) and (II.3-12) give a system of linear equations to determine A_m, B_m, K_m and L_m. The constants C_1 and C_2 can then be evaluated by

$$C_1(\alpha) = 4h \sum_{m=1,2}^{\infty} (-1)^m \frac{A_m(\alpha h)^2 m + \frac{1}{2} L_m(m^2\pi^2 + 3\alpha^2 h^2) m}{(m^2\pi^2 + \alpha^2 h^2)^2} \cdot \frac{1}{\left(1 + \frac{2\alpha h}{\sinh 2\alpha h}\right)}$$

$$C_2(\alpha) = 4h \sum_{m=1,2}^{\infty} (-1)^m \frac{B_m(\alpha h)^2 m - \frac{1}{2} L_m(m^2\pi^2 + 3\alpha^2 h^2)}{(m^2\pi^2 + \alpha^2 h^2)^2} \cdot \frac{1}{\left(1 + \frac{2\alpha h}{\sinh 2\alpha h}\right)} \cdot \qquad \text{(II.3-15)}$$

It is noted that the above solution differs from that of a bimetallic plate under uniform tension $\sigma_{xx} = \sigma_a$ by changing the term $(-1)^{m+1}$ $2\sigma_a(1/E_1 - 1/E_2)$ in Eq. (II.3-12) to $(-1)^{m+1}$ $2\sigma_a(\nu_2/E_2 - \nu_1/E_1)$.

Consider the case in which a 2 cm thick plate is subjected to unit compressive stress on the surfaces. It is assumed that $E_1/E_2 = 2$ and $\nu_1 = \nu_2 = 1/3$. Owing to the slowness of the convergence of series in Eqs. (II.3-7), (II.3-8), (II-3-11),and (II.3-12), four leading terms of each coefficient are evaluted. The implication of the results are discussed in the following section.

b. Conclusion

(1) The tensile stress σ_{xx}, induced around the plane $x=0$ tends to cause debonding at the interface. The maximum of this normal stress occurs at both ends of the interface. The magnitude of this tensile stress there is about 9 percent of the applied stress. As the center of the plate is approached, this tensile stress diminishes and finally becomes a compressive stress.

(2) The magnitude of shear component σ_{xy} at the interface can be as high as 25 percent of the applied stress as shown in Fig. II-9. This shear component also falls off with the distance from the interface. In composite materials with weakly bonded interfaces, this shear component can be the primary cause of splitting of phase boundaries. Consequently, this might lead to crack blunting at the interface.

Both normal and shear stresses at the phase boundary are caused by the inhomogeneity of the medium. The effect becomes more distinct as the differences in elastic constants of the two constituent phases increase.

(3) The normal stress component σ_{yy} on the middle plane of the plate varies with plate thickness as shown in Fig. II-10. It is noted that a nearly constant stress is attained in the vicinity of the interface as the plate becomes thick. Consequently, in discussing cracks and edge dislocation pileups ahead of a bi-material interface, a uniformly applied stress field can be achieved in this manner.

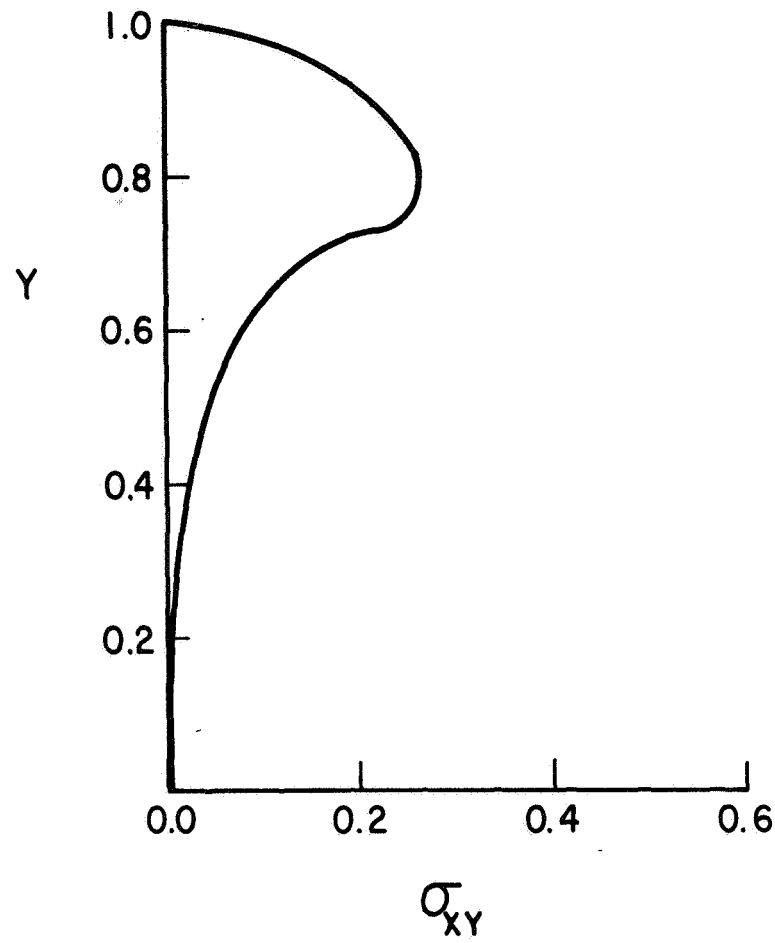

Fig. II-9. SHEAR STRESS ALONG THE INTERFACE IN A BI-MATERIAL PLATE OF UNIT THICKNESS WITH $E_1/E_2=2$ and $\nu_1=\nu_2=1/3$.

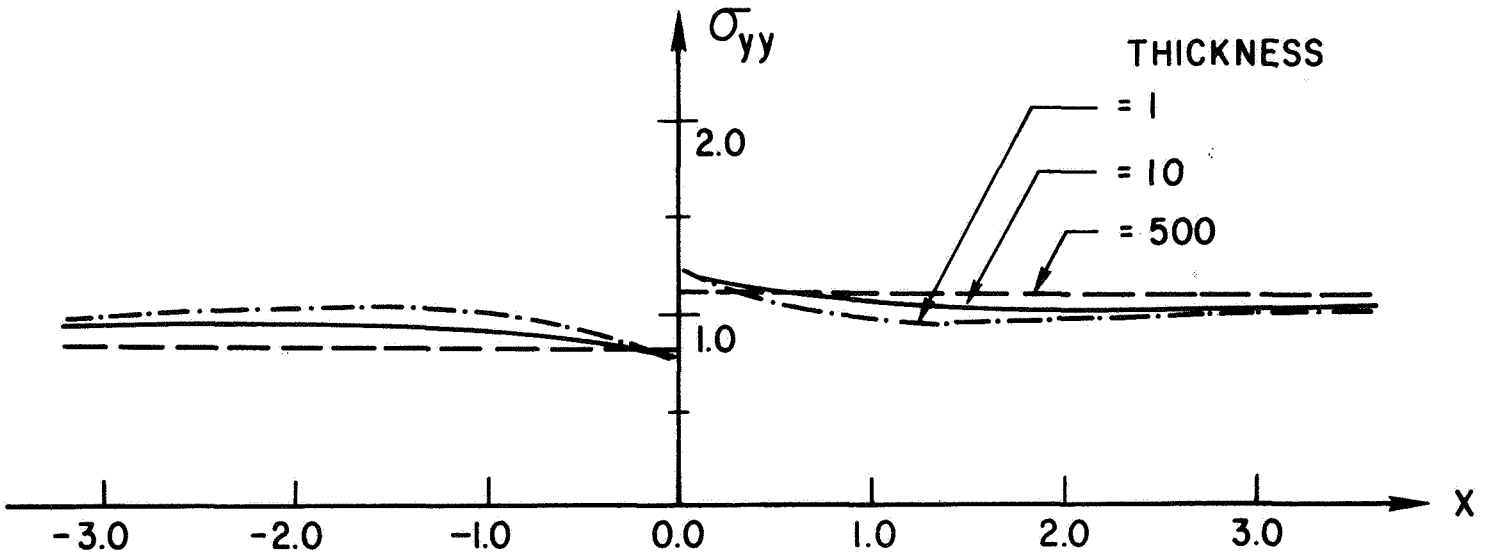

Fig. II-10. THE VARIATION OF σ_{yy} WITH PLATE THICKNESS ON THE PLANE y=0.

(4) One further implication of the present solution was pointed out by Hirth, Tiller and Pound [24] in discussing the mathematical theory of spinodal decomposition. If a finite system underwent an one-dimensional sinusoidal fluctuation in composition, the resultant configuration would resemble that shown in Fig. II-11a. This is an improvement of the theory originally proposed by Cahn [29]. In Cahn's theory, it was assumed that no y and z displacements are allowed (Fig. II-11b). This is certainly unrealistic.

An exact elastic solution of a non-homogeneous medium with sinusoidally varying elastic constants would be very complicated. However, the present solution does simulate the elastic field around the interface in Fig. II-11a. It indicates that an exact solution for such a relaxed configuration will yield a stress tensor that contains both normal and shear components. These stress components would fall off exponentially with distance from the interface.

Furthermore, an exact elastic solution of the relaxed configuration in Fig. II-11a, containing general stress tensor, would lead to a revision of the strain energy calculation as proposed by Cahn.

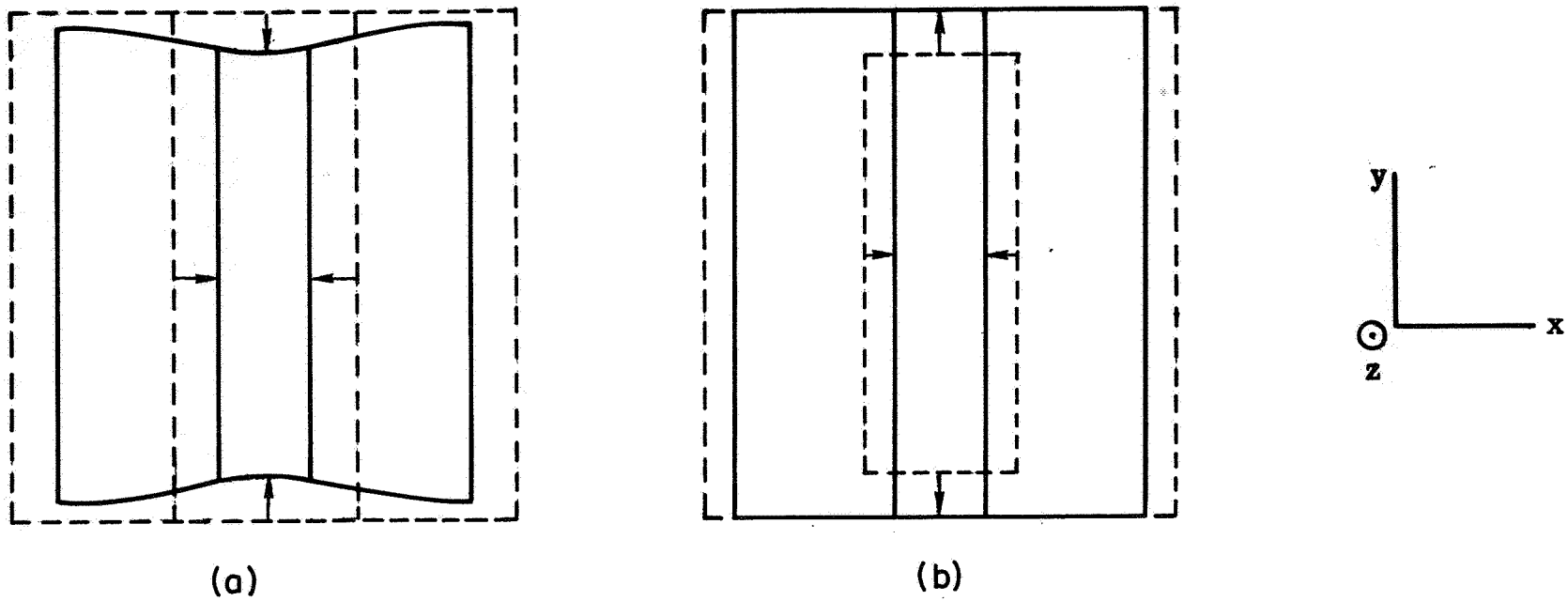

Fig. II-11. RESULTANT CONFIGURATION OF A FINITE SYSTEM UNDERWENT ONE-DIMENSIONAL SINUSOIDAL FLUCTUATION IN COMPOSITION. (a) Hirth, Tiller and Pound's theory, (b) Cahn's theory [24].

CHAPTER III

ELASTIC CRACKS AT A BI-MATERIAL INTERFACE

1. Introduction

The aim of the present chapter is to discuss the stress field about a crack perpendicular to a bi-material interface, under the three modes of deformation. The stress concentration at the tip of a crack in one phase determines the extent of plastic yielding and crack nucleation in the neighboring matrix. It also indicates if a splitting of interface and a subsequent blunting of crack tip are possible.

Analytical solutions for dislocation pileups at phase boundary in a two-phase system have been discussed by Barnett [20] and Kuang and Mura [30] for different loading conditions. The mathematical procedures for analyzing these problems are equivalent to that of semi-infinite wedges. The present work deals with the problem of elastic cracks of finite length. The displacement of crack surfaces has been represented by that of a continuously distributed dislocations [31]. The exact expression for applied stress on dislocations as discussed in Chapter II is employed in this investigation.

2. Mode III Crack

a. Dislocation Distribution Function

Consider a plate composed of two semi-infinite strips welded together at the interface. The coordinate axes are chosen to be the same as that depicted in Fig. II-1. Let G_1 and G_2 be the shear moduli and ν_1 and ν_2 the Poisson's ratios with reference to phase 1 and 2. A

crack of length L in phase 1 is perpendicular to the interface (Fig. III-1). The elastic field of the crack is represented by that of a continuous distribution of infinitesimal dislocations.

It has been pointed out in Chapter I that three kinds of stresses need to be considered in discussing the equilibrium configuration of dislocations. These are the dislocation stress, σ_d, the effective stress on dislocations due to externally applied stress, σ_a, and the friction stress, σ_o.

When the thickness of the bi-material plate is much larger than the length of cracks in consideration, the stress field of dislocations in an infinite medium can be employed. Let a single right-hand screw dislocation of Burgers vector b be situated in $x > 0$ at $(t,0)$. The line direction is parallel to the z-axis. Assuming perfect bonding at the weld, the stress field due to the dislocation is:

$$\sigma_{xz} = \begin{cases} -\frac{G_1 b}{2\pi} \frac{y}{(x-t)^2 + y^2} - \frac{G_1 b}{2\pi} \frac{ky}{(x+t)^2 + y^2} & (x > 0) \\ -\frac{G_1 b}{2\pi} \frac{(1+k)\, y}{(x-t)^2 + y^2} & (x < 0) \end{cases} \qquad \text{(III.2-1)}$$

and

$$\sigma_{yz} = \begin{cases} \frac{G_1 b}{2\pi} \frac{x-t}{(x-t)^2 + y^2} + \frac{G_1 b}{2\pi} \frac{k(x+t)}{(x+t)^2 + y^2} & (x > 0) \\ \frac{G_1 b}{2\pi} \frac{(1+k)(x-t)}{(x-t)^2 + y^2} & (x < 0) \end{cases} \qquad \text{(III.2-2)}$$

where $k = (G_2 - G_1)/(G_2 + G_1)$.

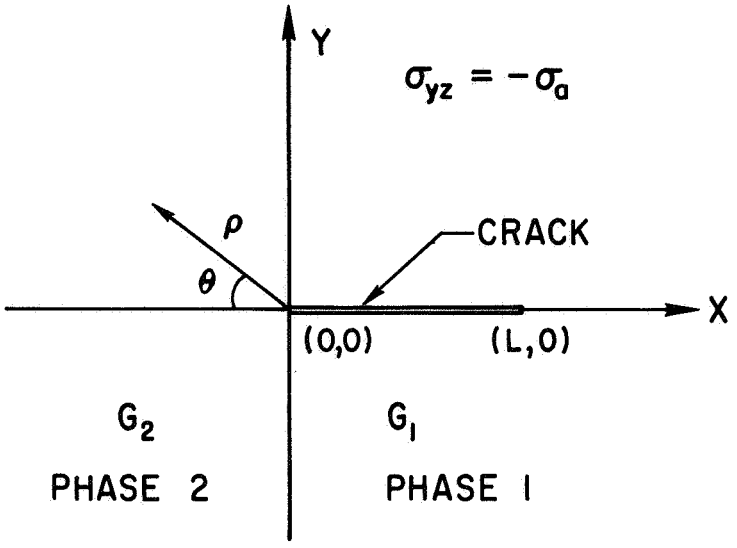

Fig. III-1. A MODE III CRACK PERPENDICULAR TO A BI-MATERIAL INTERFACE.

On the plane $y=0$, Eq. (III.2-2) reduces to:

$$\sigma_{yz} = \begin{cases} \frac{G_1 b}{2\pi}\left(\frac{1}{x-t} + \frac{k}{x+t}\right) & (x > 0) \\ \frac{G_1 b}{2\pi}\,\frac{1+k}{x-t} & (x < 0)\ . \end{cases} \qquad \text{(III.2-3)}$$

The effective stress on the middle plane due to a uniformly applied stress $\sigma_{yz} = -\sigma_a$ is found to be $-\sigma_a(1-k)$ as discussed in Chapter II. Inside the crack, the resistence stress, σ_o, to the motion of dislocations vanishes.

Let $f(t)$ be the unknown distribution function of dislocations of strength b. The force equilibrium on a single dislocation at $(x,0)$ leads to the following singular integral equation:

$$\int_0^L \frac{f(t)}{x-t}\,dt + k\int_0^L \frac{f(t)}{x+t}\,dt - \frac{2\pi\sigma_a(1-k)}{G_1 b} = 0 \qquad (0 < x < L)\ . \qquad \text{(III.2-4)}$$

The first integral is understood to be a Cauchy principal value intregal. The physics of the problem requires that $f(t)$ is unbounded at both ends of the crack.

Equation (III.2-4) is sufficient to determine the solution for dislocations piling up at one end. However, in discussing cracks, an additional condition is needed in order to determine the solution completely. Suppose dislocations neither leave nor enter the crack. Then

the line integral of displacement along any closed circuit not crossing the crack region should vanish.

The z-component of displacement at $x > 0$ due to a single right-hand screw dislocation at $t > 0$ is:

$$w(x,y,t) = \frac{b}{2\pi}\left[\tan^{-1}\frac{y}{x - t} + k\tan^{-1}\frac{y}{x + t}\right] . \qquad \text{(III.2-5)}$$

Consider the closed circuit around the crack (Fig. III-2). The resultant displacements on the upper and lower paths due to all the dislocations inside the crack are:

$$W(x, +\epsilon) = \int_0^L w(x, +\epsilon,t)\, f(t)\, dt$$

$$W(x, -\epsilon) = \int_0^L w(x, -\epsilon,t)\, f(t)\, dt \qquad \text{(III.2-6)}$$

As $\epsilon \to 0$, the total displacement integrated along the circuit vanishes:

$$\int_0^L W(x, -\epsilon)\, dx + \int_L^0 W(x, +\epsilon)\, dx$$

$$= \int_0^L -2b(1 + k)\left[\int_0^L f(t)\, dt\right] dx$$

$$= 0 .$$

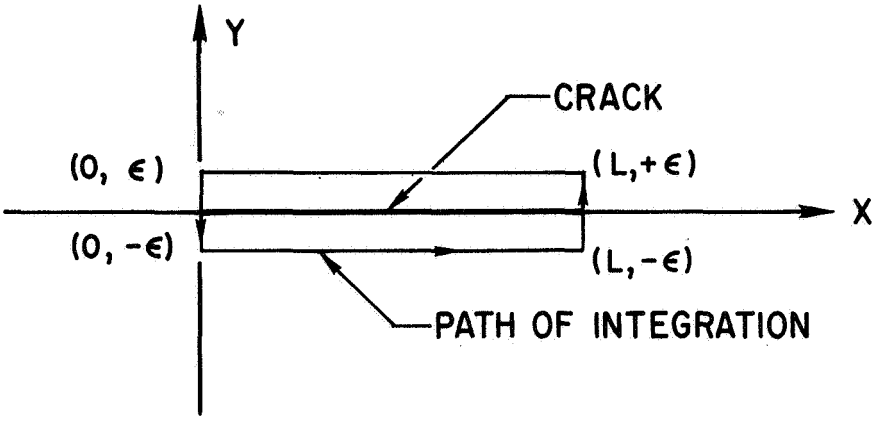

Fig. III-2. PATH FOR INTEGRATION OF DISPLACEMENT AROUND THE CRACK.

Consequently, it yields

$$\int_0^L f(t)\, dt = 0 \ . \qquad \text{(III.2-7)}$$

In fact, Eq. (III.2-7) is equivalent to the compatibility condition in linear elasticity. However, the above condition can be deduced immediately from the crack opening displacement consideration. Since it is assumed that there is no dislocation leaving nor entering the crack, the crack surfaces must close at both ends. Consequently, the integration of Burgers vectors of all dislocations in the crack vanishes:

$$\int_0^L bf(t)\, dt = 0 \ . \qquad \text{(III.2-8)}$$

This is identical with Eq. (III.2-7), as expected. Equations (III.2-4) and (III.2-7) are sufficient to determine $f(t)$.

Integral equations with kernel function of the type $K(x-t)$ can be solved by the very ingenious Wiener-Hopf technique [30,32,33,34]. An outline of this method is given in Appendix B. To avoid the very combersome mathematical procedures involved, only the essential steps in solving Eqs. (III.2-4) and (III.2-7) are shown below.

Let $\frac{x}{L} = u$ and $\frac{t}{L} = v$, Eq. (III.2-4) can be rewritten as:

$$\int_0^1 \frac{f(v)}{u - v}\, dv + k \int_0^1 \frac{f(v)}{u + v}\, dv = \frac{2\pi\sigma_a(1-k)}{G_1 b} = g(u) \quad (0 < u < 1) \ . \qquad \text{(III.2-9)}$$

Further extend Eq. (III.2-9) to the interval $L < x < \infty$ by defining the new function $h(u)$:

$$\int_0^1 \frac{f(v)}{u - v}\, dv + k \int_0^1 \frac{f(v)}{u + v}\, dv = h(u) \qquad (1 < u < \infty) \ . \tag{III.2-10}$$

Let $\frac{u}{v} = s$ and apply Mellin transform to the variable u in the above two equations. The transformed equations can be recast in the general form in terms of the transform variable ω:

$$F_+(\omega)\, K(\omega) = G_+(\omega) + H_-(\omega) \tag{III.2-11}$$

where

$$F_+(\omega) = \int_0^1 v^{\omega-1} f(v)\, dv$$

$$K_+(\omega) = \frac{2\pi^2 \Gamma(\omega)\, \Gamma(1-\omega)}{\Gamma(\frac{\omega+a}{2})\, \Gamma(1 - \frac{\omega+a}{a})\, \Gamma(\frac{\omega-a}{2})\, \Gamma(1 - \frac{\omega-a}{2})}$$

$$G_+(\omega) = \frac{2\pi\sigma_a(1-k)}{G_1 b} \frac{1}{\omega}$$

$$H_-(\omega) = \int_1^\infty h(u)\, u^{\omega-1}\, du$$

and

$$\omega = \sigma + i\tau \ .$$

Denoting $\sigma_+=1$ and $\sigma_- = a = \frac{2}{\pi}\sin^{-1}\sqrt{(1-k)/2}$, it can be shown that $G_+(\omega)$ is regular in the strip $\sigma_- < \sigma < \sigma_+$ and $K(\omega)$ is regular and non-zero in the same strip. We are then looking for the unknown function $F_+(\omega)$ and $H_-(\omega)$ which are analytical in the half planes $\sigma > \sigma_-$ and $\sigma < \sigma_+$ respectively.

Equation (III.2-11) is in the general functional relation to which the Wiener-Hopf technique can be applied. By carrying out the procedures outlined in Appendix B, the resulting expression is in the form of Eq. (B-7). In this expression, there is an unknown constant which has to be determined by employing Eq. (III.2-7).

Finally, the solution of the distribution function can be found:

$$f\left(\frac{t}{L}\right) = \frac{2\sigma_a(1-k)}{G_1 b}\sqrt{\frac{2}{1-k}}\left\{\sinh\left(\frac{2}{\pi}\sin^{-1}\sqrt{\frac{1-k}{2}}\cosh^{-1}\frac{L}{t}\right)\right.$$

$$\left. - \frac{a}{\sqrt{1-\left(\frac{t}{L}\right)^2}}\cosh\left(\frac{2}{\pi}\sin^{-1}\sqrt{\frac{1-k}{2}}\cosh^{-1}\frac{L}{t}\right)\right\}$$

$$= \frac{2\sigma_a(1-k)}{G_1 b}\sqrt{\frac{2}{1-k}}\left\{\left(\frac{L}{t}\right)^a\left[\left(1+\sqrt{1-\left(\frac{t}{L}\right)^2}\right)^a - \left(1-\sqrt{1-\left(\frac{t}{L}\right)^2}\right)^a\right]\right.$$

$$\left. - \frac{a}{\sqrt{1-\left(\frac{t}{L}\right)^2}}\left(\frac{L}{t}\right)^a\left[\left(1+\sqrt{1-\left(\frac{t}{L}\right)^2}\right)^a + \left(1-\sqrt{1-\left(\frac{t}{L}\right)^2}\right)^a\right]\right\}. \qquad \text{(III.2-12)}$$

The terms in the first bracket of the distribution function expression correspond to those of a semi-infinite wedge. The terms in the second bracket are necessary due to the unboundedness of $f(t)$ at $t=L$.

In the limiting case of an infinite homogeneous medium, $k=0$, Eq. (III.2-12) reduces to:

$$f(\frac{t}{L}) = \frac{\sigma_a}{G_1 b} \frac{L - 2t}{\sqrt{t(L - t)}} \quad . \qquad \text{(III.2-13)}$$

in agreement with the previous result [31].

As pointed out in the last chapter, the stress which tends to open the crack vanishes when the second phase is rigid, i.e., $k \rightarrow 1$. Figure III-3 depicts $f(t)$ for various values of k. Furthermore, when an uniform strain $\epsilon_{yz} = -\epsilon_a$ is applied at the plate surfaces the solution is obtained simply by changing $\sigma_a(1-k)$ to $G_1\epsilon_a$ in Eq. (III.2-12).

If, instead of cracks, a double dislocation pileup is considered, the mathematical procedures employed above still can be applied. However, in this case a certain frictional stress, σ_o, should be specified on the slip plane. This only changes the last term in Eq. (III.2-4).

Finally, it needs to be pointed out that the change of distribution function is small for small variation of G_2/G_1 (Fig. III-3). The practical implication of this result is that the effect of inhomogeneity can be neglected for small fluctuation of elastic constants. The elastic solution obtained from homogeneous medium can be used as a first approximation for these problems.

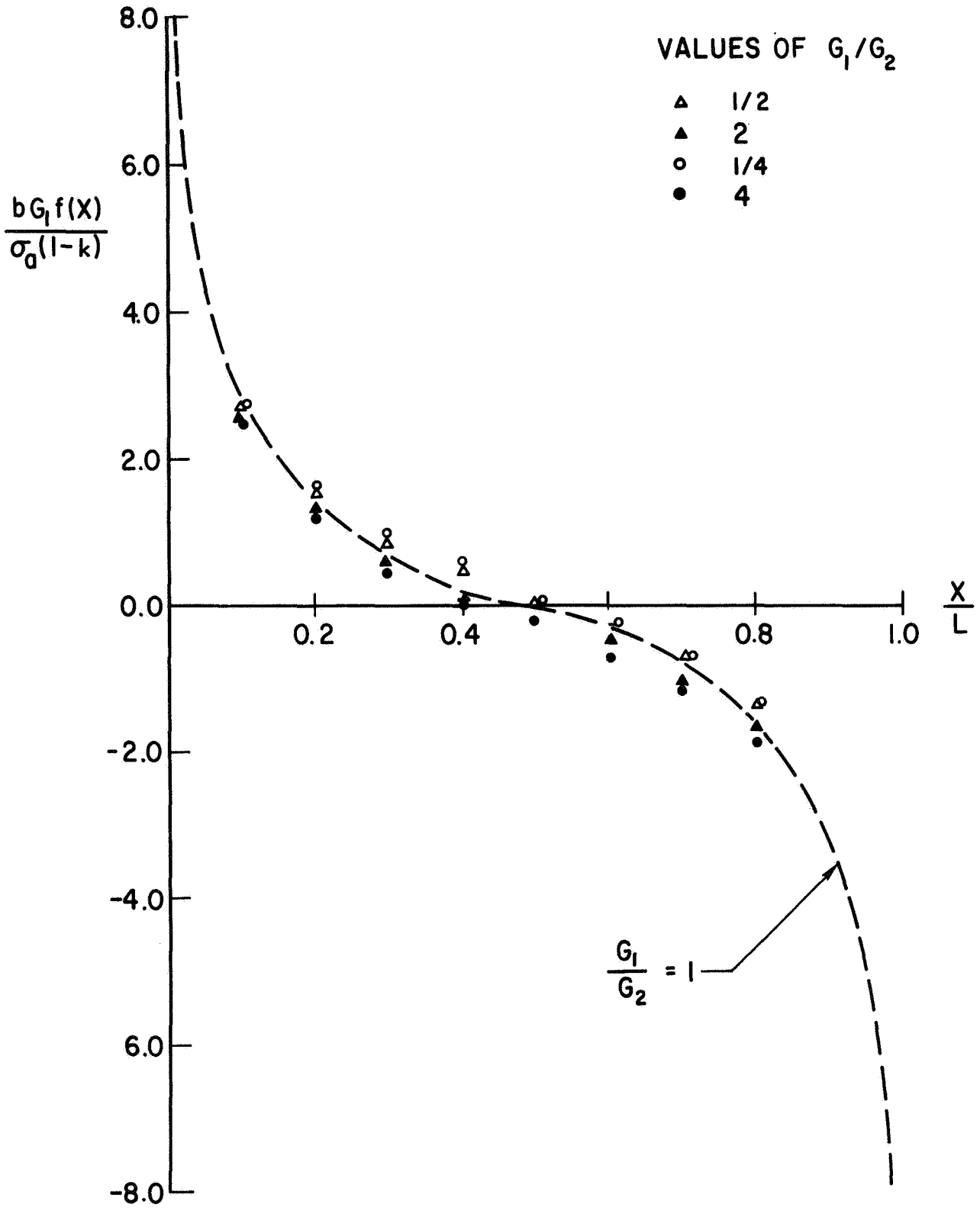

Fig. III-3. DISTRIBUTION FUNCTIONS OF DISLOCATIONS REPRESENTING THE CRACK.

b. Stress Field

The stress field of the crack is calculated from

$$\sigma_{ij}(x,y) = \int_0^L \sigma_{ij}(x,y,t)\, f(t)\, dt \qquad (i = 1,2 \text{ and } j = 3) . \tag{III.2-14}$$

Making the substitution $v = \cosh^{-1}\left(\frac{L}{t}\right)$ and integrating in the complex plane $v = \omega_o + i\phi_o$ as described by Barnett [20], stresses in the second phase can be obtained:

$$\sigma_{xz} = \frac{\sigma_a(1-k^2)\ \text{sgn}\ (y)}{\sin \pi a \sin \frac{\pi a}{2}} \Bigg[- \sinh a\omega_o \sin a\phi_o$$

$$+ \frac{a}{(\sinh^2\omega_o + \sin^2 \phi_o)} (\cosh \omega_o \sinh \omega_o \cosh a\omega_o \sin a\phi_o$$

$$- \cos \phi_o \sin \phi_o \sinh a\omega_o \cos a\phi_o) \Bigg] \tag{III.2-15}$$

and

$$\sigma_{yz} = \frac{\sigma_a(1 - k^2)}{\sin \pi a \sin \frac{\pi a}{a}} \Bigg\{ -\cosh a\omega_o \cos a\phi_o + \cos \frac{\pi a}{2}$$

$$+ \frac{a}{(\sinh^2\omega_o + \sin^2\phi_o)} \Bigg[\cos \phi_o \cosh a\omega_o \sin a\phi_o \sin \phi_o$$

$$+ \text{ctnh}\omega_o \sinh a\omega_o \cos a\phi_o \left(\frac{L^2}{\rho^2} - \cos^2 \phi_o\right) \Bigg] \Bigg\} \tag{III.2-16}$$

where

$$\sinh^2\omega_o = \frac{1}{2}\left[\left(\frac{L}{\rho}\right)^2 - 1 + \sqrt{\left(\left(\frac{L}{\rho}\right)^2 - 1\right)^2 + \left(\frac{2L}{\rho}\sin\theta\right)^2}\right] \qquad \text{(III.2-17)}$$

and

$$\sin^2\phi_o = \frac{1}{2}\left[1 - \left(\frac{L}{\rho}\right)^2 + \sqrt{\left(\left(\frac{L}{\rho}\right)^2 - 1\right)^2 + \left(\frac{2L}{\rho}\sin\theta\right)^2}\right]. \qquad \text{(III.2-18)}$$

ρ and θ are plar coordinates as depicted in Fig. III-1.

At the tip of crack, i.e., $\frac{L}{\rho} \gg 1$, Eqs. (III.2-15) and (III.2-16) can be simplified as

$$\sigma_{xz} = \frac{\sigma_a(1-k)^2\,\mathrm{sgn}(y)}{\sin\pi a \sin\frac{\pi a}{2}}\left(\frac{L}{\rho}\right)^a 2^{a-1}(a-1)\sin a\phi_o \qquad \text{(III.2-19)}$$

and

$$\sigma_{yz} = \frac{\sigma_a(1-k^2)}{\sin\pi a \sin\frac{\pi a}{2}}\left(\frac{L}{\rho}\right)^a 2^{a-1}(a-1)\cos a\phi_o \,. \qquad \text{(III.2-20)}$$

The stress singularity at the tip of the crack is of the type $\left(\frac{L}{\rho}\right)^a$ which becomes the inverse square root type only when $k=0$, namely, the two phases are identical. It is also noted that the stress concentration at the tip of a finite crack is smaller than that of a semi-infinite wedge [20] by the factor of (1-a).

Figure III-4 depicts the variation of σ_{yz}/σ_a with the distance from the tip of crack on the plane $y=0$ for various k values.

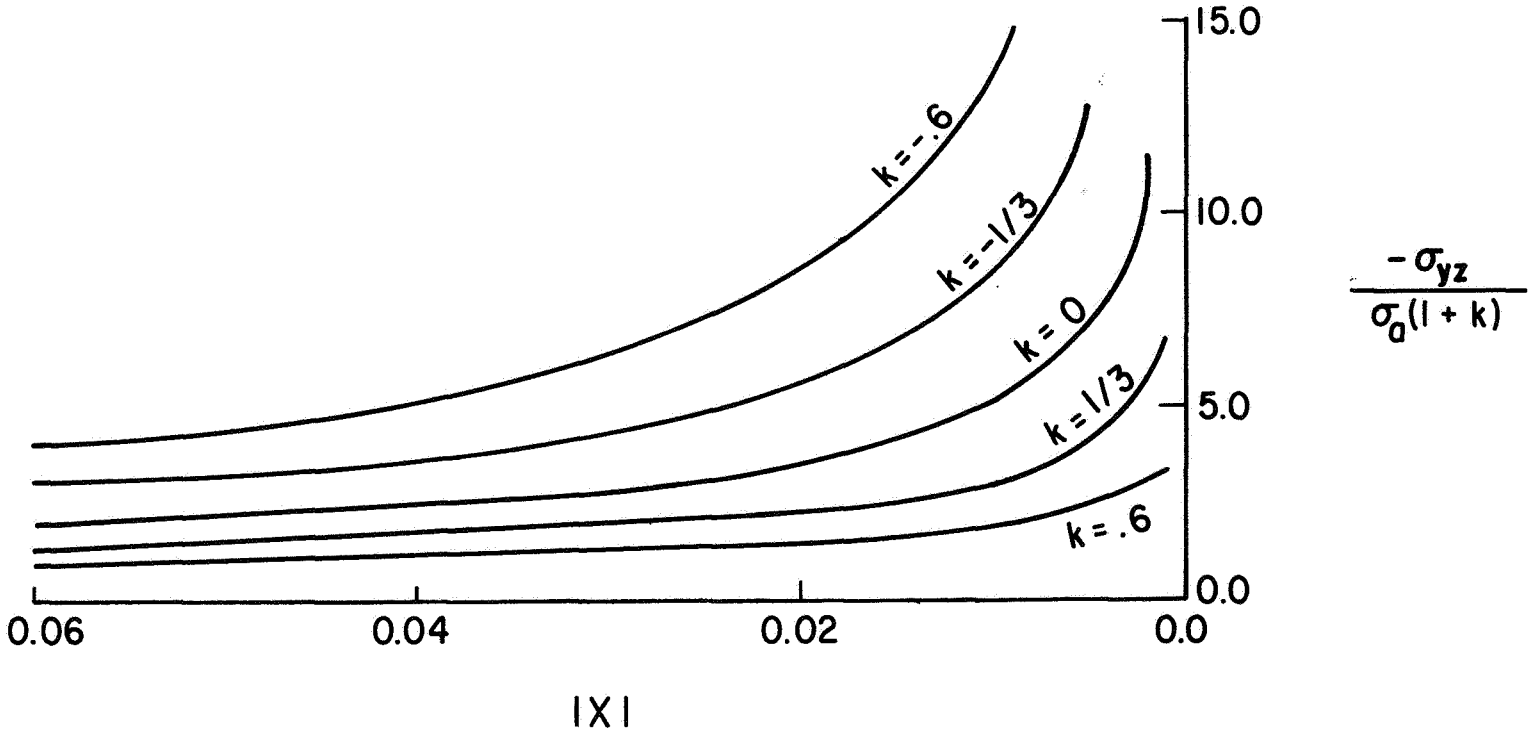

Fig. III-4. STRESS σ_{yz} AT THE CRACK TIP ON THE PLANE y=0 IN PHASE 2.

The resultant shear stress at the tip of the crack is

$$\sigma = \frac{\sigma_a(1 - k^2)}{\sin \pi a \sin \frac{\pi a}{2}} 2^{a-1}(a-1)\left(\frac{L}{\rho}\right)^a \cdot \qquad \text{(III.2-21)}$$

Just as in the case of a homogeneous medium, the resultant stress at the tip of the crack against a bi-material interface is independent of θ.

If the second phase is harder than the first phase, $0 < k < 1$, we have $0 < a < \frac{1}{2}$. When $-1 < k < 0$, then $\frac{1}{2} < a < 1$. Consequently, the stress concentration at the tip of a crack in the harder phase is higher than that in the softer phase. This finding is consistent with that of Zak and Williams and Barnett [40,20].

3. Modes I and II Cracks

a. Dislocation Distribution Function

Consider the same thick bi-material plate as discussed in the last section. A crack of unit length is situated perpendicular to the interface in phase 1. Tensile stress $\sigma_{yy} = -\sigma_a$ is applied uniformly over the plate surfaces to open the crack (Fig. III-5). The effective stress σ_{yy} on the crack plane can be found by the method illustrated in Chapter II and is denoted as $-\sigma'_a$.

Again, the displacement field of the crack is represented by that of an array of dislocations. The y-component of the normal stress at $(x,0)$ due to a single edge dislocation at $(t,0)$ in phase 1 is [35,36]:

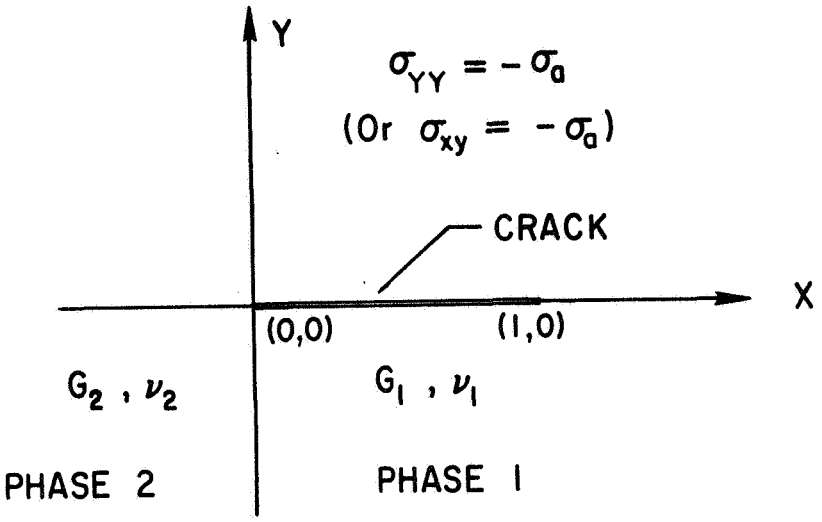

Fig. III-5. A MODE I OR II CRACK PERPENDICULAR TO A BI-MATERIAL INTERFACE.

$$\sigma_{yy} = \frac{G_1 b}{\pi(\eta_1+1)} \left[\frac{2}{x - t} - \frac{A + B}{x + t} - \frac{4At(x-t)}{(x+t)^3} \right] \qquad \text{(III.3-1)}$$

where

$$A = \frac{1 - r}{1 + r\eta_1} , \quad B = \frac{\eta_2 - r\eta_1}{\eta_2 + r} , \quad r = \frac{G_2}{G_1} ,$$

and

$$\eta_1 = 3 - 4\nu_1 ,$$

$$\eta_2 = 3 - 4\nu_2 .$$

The Burgers vector $\overline{b}$ is parallel to the interface for mode I cracks and perpendicular for mode II cracks.

Let $f(t)$ be the unknown distribution function of dislocations of strength b. The force equilibrium for a single dislocation leads to the following singular integral equation:

$$\int_0^1 \frac{\gamma}{\pi} \left[\frac{1}{x - t} - \frac{\alpha}{x + t} - \frac{\beta t(x-t)}{(x+t)^3} \right] f(t)\, dt = \sigma'_a \qquad \text{(III.3-2)}$$

where $\gamma = \frac{2G_1 b}{(1+\eta_1)}$, $\alpha = \frac{1}{2}(A+B)$ and $\beta = 2A$. $f(t)$ is unbounded at both ends of the crack.

By defining

$$\phi(t) = -i\gamma f(t)$$

and $k(x,t) = \frac{\alpha}{x+t} + \frac{\beta t(x-t)}{(x+t)^3}$, the left-hand side of Eq. (III.3-2) can be separated into singular and non-singular parts as follows:

$$\frac{1}{\pi i}\int_0^1 \frac{\phi(t)\,dt}{x-t} + \frac{1}{\pi i}\int_0^1 \phi(t)\,k(x,t)\,dt = \sigma_a' \,. \qquad \text{(III.3-3)}$$

Singular integral equation of this type can be inverted according to the method outlined in Appendix A and $\phi(t)$ is solved "formly." The resulting equation is a Fredholm integral equation of the second kind:

$$\Phi(x) = \int_0^1 K(x,t')\,\Phi(t')\,dt' + F(x) \qquad \text{(III.3-4)}$$

where

$$\Phi(x) = \frac{i\phi(x)}{\sigma_a'}$$

$$K(x,t') = \frac{1}{\pi\sqrt{x(1-x)}}\left[\frac{-\alpha}{x+t'}\left(x + t' - \sqrt{t' + t'^2}\right)\right.$$

$$+ \frac{2\beta t'^2}{x+t'}\left(\frac{1+2t'}{2t'^2\,(1+t'^2)\,\pi} + \frac{1}{8(t'+t'^2)\sqrt{t'+t'^2}}\right)$$

$$+ \frac{\beta t'(t'-x)}{(t'+x)^2}\left(-1 + \frac{2t'+1}{2\sqrt{t'+t'^2}}\right)$$

$$\left. + \frac{\beta t'(t'-x)}{(t'+x)^3}\left(x + t' - \sqrt{t' + t'^2}\right)\right]$$

and

$$F(x) = \frac{c}{\sqrt{x(1-x)}} + \frac{1 - 2x}{2\sqrt{x(1-x)}} \quad .$$

The constant c is to be determined by the condition of conservation of Brugers vectors:

$$\int_0^1 f(t)\, dt = 0 \qquad \text{(III.3-5)}$$

The physical basis of its derivation is shown in the last section.

Equations (III.3-4) and (III.3-5) have to be solved simultaneously. First define

$$F_1(x) = \frac{1 - 2x}{2\sqrt{x(1-x)}} \quad , \quad F_2(x) = \frac{1}{\sqrt{x(1-x)}}$$

and

$$\Phi(x) = \Phi_1(x) + c\Phi_2(x) \quad . \qquad \text{(III.3-6)}$$

Since Eq. (III.3-4) is linear, it can be considered as the linear combination of the following two equations:

$$\Phi_1(x) = \int_0^1 K(x,t')\, \Phi_1(t')\, dt' + F_1(x) \qquad \text{(III.3-7)}$$

and

$$\Phi_2(x) = \int_0^1 K(x,t')\ \Phi_2(t')\ dt' + F_2(x)\ . \qquad \text{(III.3-8)}$$

$\Phi_1(x)$ and $\Phi_2(x)$ are then solved separately. Because of the complicated form of the kernel in Eq. (III.3-4), a numerical solution of the Fredholm integral equation is attempted. Using the method outlined in Appendix C, Eq. (III.3-7) is replaced by a system of n linear equations. n is the number of subdivisions in the interval of integration. By solving this system of linear equations, an approximate expression for $\Phi_1(x)$ in the whole interval can be obtained. Same procedures can be carried out to solve $\Phi_2(x)$.

With the known values of $\Phi_1(x)$ and $\Phi_2(x)$, Eq. (III.3-6) can then be substituted into Eq. (III.3-5) and solved for the constant c. Consequently, $\Phi(x)$, hence $f(x)$, is obtained from Eq. (III.3-6).

If $\beta=0$, $\alpha = -k$, $\gamma = G_1 b/2$ and $\sigma_a' = \sigma_a(1-k)$ in Eq. (III.3-4), the solution reduces to that of a mode III crack. A comparison of the exact solution obtained from Eq. (III.2-12) and the numerical solution of this case is shown in Fig. III-6. The solid line depicts the exact solution and the crosses are obtained from the numerical solution. It can be seen that the agreement is excellent. As a consequence of this comparison, the numerical approximation to the singular integral equation can be employed with confidence.

b. Crack Opening Displacement

The configuration of the crack opening displacement can most easily be obtained by integrating the dislocation density. At any point

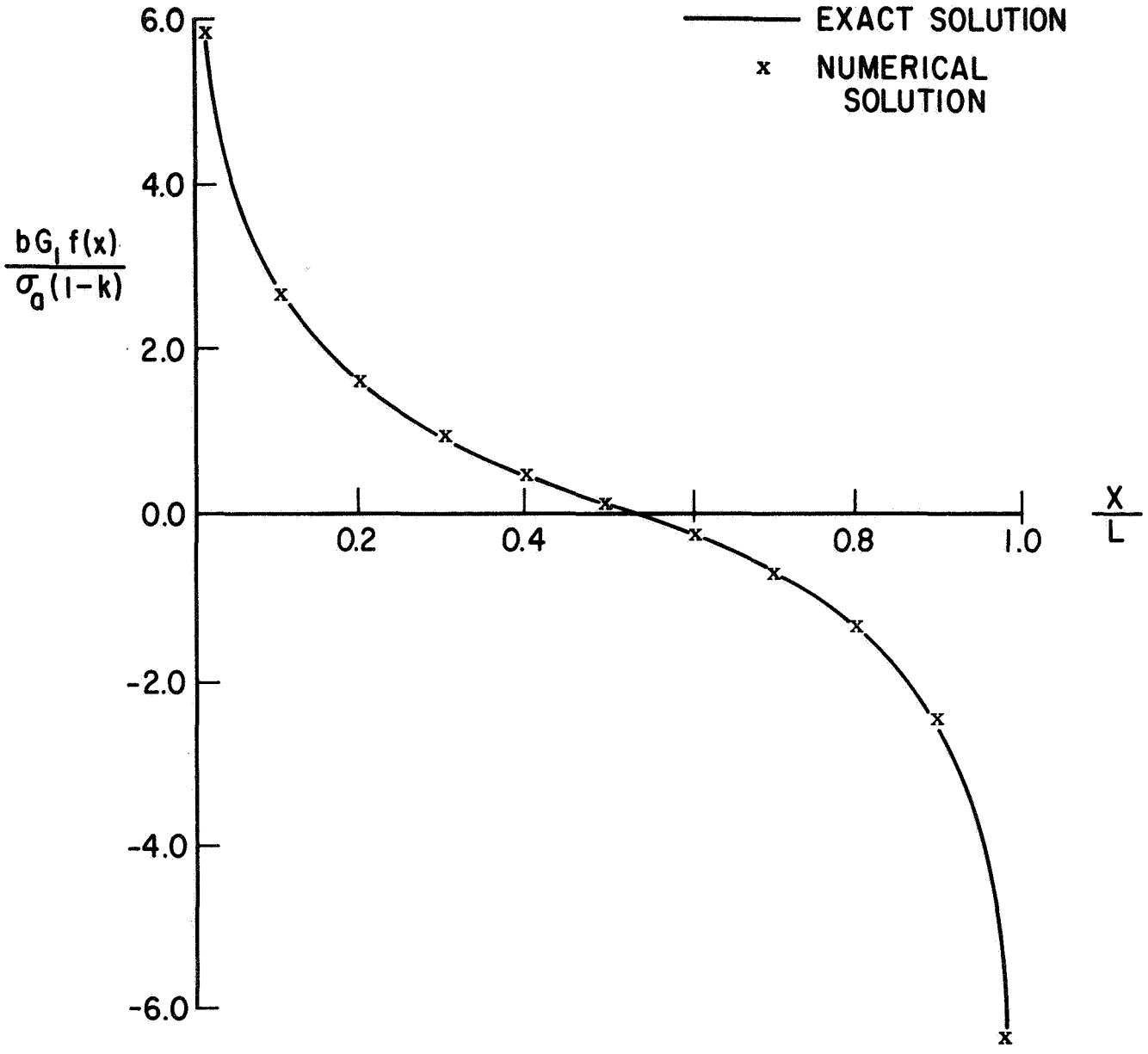

Fig. III-6. A COMPARISON OF THE EXACT AND NUMERICAL SOLUTIONS (k=.4).

$(x,0)$ in the region $(0 < x < 1)$, the crack opening displacement, $\delta(x)$, is defined as:

$$\delta(x) = b\int_0^x f(t)\, dt \ . \qquad \text{(III.3-9)}$$

Figure III-7 depicts the variation of crack opening displacements with the ratio of shear moduli of the two constituent phases. Comparing to the homogeneous case, it is noted that larger elastic relaxation occurs near the interface if phase 2 is softer than phase 1. This consequence is consistent with physical expectation.

Figure III-8 illustrates the variation of crack opening displacements with Poisson's ratios of both phases. The result shows that larger elastic relaxation takes place in material with higher Poisson's ratio.

The stress field at crack tip can easily be found from the dislocation distribution function:

$$\sigma_{ij}(x,y) = \int_0^1 \sigma_{ij}(x,y,t)\, f(t)\, dt \qquad (i,j = 1,2) \qquad \text{(III.3-10)}$$

where $\sigma_{ij}(x,y,t)$ is the stress field due to a single edge dislocation. By plotting the contour lines of stress at the crack tip, the type of stress singularity can be obtained. Zak and Williams [40] have shown the crack point stress singularities at a bi-material interface. They concluded that as phase 1 becomes harder with respect to phase 2, that is,

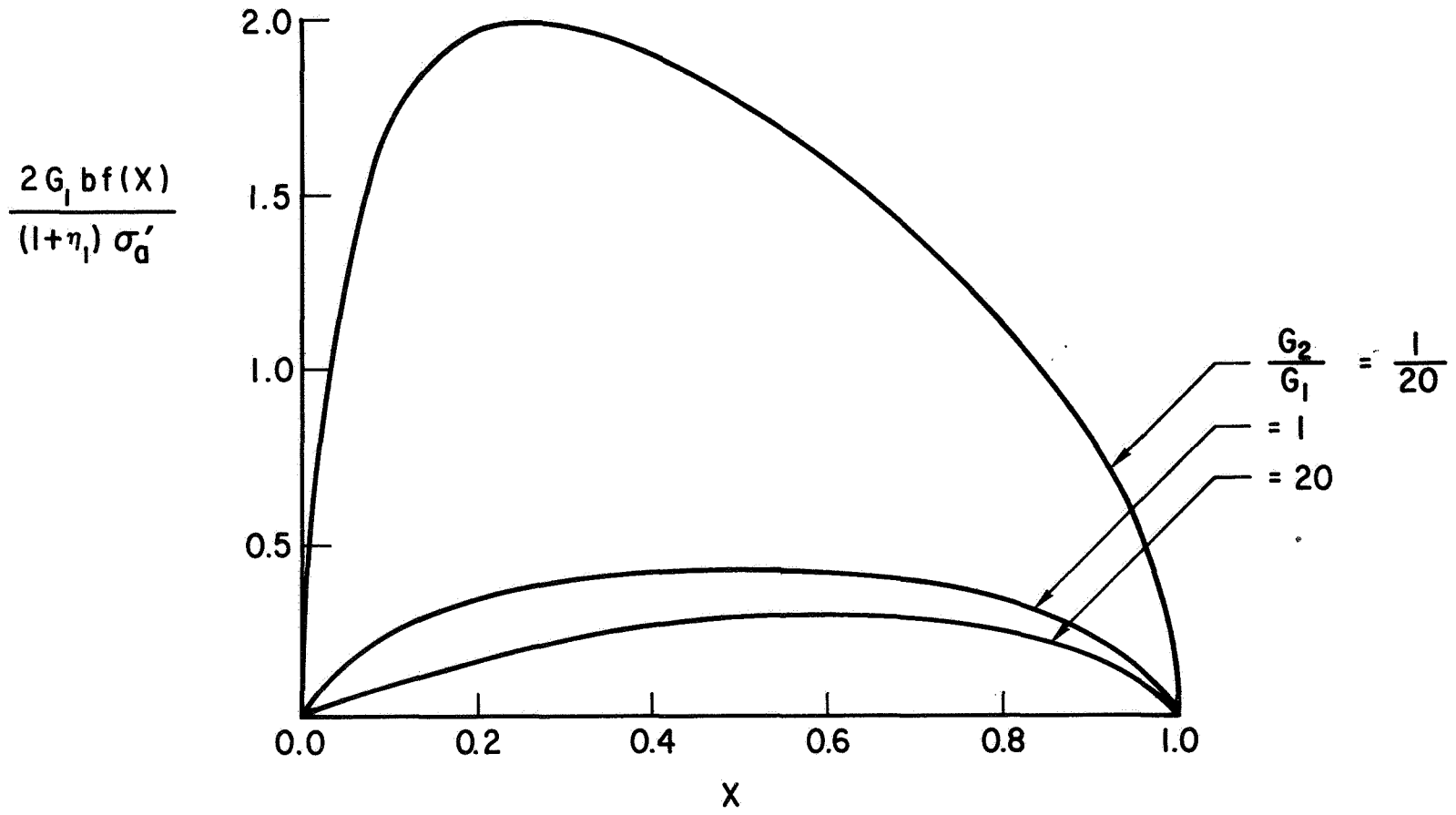

Fig. III-7. VARIATION OF CRACK OPENING DISPLACEMENTS WITH THE RATIO OF SHEAR MODULI OF THE TWO CONSTITUENT PHASES ($\nu_1=\nu_2=1/3$).

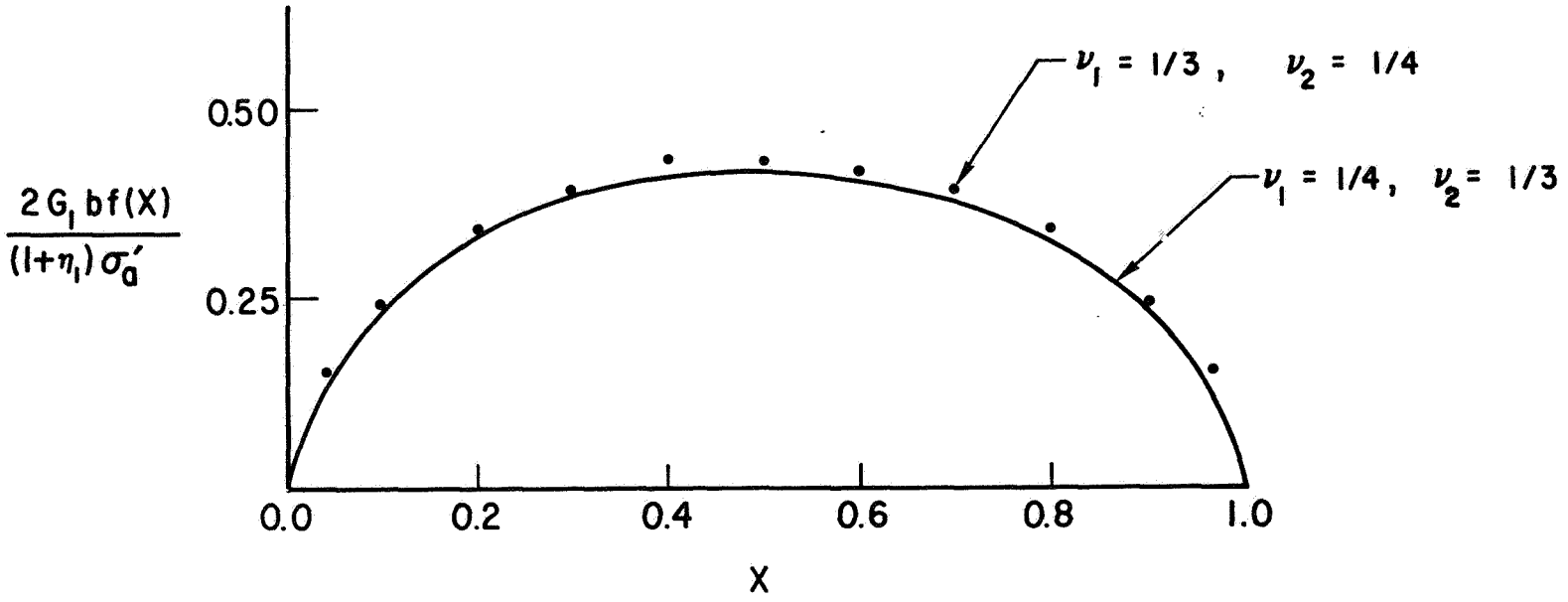

Fig. III-8. VARIATION OF CRACK OPENING DISPLACEMENTS WITH POISSON'S RATIOS OF THE TWO CONSTITUENT PHASES (G_1=G_2).

G_1 is higher than G_2, the strength of singularity increases. In fact, this conclusion can easily be obtained by examining the crack opening configuration in Fig. III-7. It is noted that the larger G_1/G_2 is, the higher is the dislocation density near the interface. This will certainly lead to high stress singularity at the crack tip.

CHAPTER IV

ELASTIC CRACKS CROSSING A BI-MATERIAL INTERFACE

1. Introduction

The general problems of nonhomogeneous media with cracks and slip bands have not yet been attacked. The special cases that have been treated can be grouped into two categories. The first type of problem deals with cracks and dislocation pileups which are limited in one constituent phase of a two-phase system or within one grain in a bicrystal. These have been discussed in the last chapter. The second type of problem deals with two-phase media where the interfaces contain cracks [41-44].

However, the problems involving cracks and slip bands crossing a bicrystal interface or a grain boundary have not yet been discussed in an analytical fashion. This is primarily due to the fact that the associated mixed boundary value problems in such cases are complicated by the unknown boundary conditions at the interface.

In spite of the difficulties involved in the analysis, problems of these kinds are certainly of great practical importance. Examples of these sorts can be seen in transgranular fractures of polycrystaline materials containing brittle inclusion particles, and also for plastic yielding crossing phase boundaries when the slip planes of neighboring grains are appropriately aligned.

It is the aim of this chapter to investigate the problem of cracks and slip bands crossing a boundary. The elastic fields of cracks are replaced by that of an appropriate distribution of dislocations. By obtaining the crack opening displacements, a condition for the extension

of cracks under the applied stress can be reached. Furthermore, the crack tip stress field has been studied in detail.

2. Analysis

Consider a plate composed of two elastic semi-infinite strips welded together at the interface. The coordinate system is chosen to be the same as that depicted in Fig. II-1. The shear modulus is G_1 for $x > 0$ and is G_2 for $x < 0$. Let a crack, crossing the interface, be situated on the plane $y=0$ with tips at $(-1,0)$ and $(1,0)$ (Fig. IV-1). The elastic field of the crack is again represented by that of continuously distributed dislocations.

Just as the case examined in Chapter III, there are three kinds of stresses needed to be considered in discussing the equilibrium configuration of dislocations. These are the dislocation stress, σ_d, the effective stress on dislocations due to an externally applied stress, σ_a, and the friction stress σ_o.

If the thickness of the plate is much larger than the length of the crack, the medium can practically be considered as "infinite." Hence, the stress field of dislocations in an infinite medium can be employed. Consider the right-hand screw dislocations at $(t,0)$ with Burgers vector $\bar{b}_1$ for $t > 0$ and $\bar{b}_2$ for $t < 0$. The non-vanishing stress component σ_{yz} at (x,y) is:

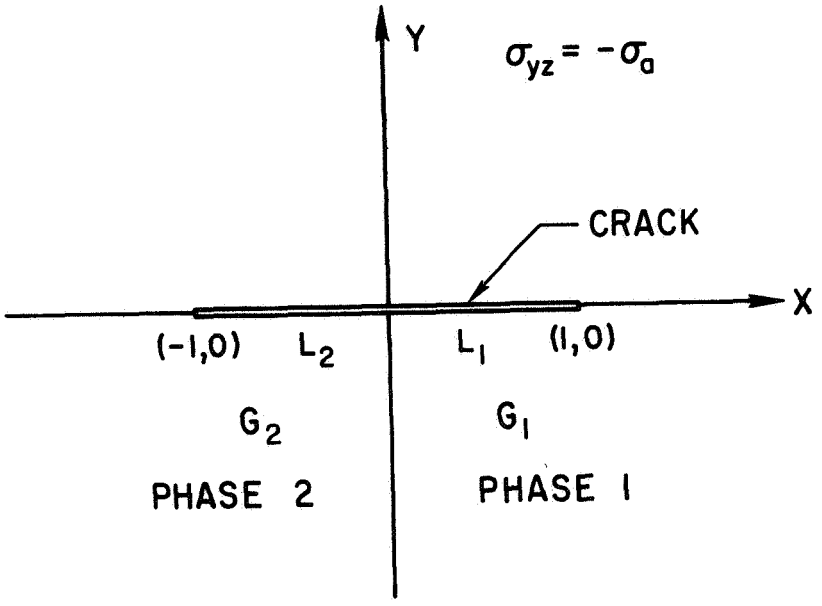

FIG. IV-1. A MODE III CRACK CROSSING A BI-MATERIAL INTERFACE.

(1) $t > 0$

$$\sigma_{yz} = \begin{cases} \dfrac{G_1 b_1}{2\pi} \dfrac{x-t}{(x-t)^2 + y^2} + \dfrac{G_1 b_1}{2\pi} \dfrac{k(x+t)}{(x+t)^2 + y^2} & (x > 0) \\ \dfrac{G_1 b_1}{2\pi} \dfrac{(1+k)(x-t)}{(x-t)^2 + y2} & (x < 0) \end{cases} \qquad \text{(IV.2-1)}$$

(2) $t < 0$

$$\sigma_{yz} = \begin{cases} \dfrac{G_2 b_2}{2\pi} \dfrac{(1-k)(x-t)}{(x-t)^2 + y^2} & (x > 0 \\ \dfrac{G_2 b_2}{2\pi} \dfrac{x - t}{(x-t)^2 + y^2} - \dfrac{G_2 b_2}{2\pi} \dfrac{k(x+t)}{(x+t)^2 + y^2} & \end{cases} \qquad \text{(IV.2-2)}$$

where

$$k = \frac{G_2 - G_1}{G_2 + G_1} .$$

On the middle plane of the plate, $y=0$, the above expressions are simplified as:

(1) $t > 0$

$$\sigma_{yz} = \begin{cases} \dfrac{G_1 b_1}{2\pi} \left(\dfrac{1}{x - t} + \dfrac{k}{x + t} \right) & (x > 0) \\ \dfrac{G_1 b_1}{2\pi} \dfrac{(1+k)}{x - t} & (x < 0) \end{cases} \qquad \text{(IV.2-3)}$$

(2) $t < 0$

$$\sigma_{yz} = \begin{cases} \dfrac{G_2 b_2}{2\pi} \dfrac{1-k}{x-t} & (x > 0) \\ \dfrac{G_2 b_2}{2\pi} \dfrac{1}{x-t} - \dfrac{G_2 b_2}{2\pi} \dfrac{k}{x+t} & (x < 0) \end{cases} . \qquad \text{(IV.2-4)}$$

The effective stress on the middle plane of the plate due to an uniformly applied stress $\sigma_{yz} = -\sigma_a$ is $\sigma_1 = -\sigma_a(1-k)$ for $x > 0$ and $\sigma_2 = -\sigma_a(1+k)$ for $x < 0$ (Chapter II). Inside the crack, the resistance stress to the motion of dislocations vanishes.

Let $f(t)$ be the unknown distribution function of dislocations representing the crack. The regions L_1 and L_2 are defined as $0 \leq x < 1$ and $-1 < x \leq 0$ respectively. The union of L_1 and L_2 is denoted by L. Because of the different expressions of σ_{yz} in L_1 and L_2, the equilibrium of dislocations should be considered separately for both regions. Under the applied stress $\sigma_{yz} = -\sigma_a$, the equilibrium configuration of dislocations is determined by the following set of dual singular integral equations:

$$\left.\begin{aligned} \int_{L_1} \frac{G_1 b_1}{2\pi} \left[\frac{1}{x-t} + \frac{k}{x+t}\right] f(t)\, dt + \int_{L_2} \frac{G_2 b_2}{2\pi} \left[\frac{1-k}{x-t}\right] f(t)\, dt &= \sigma_1 \quad (x \in L_1) \\ \int_{L_1} \frac{G_1 b_1}{2\pi} \left[\frac{1+k}{x-t}\right] f(t)\, dt + \int_{L_2} \frac{G_2 b_2}{2\pi} \left[\frac{1}{x-t} + \frac{-k}{x+t}\right] f(t)\, dt &= \sigma_2 \quad (x \in L_2) . \end{aligned}\right\} \qquad \text{(IV.2-5)}$$

It is noted that only two terms in the above equations are singular and are understood to be Caucy principal value integrals.

In discussing cracks, an additional condition is needed in order to determine the solution completely. This is the compatibility condition of displacement. Derivation of this condition is to be discussed in the following paragraphs.

The z-component of displacement at $(x,0)$ due to a single right-hand screw dislocation at $(t,0)$ is given below:

(1) $t > 0$

$$w(x,y,t) = \begin{cases} w_1(x,y,t) = \frac{b_1}{2\pi}\left[\tan^{-1}\frac{y}{x-t} + k\tan^{-1}\frac{y}{x+t}\right] & (x > 0) \\ w_2(x,y,t) = \frac{b_1}{2\pi}(1-k)\tan^{-1}\frac{y}{x-t} & (x < 0) \end{cases} \qquad \text{(IV.2-6)}$$

(2) $t < 0$

$$w_3(x,y,t) = \frac{b_2}{2\pi}(1+k)\tan^{-1}\frac{y}{x-t} \qquad (x > 0)$$

$$w_4(x,y,t) = \frac{b_2}{2\pi}\left(\tan^{-1}\frac{y}{x-t} - k\tan^{-1}\frac{y}{x+t}\right) \qquad (x < 0)\ . \qquad \text{(IV.2-7)}$$

Consider the closed circuit around the crack (Fig. IV-2). The displacement components along the path are:

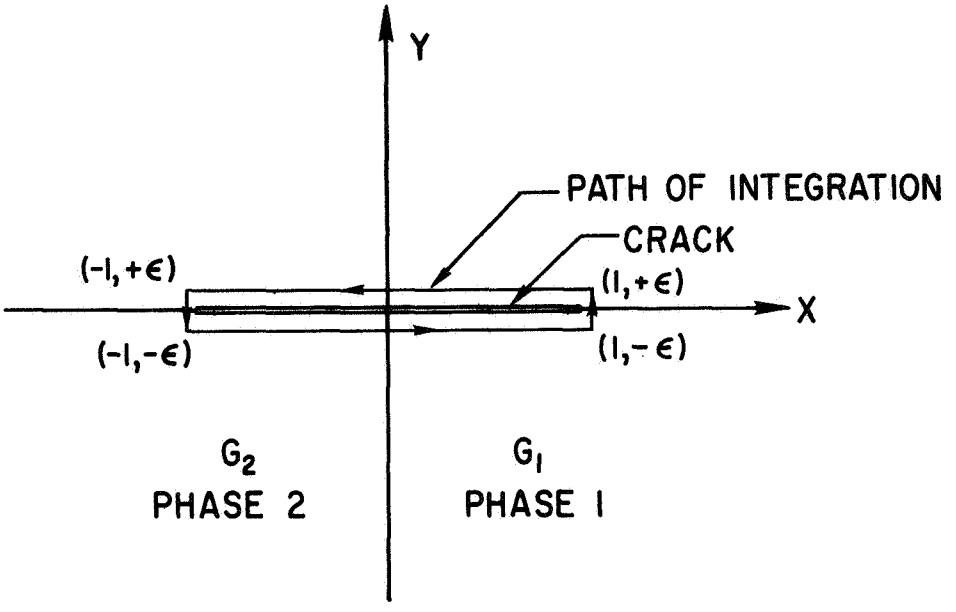

Fig. IV-2. PATH OF INTEGRATION OF DISPLACEMENT.

(1) $x > 0$

$$W_3(x,-\epsilon) = \int_{L_1} w_1(x,-\epsilon,t)\, f(t)\, dt + \int_{L_2} w_3(x,-\epsilon,t)\, f(t)\, dt$$

$$W_4(x,+\epsilon) = \int_{L_1} w_1(x,+\epsilon,t)\, f(t)\, dt + \int_{L_2} w_3(x,+\epsilon,t)\, f(t)\, dt$$

(2) $x < 0$

$$W_1(x,-\epsilon) = \int_{L_1} w_2(x,-\epsilon,t)\, f(t)\, dt + \int_{L_2} w_4(x,-\epsilon,t)\, f(t)\, dt$$

$$W_2(x,+\epsilon) = \int_{L_1} w_2(x,+\epsilon,t)\, f(t)\, dt + \int_{L_2} w_4(x,+\epsilon,t)\, f(t)\, dt \ .$$

Assuming that no dislocation entering nor leaving the crack, the integration of displacement about the closed path should vanish:

$$\int_{-1}^{0} W_1(x,-\epsilon)\, dx + \int_{0}^{1} W_3(x,-\epsilon) + \int_{0}^{1} W_4(x,+\epsilon)\, dx + \int_{0}^{-1} W_2(x,+\epsilon)\, dx$$

$$= 0 \ .$$

In the limiting case where $\epsilon \to 0$, the above equation leads to the condition

$$\int_{L_1} b_1 f(t)\, dt + \int_{L_2} b_2 f(t)\, dt = 0 \ . \qquad \text{(IV.2-8)}$$

Again this condition can most easily be derived from the crack opening displacement consideration.

Equations (IV.2-5) and (IV.2-8) are necessary to determine the solution completely. A method of solving the dual singular integral equations is first discussed. It is then shown how the solution of integral equations can be incorporated with the compatibility condition.

First, a new function is defined as:

$$\phi(t) = \begin{cases} \frac{-i}{2} G_1 b_1 f(t) & (x \in L_1) \\ \\ \frac{-i}{2} G_2 b_2 f(t) & (x \in L_2) \end{cases} \qquad \text{(IV.2-9)}$$

and $f(t)$ can be found if $\phi(t)$ is known. By employing the function $\phi(t)$, the coupled integral equations can be rewritten as:

$$\frac{1}{\pi i} \int_L \frac{\phi(t)\, dt}{t-x} + \frac{1}{\pi i} \int_L \phi(t)\, K(x,t)\, dt = \begin{cases} \sigma_1 & (x \in L_1) \\ \\ \sigma_2 & (x \in L_2) \end{cases} \qquad \text{(IV.2-10)}$$

where

$$K(x,t) = \begin{cases} \frac{-k}{x+t} & (x \in L_1 \ , \ t \in L_1) \\ \\ \frac{k}{x-t} & (x \in L_1 \ , \ t \in L_2) \\ \\ \frac{-k}{x-t} & (x \in L_2 \ , \ t \in L_1) \\ \\ \frac{k}{x+t} & (x \in L_2 \ , \ t \in L_2) \end{cases} \qquad \text{(IV.2-11)}$$

In Eq. (IV.2-10), the singular and non-singular parts of integrals have been separated. The kernel expression $K(x,t)$ is non-singular as can be seen from Eq. (IV.2-11). Further defining:

$$g(x) = -\frac{1}{\pi i}\int_L \phi(t')\,K(x,t')\,dt' + \begin{cases} \sigma_1 & (x \in L_1) \\ \sigma_2 & (x \in L_2)\ , \end{cases} \qquad \text{(IV.2-12)}$$

Equation (IV.2-10) becomes

$$\frac{1}{\pi i}\int_L \frac{\phi(t)\,dt}{t-x} = g(x) \qquad (x \in L)\ . \qquad \text{(IV.2-13)}$$

The physics of the problem requires that $f(x)$, hence $\phi(x)$, is unbounded at the end points of L. If $g(x)$ is considered temporarily to be known, then Eq. (IV.2-13) can be formally inverted according to the procedure outlined in Appendix A. The resulting equation is a Fredholm integral equation of the second kind:

$$\phi(x) = \frac{\sqrt{R_1(x)}}{\pi i\sqrt{R_2(x)}}\int_L \frac{\sqrt{R_2(t)}\,g(t)\,dt}{t-x} + \frac{c}{\sqrt{R_2(x)}} \qquad \text{(IV.2-14)}$$

where $R_1(t) = 1$, $R_2(t) = (t-1)(t+1)$, and c is a constant to be determined otherwise.

By carrying out the integration in Eq. (IV.2-14) and defining

$$\Phi(x) = \begin{cases} \frac{2i}{\sigma_1}\,\phi(x) = \frac{G_1 b_1}{\sigma_1}\,f(x) & (x \in L_1) \\ \frac{2i}{\sigma_2}\,\phi(x) = \frac{G_2 b_2}{\sigma_2}\,f(x) & (x \in L_2) \end{cases} \qquad \text{(IV.2-15)}$$

the above integral equation becomes

$$\Phi(x) = \frac{k}{\pi^2}\int_L K(x,t)\,\Phi(t)\,dt + F_1(x) + cF_2(x) \qquad \text{(IV.2-16)}$$

where

$$K(x,t) = \begin{cases} K_2(x,t) & (-1 < t \leq 0) \\ K_1(x,t) & (0 \leq t < +1) \end{cases} \qquad \text{(IV.2-17)}$$

$$K_1(x,t) = \frac{1}{\sqrt{1-x^2}}\left\{\pi - 2\sum_{n=1}^{\infty}\frac{t}{2n-1}\left[(1-t^2)^{n-1} + (1-t^2)^{n-2}(1-x^2) + \cdots\right.\right.$$

$$\left.\left. + (1-t^2)(1-x^2)^{n-2} + (1-x^2)^{n-1}\right]\right\}$$

$$K_2(x,t) = \frac{1}{\sqrt{1-x^2}}\left\{-\pi - 2\sum_{n=1}^{\infty}\frac{t}{2n-1}\left[(1-t^2)^{n-1} + (1-t^2)^{n-2}(1-x^2) + \cdots\right.\right.$$

$$\left.\left. + (1-t^2)(1-x^2)^{n-2} + (1-x^2)^{n-1}\right]\right\}$$

$$F_1(x) = \frac{-2x}{\sqrt{1-x^2}}$$

$$F_2(x) = \frac{c}{\sqrt{1-x^2}}$$

and

$$c = \begin{cases} \dfrac{2c_1}{\sigma_1} & (x \in L_1) \\ \dfrac{2c_2}{\sigma_2} & (x \in L_2) \end{cases} \qquad \text{(IV.2-18)}$$

The constant c have different expressions in terms of constants c_1 and c_2 in regions L_1 and L_2 respectively. By employing the continuity condition imposed at the interface, however, it can be shown that these two expressions are in fact the same. It has been assumed that at the welded interface the z-component of displacement is continuous. This implies that for the dislocation distribution function we have:

$$b_1 f(0^+) = b_2 f(0^-) \ , \qquad \text{(IV.2-19)}$$

namely,

$$\Phi(0^+) - \Phi(0^-) = 0 \ . \qquad \text{(IV.2-20)}$$

Substituting the values of $\Phi(0^+)$ and $\Phi(0^-)$ from Eq. (IV.2-16) into the above relationship, we obtain

$$c = \frac{2c_1}{\sigma_1} = \frac{2c_2}{\sigma_2} \qquad (-1 < x < 1) \qquad \text{(IV.2-21)}$$

When k approaches zero, the medium becoming homogeneous, the expression of (IV.2-16) check with the solution of cracks in homogeneous materials.

Equations (IV.2-8), (IV.2-16) and (IV.2-21) are sufficient for the determination of $f(x)$ and the constant c. By using the constant value of c from Eq. (IV.2-16), the Fredholm integral equation of (IV.2-8) can be written for the whole region L as:

$$\Phi(x) = \frac{k}{\pi^2} \int_L K(x,t)\, \Phi(t)\, dt + F_1(x) + cF_2(x) \qquad (x \in L) \,. \tag{IV.2-21}$$

To incorporate this equation with the compatibility condition, $\Phi(x)$ is considered to be a linear combination of two functions:

$$\Phi(x) = \Phi_1(x) + c\Phi_2(x) \tag{IV.2-22}$$

where

$$\Phi_1(x) = \frac{k}{\pi^2} \int_L K(x,t)\, \Phi_1(t)\, dt + F_1(x) \tag{IV.2-23}$$

and

$$\Phi_2(x) = \frac{k}{\pi^2} \int_L K(x,t)\, \Phi_2(t)\, dt + F_2(x) \,. \tag{IV.2-24}$$

$\Phi_1(x)$ and $\Phi_2(x)$ have to be solved separately. Substituting the known values of $\Phi_1(x)$ and $\Phi_2(x)$ into Eq. (IV.2-8), the constant c can be obtained and Eq. (IV.2-22) gives the complete solution.

A method of solving Eqs. (IV.2-23) and (IV.2-24) is now outlined as following. As noted in Eq. (IV.2-17), the kernel of the Fredholm integral

equation is degenerate. In principle, the infinite series expression of the kernel can be truncated and the integral equation with degenerate kernel can be solved analytically. However, because of the different expressions of the kernel in L_1 and L_2, this process can be very tedious. Instead, a direct procedure as outlined in Appendix C is employed. The definite integral on the right-hand side of Eq. (IV.2-16) is first approximated by a quadrature formula. Then the integral equation is transformed into a system of linear algebraic equations. The number of equations is equal to the number of subdivisions, n, in L. The system of linear equations can then be solved numerically.

In the process of approximating the integral portions in Eqs. (IV.-2-23) and (IV.2-24) by quadrature formulas, the Simpson's rule has been used. This approximation is pretty accurate and dependable. It is due to the fact that the integrands in the above equations are well behaved polynomials.

In the present analysis, numerical solution of the Fredholm integral equations have been carried out for n=102. Solution for the plate under uniform strain ϵ_a can be obtained simply by defining $\sigma_1 = G_1\epsilon_a$ and $\sigma_2 = G_2\epsilon_a$ in the formulation.

Figure IV-3 shows the dislocation distribution function for cracks under both uniform strain and stress. It is obvious from Fig. IV-3 that the distribution function is discontinuous at the interface if the lattice parameters of the two media are different.

Before leaving this section, it is worthwhile to examine the behavior of the distribution function at both ends of the crack. From

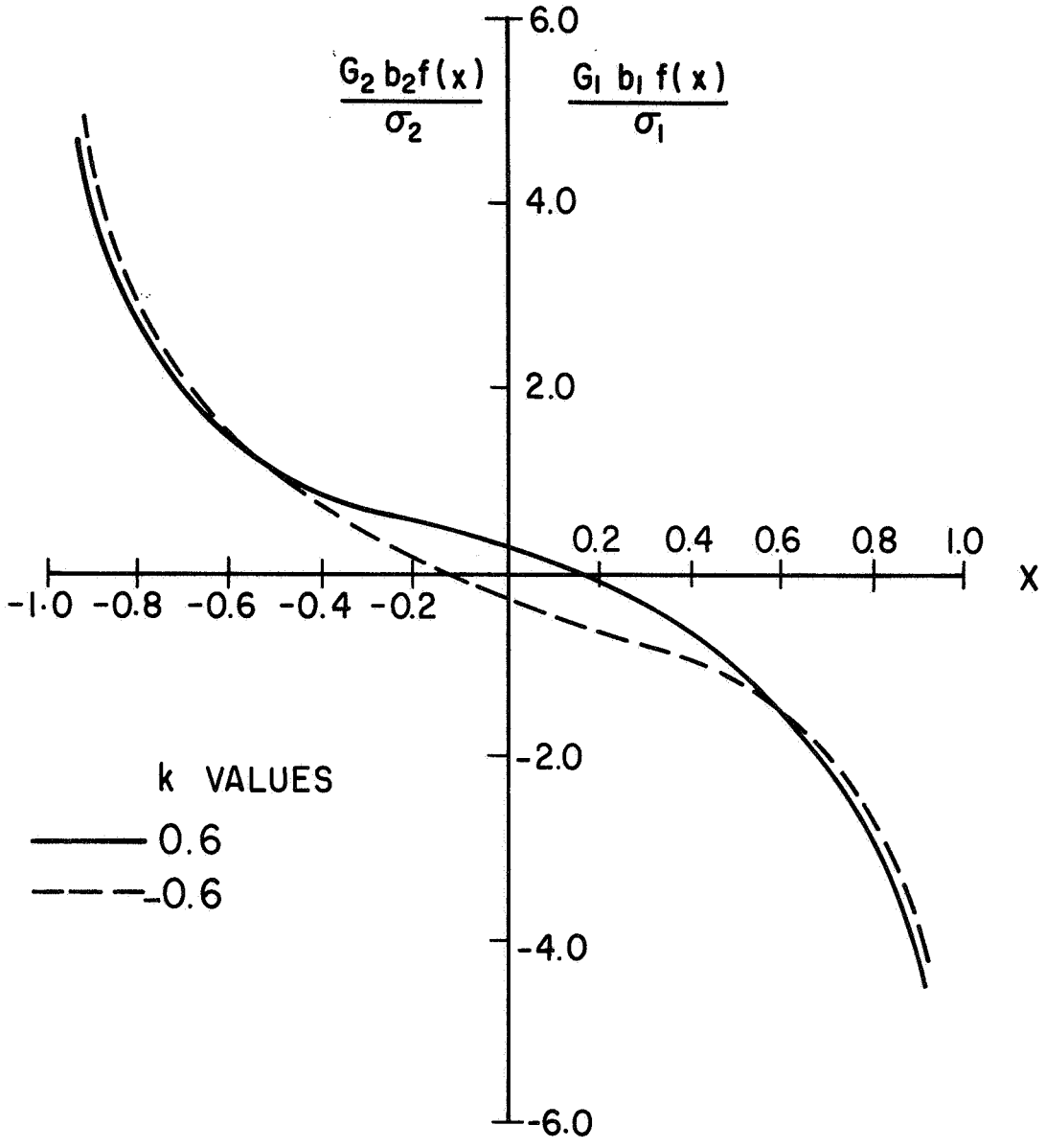

Fig. IV-3. DISTRIBUTION FUNCTIONS OF DISLOCATIONS REPRESENTING CRACKS CROSSING A PHASE BOUNDARY.

Eq. (IV.2-17) we notice that the function $\Phi(x)$, hence $f(x)$, varies with the inverse square root of the distances from the crack tips as x approaches ± 1. This can also be shown readily by plotting $\Phi(x)$ as functions of the distances from the crack tips (Fig. IV-4).

As a consequence, we can write

$$\Phi(r) = Ar^{-\frac{1}{2}} \qquad \text{(IV.2-25)}$$

for the crack tip $(1,0)$ and

$$\Phi(r) = Br^{-\frac{1}{2}} \qquad \text{(IV.2-26)}$$

for the crack tip $(-1,0)$. In the above equations, r denotes the distances from the crack tips. The constants A and B can immediately be obtained from Fig. IV-4.

Moreover, in applying Eq. (IV.2-8) to the functions $\Phi_1(x)$ and $\Phi_2(x)$, numerical integrations have been performed. To circumvent the singularities of the functions at $x = \pm 1$, the ranges of L_1 and L_2 used are $0 \leq x \leq 0.999$ and $-0.999 \leq x \leq 0$ respectively. The contributions of the portions of $\Phi_1(x)$ and $\Phi_2(x)$ neglected are now investigated. At the crack tips the function $\Phi_1(r)$ behaves as in Eqs. (IV.2-25) and (IV.2-26). Constants A and B are obtained from plots of $\ell n\, \Phi_1(r)$ vs. $\ell n\, r$ at both crack tips. Similar expressions are valid for $\Phi_2(r)$. By carrying out the integration of Eq. (IV.2-8) for $-1 < x \leq -0.999$ and $0.999 \leq x < 1$, it is found that the error involved is negligibly small.

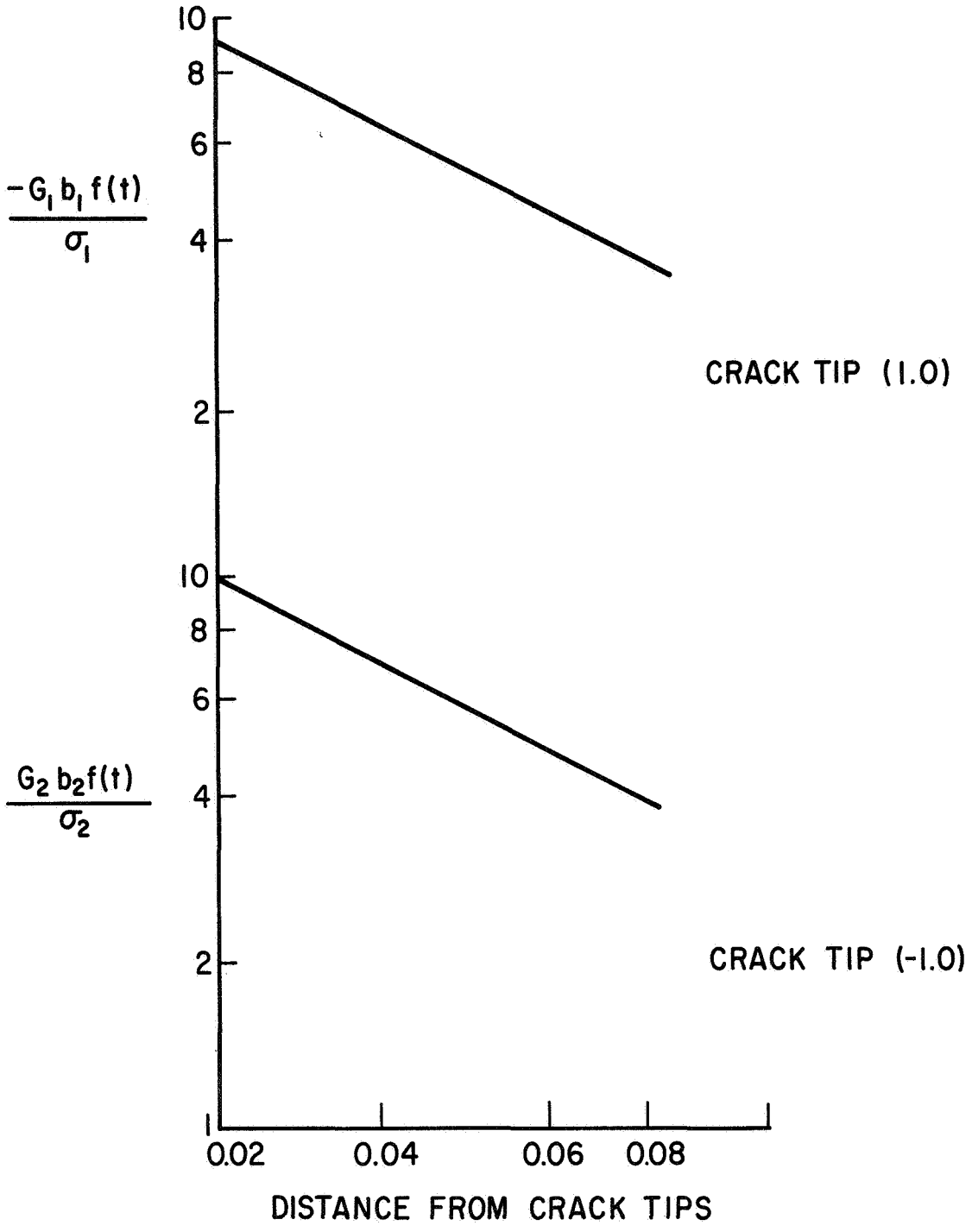

Fig. IV-4. DISTRIBUTION FUNCTION-DISTANCE RELATIONSHIP AT THE CRACK TIP (k=-.4).

3. Crack Opening Displacement

The crack opening displacement $\delta(x)$ can readily be obtained by integrating the dislocation distribution function:

$$\delta(x) = \frac{2\sigma_a}{G_1 + G_2} \int_{-1}^{x} \Phi(t)\, dt \ . \qquad \text{(IV.3-1)}$$

Although the dislocation density can be discontinuous at $x = 0$, the crack opening displacement is a continuous function in the entire region of L.

Numerical results of crack opening displacements are shown in Fig. IV-5. The validity of the solutions can be readily checked by the symmetry of curves, for $k = .4$ and $k = -.4$. The broken line in the middle shows the crack opening displacement in a homogeneous medium. By comparing these curves, it is noted that larger elastic relaxation takes place in the comparatively softer phase. However, the deviation from the solution for a homogeneous medium is small.

Again, by employing the argument similar to that in the last section, the error involved in the numerical integration of Eq. (IV.3-1) can be estimated.

The behavior of the crack opening displacements $\delta(x)$, near crack tips can easily be determined. From the last section we have learned that $\Phi(t)$ near crack tips varies with the inverse square root of the distances from the tips. Since crack opening displacements are derived from the integration of $\Phi(t)$, it is legitimate to conclude that close to the crack tip, $\delta(x)$ varies with the square root of the distances from crack tips.

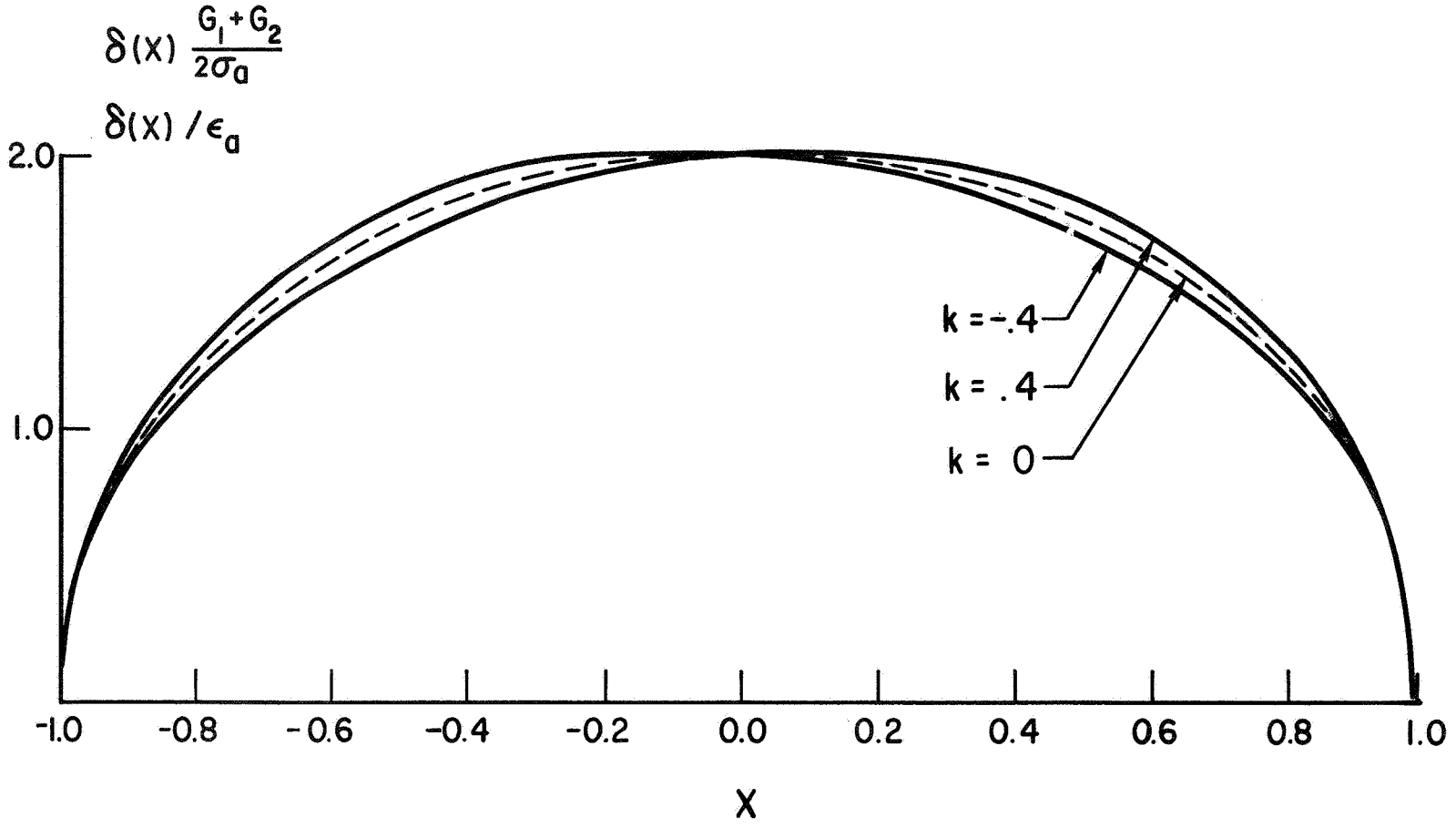

Fig. IV-5. CRACK OPENING DISPLACEMENTS FOR CRACKS CROSSING A PHASE BOUNDARY.

4. Stress Fields at the Crack Tips

It is known that for cracks imbeded in homogeneous media, displacements at the crack tips have the general expression [41]:

$$W = \frac{K_{III}}{G}\left[\frac{2r}{\pi}\right]^{1/2} \sin\frac{\theta}{2} \qquad \text{(IV.3-2)}$$

where r is the distance from the crack tip and θ is the angle made with the x-axis about the crack tip. K_{III} is the stress intensity factor. At the crack surface, $\theta = \pi$,

$$W = \frac{K_{III}}{G}\left[\frac{2r}{\pi}\right]^{1/2} . \qquad \text{(IV.3-3)}$$

It is noted from the above equation that in a homogeneous medium the crack opening displacement varies with the square root of the distance from the crack tip. This in turn implies that for crack crossing a bimaterial interface the stress singularity at the immediate vicinity of the crack tip behaves as if the crack were imbeded in a homogeneous medium.

Hence, the stress expression at the tip of a crack in a homogeneous medium can be employed for our problem:

$$\sigma_{xz} = \frac{-K_{III}}{(2\pi r)^{1/2}} \sin\frac{\theta}{2}$$

$$\sigma_{yz} = \frac{K_{III}}{(2\pi r)^{1/2}} \cos\frac{\theta}{2} \qquad \text{(IV.3-4)}$$

where θ is measured from the x-axis. The stress intensity factor, K_{III}, has different values at the two crack tips, and these values can be determined by Eq. (IV.3-3) combined with the data of Fig. IV-4.

Although the types of stress singularities are the same at both crack tips, the strength of these singularities can be different. It is found that when $k = -.4$, the magnitude of the stress intensity factor, K_{III}, at the crack tip $(1,0)$ is about twice of that at the tip $(-1,0)$. This leads us to the following conclusion: for a crack lying across a phase boundary, the stress concentration near the crack tip in the comparatively harder phase is higher than that in the softer phase.

5. Discussion

The solution of the present problem can also be achieved by employing the method of linear elasticity theory. Boundary value problems can be set up for both regions, for $x > 0$ and $x < 0$ (Fig. IV-6). It is required that σ_{zx} and the z-component of displacement, W, be continuous at the interface.

The problem is complicated by the fact that both σ_{zx} and W are unknown on the boundary $x = 0$. Moreover, the boundary conditions on $y=0$ are mixed. It is suggested that both σ_{zx} and W can be assumed in the form of Fourier series. By taking a sine transform on the variable x of the Laplace equation and applying the boundary conditions on $y=0$, one obtains a set of dual integral equations in each region. These two sets of dual integral equations should be solved separately for W while the continuity of σ_{zx} at the interface is also satisfied.

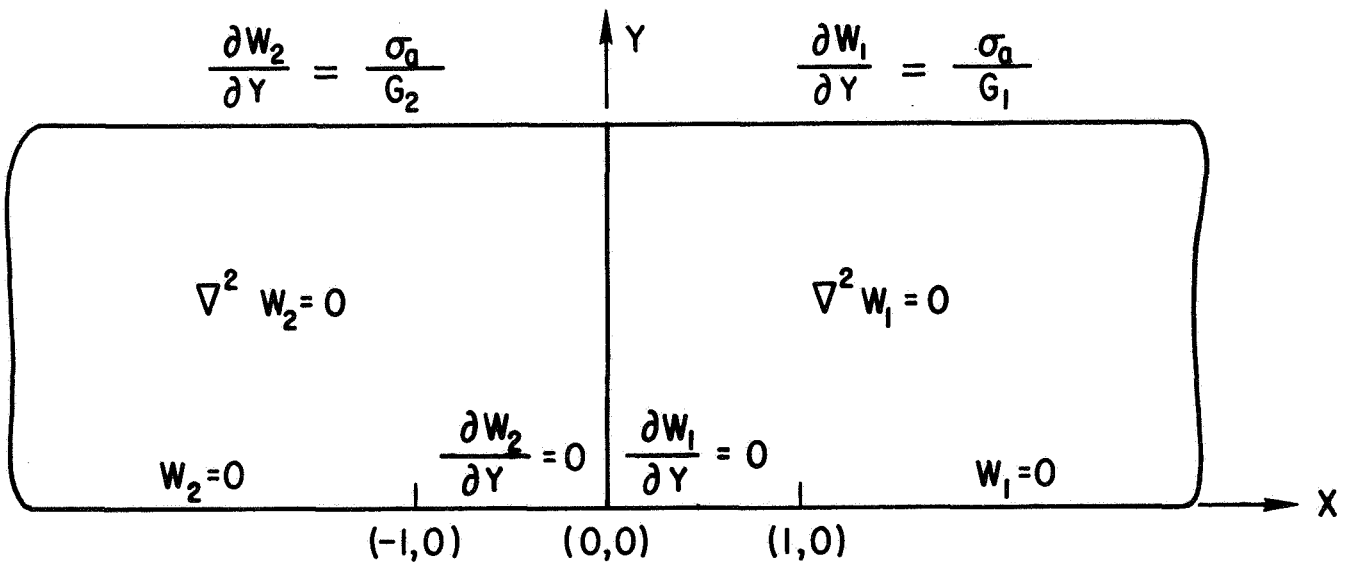

AT $X = 0$ $\quad W_1 = W_2$

$$G_1 \frac{\partial W_1}{\partial X} = G_2 \frac{\partial W_2}{\partial X}$$

Fig. IV-6. THE BOUNDARY VALUE PROBLEM.

The difficulty in solving this problem by elasticity theory is due to the unknown boundary conditions at $x=0$. However, this difficulty is circumvented in the present analysis. Using the stress field of screw dislocations in a two phase medium, the continuity conditions at the interface have already been built in the stress expressions. Furthermore, since dislocation distributions in both phases are treated as one unknown function only one set of dual integral equations has to be considered.

The dislocations representing the crack can also be viewed as dislocations on a slip band crossing a grain boundary. This can be justified simply by specifying an appropriate resistance stress to the motion of dislocations on the slip band. Hence, the mathematical procedure employed in the present analysis is equivalent to that of solving a dislocation pileup problem. The only term needed to be changed in Eq. (IV.2-5) is the term of externally applied stresses.

Finally, a crucial point in the derivation of Eqs. (IV.2-8) and (IV.2-20) needs to be pointed out. It is noted that in deriving both equations, the effective stress expressions of both phases have been employed. The implication is two-fold.

First, if the stress on the middle plane of the plate, due to some internal sources, is other than σ_1 for $x > 0$ and σ_2 for $x < 0$, Eq. (IV.2-8) will not hold. This implies that dislocations have to enter or leave the crack in order to reach equilibrium. Secondary, any discontinuity of displacement at the interface should be taken into account in the formulation of the problem. This can be done by setting $b_1 f(0^+) - b_2 f(0^-)$ equal to the magnitude of this discontinuity.

CHAPTER V

AN ELASTIC-PLASTIC CRACK IN A TWO-PHASE SYSTEM

1. Introduction

The matrix phase in a composite material serves several important functions [1]. It binds the hard particles together to protect their surfaces from flaws and transfers both local and nominal stresses to the hard phase. The matrix should be inherently notch-tough, so that cracks initiated at the brittle phase will be blunted when they reach the soft matrix.

Blunting of crack tips can be caused by either the splitting of interface or the plastic relaxation in the matrix. Typical observations in these respects can be found in the work of Cooper and Kelley [45]. They have studied how a material reinforced with aligned fibers fails at the root of a notch by the propagation of transverse cracks. The composite examined consists of brittle tungsten wires in vacuum-cast copper with very strong interfacial bonding. This system constitutes an extreme combination of brittle and ductile phases. A representative series of micrographs are shown in Fig. V-1.

It is noted that the ductile matrix phase has been plastically deformed at the crack tip. The plastic strain concentrated at the crack tips will cause subsequent failure of the matrix phase. As a consequence of these experimental observations, we are led to believe that a realistic discussion of problems concerning crack propagation in most metal-matrix composites should consider both the elastic and plastic behavior of constituent phases.

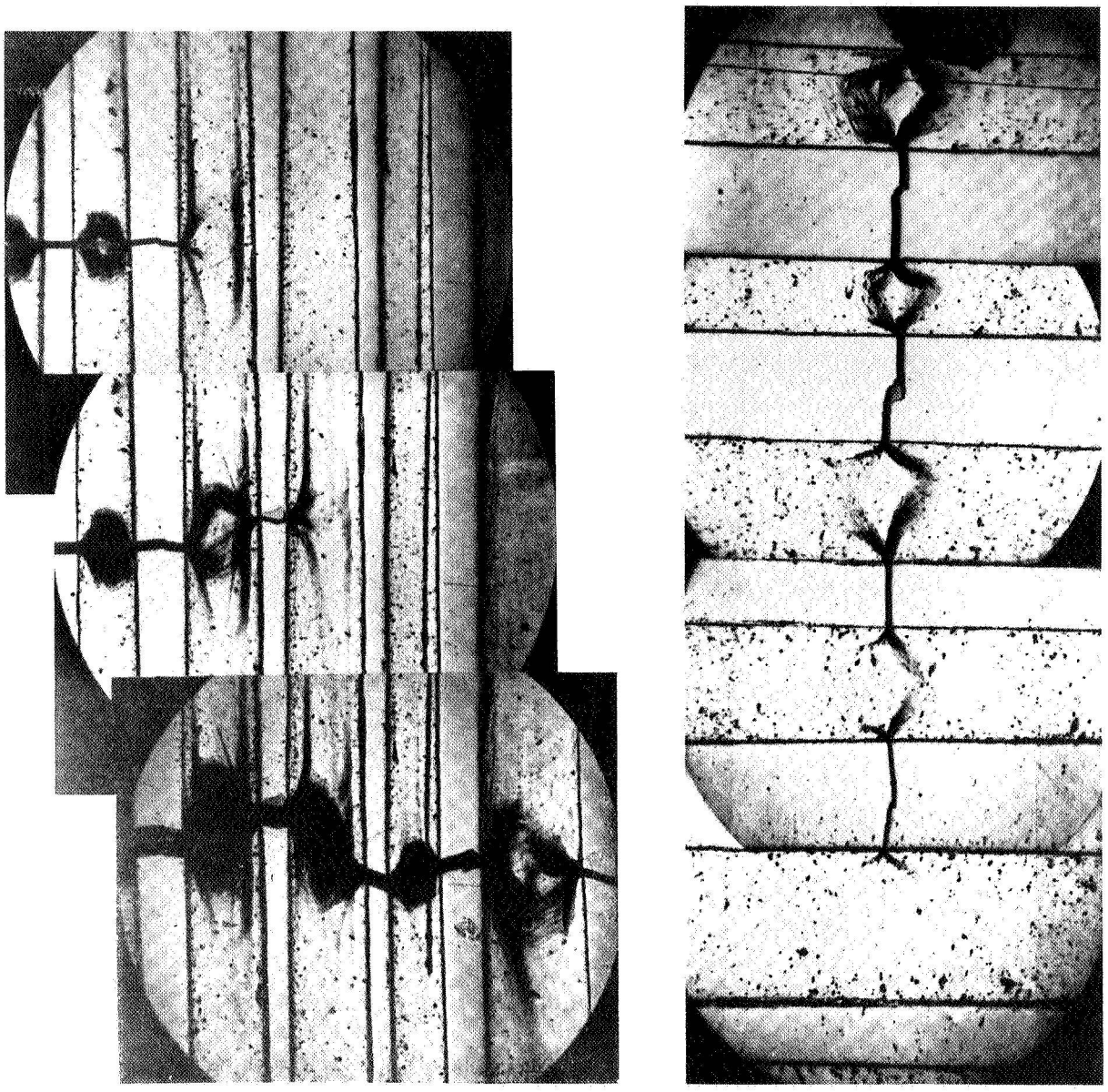

Fig. V-1. PROGRESSIVE SLOW ADVANCE OF THE CRACK. The three micrographs on the left were taken in the order top, middle, bottom showing growth of the crack. x20. [45]

In this chapter an idealized model of a mode III elastic-plastic crack in a two-phase medium has been set up. Relation between the applied stress and the length of plastic zone has been found for various ratios of rigidities. By employing the critical crack opening displacement criteria for fracture, the fracture load can be determined.

2. Analysis

Consider a plate composed of two elastic semi-infinite strips welded together at the interface. The shear modulus is G_1 for $x > 0$ and is G_2 for $x < 0$. Let a crack in phase 1 be situated on the plane $y=0$ and perpendicular to the interface. To simulate the crack in laminar structures, the crack length is considered to be fixed and equal to unity. If phase 2 is much softer than phase 1, it is a valid assumption that the length of plastic zone ahead of the crack in the hard phase is much smaller than that in the soft phase and hence can be neglected. The length of plastic zone in phase 2 is set equal to b which varies with the applied stress (Fig. V-2). It has been pointed out in Chapter I that the associated displacements of both cracks and slips band are similar to those of dislocations. Consequently, linear elasticity can again be employed in the present analysis by representing the non-linear region as a packet of continuous dislocations.

There are three kinds of stresses needed to be considered in discussing the equilibrium configuration of dislocations. These are the dislocation stress, σ_d, the effective stress on dislocations due to an externally applied stress, σ_a, and the friction stress σ_o.

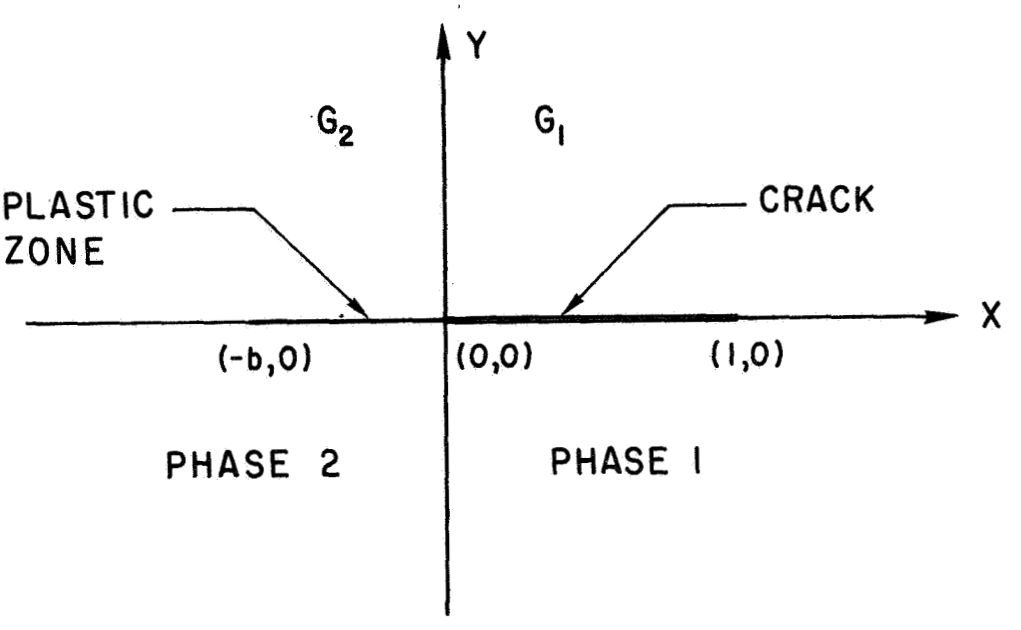

Fig. V-2. AN ELASTIC-PLASTIC CRACK.

If the thickness of the plate is much larger than the length of the crack, the medium can practically be considered as "infinite." Hence, the stress field of dislocations in an infinite medium can be employed. Consider right-hand screw dislocations at $(t,0)$ with Burgers vector $\bar{b}_1$ for $t > 0$ and $\bar{b}_2$ for $t < 0$. The non-vanishing stress component σ_{yz} at $(x,0)$ is:

(1) $t > 0$

$$\sigma_{yz} = \begin{cases} \frac{G_1 b_1}{2\pi} \left(\frac{1}{x - t} + \frac{k}{x + t} \right) & (x > 0) \\ \frac{G_1 b_1}{2\pi} \frac{1 + k}{x - t} & (x < 0) \end{cases} \qquad \text{(V.2-1)}$$

(2) $t < 0$

$$\sigma_{yz} = \begin{cases} \frac{G_2 b_2}{2\pi} \frac{1 - k}{x - t} & (x > 0) \\ \frac{G_2 b_2}{2\pi} \left(\frac{1}{x - t} - \frac{k}{x + t} \right) . & (x < 0) \end{cases} \qquad \text{(V.2-2)}$$

The effective stress on the middle plane of the plate due to an uniformly applied stress $\sigma_{yz} = -\sigma_a$ is $\sigma_1 = -\sigma_a(1-k)$, for $x > 0$ and $\sigma_2 = -\sigma_a(1+k)$, for $x < 0$ (Chapter II). The resistence stress to the motion of dislocations, σ_o, vanishes inside the crack region and is set equal to the yield stress of the material in the second phase. The medium is also assumed to behave perfectly-plastic.

The pastic relaxation at the crack tip is assumed to be caused totally by the injection of dislocations from the crack tip into the slip lines. Relaxation due to absorption of opposite sign dislocations to the crack tip is not considered in the present analysis.

Let $f(t)$ be the unknown distribution function of dislocations representing the crack. The regions L_1 and L_2 are defined as $0 \leq x < 1$ and $-b \leq x \leq 0$ respectively. The union of L_1 and L_2 is denoted by L. Because of the different expressions of σ_{yz} in L_1 and L_2, the equilibrium of dislocations should be considered separately for both regions. Under the applied stress $\sigma_{yz} = -\sigma_a$, the equilibrium configuration of dislocations is determined by the following set of dual singular integral equations:

$$\left.\begin{aligned} \int_{L_1} \frac{G_1 b_1}{2\pi}\left[\frac{1}{x-t} + \frac{k}{x+t}\right] f(t)\,dt + \int_{L_2} \frac{G_2 b_2}{2\pi}\left[\frac{1-k}{x-t}\right] f(t)\,dt &= \sigma_1 \\ & (x \in L_1) \\ \int_{L_1} \frac{G_1 b_1}{2\pi}\left[\frac{1+k}{x-t}\right] f(t)\,dt + \int_{L_2} \frac{G_2 b_2}{2\pi}\left[\frac{1}{x-t} + \frac{-k}{x+t}\right] f(t)\,dt &= \sigma_2 - \sigma_o \\ & (x \in L_2). \end{aligned}\right\} \quad \text{(V.2-3)}$$

It is noted that only two terms in the above equations are singular and are understood to be Cauchy principal value integrals.

Since it has been assumed that plastic relaxation is not due to the absorbtion of dislocations, there is no dislocation leaving nor entering the region L. As a consequence, the compatibility condition, Eq. (IV.2-8), derived in the last chapter is still valid in this case:

$$\int_{L_1} b_1 f(t)\, dt + \int_{L_2} b_2 f(t)\, dt = 0 \,. \qquad \text{(V.2-4)}$$

Equations (V.2-3) and (V.2-4) are sufficient to determine the solution completely. A method of solving the dual singular integral equations is first discussed. It is then shown how the solution of integral equations has to be incorporated with the compatibility condition in order to find the magnitude of the applied stress under which the plastic zones is extended to a length b.

First, a new function is defined as:

$$\phi(t) = \begin{cases} \frac{-i}{2} G_1 b_1 f(t) & (x \in L_1) \\ \\ \frac{-i}{2} G_2 b_2 f(t) & (x \in L_2) \end{cases} \qquad \text{(V.2-5)}$$

and $f(t)$ can be found if $\phi(t)$ is known. By employing the function $\phi(t)$, the left-hand side of the coupled singular integral equations can be rewritten as:

$$\frac{1}{\pi i}\int_L \frac{\phi(t)\, dt}{t - x} + \frac{1}{\pi i}\int_L \phi(t)\, K(x,t)\, dt = \begin{cases} \sigma_1 & (x \in L_1) \\ \\ \sigma_2 - \sigma_o & (x \in L_2) \end{cases} \qquad \text{(V.2-6)}$$

where

$$K(x,t) = \begin{cases} \dfrac{-k}{x + t} & (x \in L_1 , \quad t \in L_1) \\ \dfrac{k}{x - t} & (x \in L_1 , \quad t \in L_2) \\ \dfrac{-k}{x - t} & (x \in L_2 , \quad t \in L_1) \\ \dfrac{k}{x + t} & (x \in L_2 , \quad t \in L_2) \end{cases} \tag{V.2-7}$$

and

$$k = \frac{G_2 - G_1}{G_2 + G_1} \quad .$$

In Eq. (V.2-6), the singular and non-singular parts of integrals have been separated. The kernel expression $K(x,t)$ is non-singular as can be seen from Eq. (V.2-7). Further defining:

$$g(x) = \frac{-1}{\pi i} \int_L \phi(t') \, K(x,t') \, dt' + \begin{cases} \sigma_1 & (x \in L_1) \\ \sigma_2 - \sigma_o & (x \in L_2) \end{cases} , \tag{V.2-8}$$

Eq. (V.2-8) becomes:

$$\frac{1}{\pi i} \int_L \frac{\phi(t) \, dt}{t - x} = g(x) \qquad (x \in L) \quad . \tag{V.2-9}$$

The physics of the problem requires that $f(t)$, hence $\phi(t)$, be bounded at $(-a,0)$ and unbounded at $(1,0)$. If $g(x)$ is considered temporarily to be known, then Eq. (V.2-9) can be formally inverted according to the procedure outlined in Appendix A. The resulting equation is a Fredholm integral equation of the second kind:

$$\phi(x) = \frac{\sqrt{R_1(x)}}{\pi i \sqrt{R_2(x)}} \int_L \sqrt{\frac{R_2(t)}{R_1(t)}} \frac{g(t)}{t - x} dt \qquad \text{(V.2-10)}$$

where $R_1(t) = t + b$ and $R_2(t) = t - 1$.

The kernel of Eq. (V.2-10) is very complicated since it involves principal value integrals. The integration has been carried out for different ranges of plastic zone length, b. The resulting form of integral equations are summarized in the following:

(1) $b < 1$

$$\Phi(x) = \frac{2i}{\sigma_a}\,\phi(x) = \begin{cases} \dfrac{G_1 b_1}{\sigma_a}\, f(x) & (x \in L_1) \\ \dfrac{G_2 b_2}{\sigma_a}\, f(x) & (x \in L_2) \end{cases}$$

$$= \frac{k}{\pi^2}\int_L \Phi(t)\, K(x,t)\, dt + F_1(x) + c_1 F_2(x) \qquad \text{(V.2-11)}$$

where

$$K(x,t) = \begin{cases} K_1(x,t) & (0 \le t \le b) \\ K_2(x,t) & (b \le t < 1) \\ K_3(x,t) & (-b \le t \le 0) \end{cases} \qquad \text{(V.2-12)}$$

$$K_1(x,t) = \frac{1}{x+t}\left[\ell n(b+1)\left(\sqrt{\frac{1-x}{b+x}} - \sqrt{\frac{1+t}{b-t}}\right) - \sqrt{\frac{1-x}{b+x}}\ \ell n\ \frac{\left[\sqrt{b+x} + \sqrt{b(1-x)}\right]^2}{|x|}\right.$$

$$\left. + \sqrt{\frac{1+t}{b-t}}\ \ell n\ \frac{\left[\sqrt{b-t} + \sqrt{b(1+t)}\right]^2}{|t|}\right]\sqrt{\frac{x+b}{1-x}}$$

$$+ \frac{1}{x-t}\left[\ell n(b+1)\left(\sqrt{\frac{1-t}{b+t}} - \sqrt{\frac{1-x}{b+x}}\right) + \sqrt{\frac{1-x}{b+x}}\ \ell n\ \frac{\left[\sqrt{b+x} + \sqrt{b(1-x)}\right]^2}{|x|}\right.$$

$$\left. - \sqrt{\frac{1-t}{b+t}}\ \ell n\ \frac{\left[\sqrt{b+t} + \sqrt{b(1-t)}\right]^2}{|t|}\right]\sqrt{\frac{x+b}{1-x}}$$

$$K_2(x,t) = \frac{1}{x+t}\left[\sqrt{\frac{1+t}{t-b}}\left(\frac{\pi}{2} - \sin^{-1}\frac{2b - t + bt}{t(1+b)}\right)\right.$$

$$\left. + \sqrt{\frac{1-x}{b+x}}\left(\ell n(b+1) - \ell n\ \frac{\left[\sqrt{b+x} + \sqrt{b(1-x)}\right]^2}{|x|}\right)\right]\sqrt{\frac{x+b}{1-x}}$$

$$+\frac{1}{x-t}\left[\ell n(b+1)\left(\sqrt{\frac{1-t}{b+t}}-\sqrt{\frac{1-x}{b+x}}\right)+\sqrt{\frac{1-x}{b+x}}\ \ell n\ \frac{\left[\sqrt{b+x}+\sqrt{b(1-x)}\right]^2}{|x|}\right.$$

$$\left.-\sqrt{\frac{1-t}{b+t}}\ \ell n\ \frac{\left[\sqrt{b+t}+\sqrt{b(1-t)}\right]^2}{|t|}\right]\sqrt{\frac{x+b}{1-x}}$$

$$K_3(x,t)=\frac{1}{t-x}\left[\ell n(b+1)\left(\sqrt{\frac{1-x}{b+x}}-\sqrt{\frac{1-t}{b+t}}\right)+\sqrt{\frac{1-t}{b+t}}\ \ell n\ \frac{\left[\sqrt{b+t}+\sqrt{b(1-t)}\right]^2}{|t|}\right.$$

$$\left.-\sqrt{\frac{1-x}{b+x}}\ \ell n\ \frac{\left[\sqrt{b+x}+\sqrt{b(1-x)}\right]^2}{|x|}\right]\sqrt{\frac{x+b}{1-x}}$$

$$-\frac{1}{x+t'}\left[\ell n(b+1)\left(\sqrt{\frac{1+t}{b-t}}-\sqrt{\frac{1-x}{b+x}}\right)+\sqrt{\frac{1-x}{b+x}}\ \ell n\ \frac{\left[\sqrt{b+x}+\sqrt{b(1-x)}\right]^2}{|x|}\right.$$

$$\left.-\sqrt{\frac{1+t}{b-t}}\ \ell n\ \frac{\left[\sqrt{b-t}+\sqrt{b(1+t)}\right]^2}{|x|}\right]\sqrt{\frac{x+b}{1-x}}$$

$$F_1(x)=-2\sqrt{\frac{x+b}{1-x}}+\frac{4k}{\pi}\left(\sqrt{\frac{x+b}{1-x}}\ \sin^{-1}\frac{1-b}{1+b}-\ell n\ \frac{\left[\sqrt{x+b}+\sqrt{b(1-x)}\right]^2}{|x|\ (b+1)}\right)$$

$$F_2(x)=\sqrt{\frac{x+b}{1-x}}-\frac{2}{\pi}\left(\sqrt{\frac{x+b}{1-x}}\ \sin\frac{1-b}{1+b}-\ell n\ \frac{\left[\sqrt{x+b}+\sqrt{b(1-x)}\right]^2}{|x|\ (b+1)}\right)$$

and

$$c_1=\frac{\sigma_a}{\sigma_a}\ . \qquad \text{(V.2-13)}$$

(2) $b = 1$

$$\Phi(x) = \frac{2i}{\sigma_a}\,\phi(x) = \begin{cases} \dfrac{G_1 b_1}{\sigma_a}\, f(x) & (x \in L_1) \\ \dfrac{G_2 b_2}{\sigma_a}\, f(x) & (x \in L_2) \end{cases}$$

$$= \frac{k}{\pi^2}\int_L K(x,t)\ \Phi(t)\ dt + F_3(x) + c_2 F_4(x) \qquad \text{(V.2-14)}$$

where

$$K(x,t) = \begin{cases} K_4(x,t) & (t \in L_1) \\ K_5(x,t) & (t \in L_2) \end{cases} \qquad \text{(V.2-15)}$$

$$K_4(x,t) = \frac{1}{x+t}\left[\sqrt{\frac{1-x}{1+x}}\ \ell n\ \frac{|x|}{1+\sqrt{1-x^2}} - \sqrt{\frac{1+t}{1-t}}\ \ell n\ \frac{t}{1+\sqrt{1-t^2}}\right]\sqrt{\frac{1+x}{1-x}}$$

$$+ \frac{1}{x-t}\left[\sqrt{\frac{1-t}{1+t}}\ \ell n\ \frac{t}{1+\sqrt{1-t^2}} - \sqrt{\frac{1-x}{1+x}}\ \ell n\ \frac{|x|}{1+\sqrt{1-x^2}}\right]\sqrt{\frac{1+x}{1-x}}$$

$$K_5(x,t) = \frac{1}{t-x}\left[\sqrt{\frac{1-x}{1+x}}\ \ell n\ \frac{|x|}{1+\sqrt{1-x^2}} - \sqrt{\frac{1-t}{1+t}}\ \ell n\ \frac{|t|}{1+\sqrt{1-t^2}}\right]\sqrt{\frac{1+x}{1-x}}$$

$$- \frac{1}{t+x}\left[\sqrt{\frac{1+t}{1-t}}\ \ell n\ \frac{|t|}{1+\sqrt{1-t^2}} - \sqrt{\frac{1-x}{1+x}}\ \ell n\ \frac{|x|}{1+\sqrt{1-x^2}}\right]\sqrt{\frac{1+x}{1-x}}$$

$$F_3(x) = -2\sqrt{\frac{1+x}{1-x}} + \frac{4k}{\pi}\ \ell n\ \frac{|x|}{1+\sqrt{1-x^2}}$$

$$F_4(x) = \sqrt{\frac{1+x}{1-x}} - \frac{2}{\pi}\ \ell n\ \frac{|x|}{1+\sqrt{1-x^2}}$$

and

$$c_2 = \frac{\sigma_o}{\sigma_a}\ . \qquad \text{(V.2-16)}$$

(3) $b > 1$

$$\Phi(x) = \frac{2i}{\sigma_a}\phi(x) = \begin{cases} \dfrac{G_1 b_1}{\sigma_a} f(x) & (x \in L_1) \\ \dfrac{G_2 b_2}{\sigma_a} f(x) & (x \in L_2) \end{cases}$$

$$= \frac{k}{\pi^2}\int_L K(x,t)\ \Phi(t)\ dt + F_5 + c_3 F_6(x) \qquad \text{(V.2-17)}$$

where

$$K(x,t) = \begin{cases} K_6(x,t) & (0 \le t < 1) \\ K_7(x,t) & (-1 \le t \le 0) \\ K_8(x,t) & (-b \le t \le -1) \end{cases} \qquad \text{(V.2-18)}$$

$$K_6(x,t) = \frac{1}{x+t}\left[\ell n(b+1)\left(\sqrt{\frac{1-x}{b+x}} - \sqrt{\frac{1+t}{b-t}}\right) + \sqrt{\frac{1+t}{b-t}}\ \ell n\ \frac{[\sqrt{b-t} + \sqrt{b(1+t)}]^2}{|t|}\right.$$

$$\left. - \sqrt{\frac{1-x}{b+x}}\ \ell n\ \frac{[\sqrt{b+x} + \sqrt{b(1-x)}]^2}{x}\right]\sqrt{\frac{x+b}{1-x}}$$

$$+ \frac{1}{x-t}\left[\ell n(b+1)\left(\sqrt{\frac{1-t}{b+t}} - \sqrt{\frac{1-x}{b+x}}\right) + \sqrt{\frac{1-x}{b+x}}\ \ell n\ \frac{[\sqrt{b+x} + \sqrt{b(1-x)}]^2}{|x|}\right.$$

$$\left. - \sqrt{\frac{1-t}{b+t}}\ \ell n\ \frac{[\sqrt{b+t} + \sqrt{b(1-t)}]^2}{|t|}\right]\sqrt{\frac{x+b}{1-x}}$$

$$K_7(x,t) = \frac{1}{t-x}\left[\ell n(b+1)\left(\sqrt{\frac{1-x}{b+x}} - \sqrt{\frac{1-t}{b+t}}\right) - \sqrt{\frac{1-x}{b+x}}\ \ell n\ \frac{[\sqrt{b+x} + \sqrt{b(1-x)}]^2}{|x|}\right.$$

$$\left. + \sqrt{\frac{1-t}{b+t}}\ \ell n\ \frac{[\sqrt{b+t} + \sqrt{b(1-t)}]^2}{|t|}\right]\sqrt{\frac{x+b}{1-x}}$$

$$- \frac{1}{x+t}\left[\ell n(b+1)\left(\sqrt{\frac{1+t}{b+t}} - \sqrt{\frac{1-x}{b+x}}\right) - \sqrt{\frac{1+t}{b-t}}\ \ell n\ \frac{\left[\sqrt{b-t} + \sqrt{b(1+t)}\right]^2}{|t|}\right.$$

$$\left. + \sqrt{\frac{1-x}{b+x}}\ \ell n \frac{\left[\sqrt{b+x} + \sqrt{b(1-x)}\right]^2}{|x|}\right] \sqrt{\frac{x+b}{1-x}}$$

$$K_8(x,t) = \frac{1}{t-x}\left[\ell n(b+1)\left(\sqrt{\frac{1-x}{b+x}} - \sqrt{\frac{1-t}{b+t}}\right) - \sqrt{\frac{1-x}{b+x}}\ \ell n\ \frac{\left[\sqrt{b+x} + \sqrt{b(1-x)}\right]^2}{|x|}\right.$$

$$\left. + \sqrt{\frac{1-t}{b+t}}\ \ell n\ \frac{\left[\sqrt{b+t} + \sqrt{b(1-t)}\right]^2}{|t|}\right] \sqrt{\frac{x+b}{1-x}}$$

$$- \frac{1}{x+t}\left[\sqrt{\frac{-t-1}{b-t}}\left(\frac{\pi}{2} + \sin^{-1}\frac{2b - t + bt}{t(b+1)}\right)\right.$$

$$\left. - \sqrt{\frac{1-x}{b+x}}\left(\ell n(b+1) - \ell n\ \frac{\left[\sqrt{b+x} + \sqrt{b(1-x)}\right]^2}{|x|}\right)\right] \sqrt{\frac{x+b}{1-x}}$$

$$F_5(x) = -2\sqrt{\frac{x+b}{1-x}} + \frac{4k}{\pi}\left[\sqrt{\frac{x+b}{1-x}}\ \sin^{-1}\frac{1-b}{1+b} - \ell n\ \frac{\left[\sqrt{x+b} + \sqrt{b(1-x)}\right]^2}{|x|\ (b+1)}\right]$$

$$F_6(x) = \sqrt{\frac{x+b}{1-x}} - \frac{2}{\pi}\left[\sqrt{\frac{x+b}{1-x}}\ \sin^{-1}\frac{1-b}{1+b} - \ell n\ \frac{\left[\sqrt{x+b} + \sqrt{b(1-x)}\right]^2}{|x|\ (b+1)}\right]$$

and

$$c_3 = \frac{\sigma_o}{\sigma_a} \ . \qquad \text{(V.2-19)}$$

In each of the above integral equations (V.2-11), (V.2-14) and (V.2-17), there are two parameters which have to be determined. These are the plastic zone length and the ratio σ_o/σ_a. However, besides the integral equations, there is an additional mathematical condition available, namely, the compatibility Eq. (V.2-4). This leads to the conclusion that the plastic zone length, b, and the magnitude of applied stress, σ_a, are not independent of each other. From the physics of the problem, in fact, this is valid. It is understood that the plastic relaxation at the tip of the crack is caused by the injection of dislocations into the slip lines. Hence, each incremental growth of the plastic zone requires the injection of more dislocations which push the existing dislocations further across the load bearing section. Meanwhile, the applied stress has to be increased correspondingly.

A method of solving the integral equation is now illustrated. Consider the case where the plastic zone length is less than unity. The value of b is first assumed. $\Phi(x)$ in Eq. (V.2-11) can then be rewritten as a linear combination of two functions:

$$\Phi(x) = \Phi_1(x) + c_1\Phi_2(x) \qquad \text{(V.2-20)}$$

where $\Phi_1(x)$ and $\Phi_2(x)$ satisfying the following integral equations:

$$\Phi_1(x) = \frac{k}{\pi^2}\int_L \Phi_1(t)\, K(x,t)\, dt + F_1(x) \qquad \text{(V.2-21)}$$

and

$$\Phi_2(x) = \frac{k}{\pi^2}\int_L \Phi_2(t)\, K(x,t)\, dt + F_2(x) \qquad \text{(V.2-22)}$$

where $K(x,t)$ has been defined in Eq. (V.2-12). In view of the very complicated form of the kernel in the above integral equations, only

numerical solutions have been attempted. The definite integrals on the right-hand side of Eqs. (V.2-21) and (V.2-22) are first approximated by a quadrature formula. Then the integral equations are transformed into systems of algebraic equations. The number of equations in each system is equal to the number of subdivisions, n, in L. The systems of linear equations can then be solved numerically. Details of this procedure are outlined in Appendix C.

Knowing $\Phi_1(x)$ and $\Phi_2(x)$, the constant c_1 can be found by the following procedure. First, Eq. (V.2-4) is rewritten in terms of the known functions $\Phi_1(x)$ and $\Phi_2(x)$ as:

$$\int_{L_2} b_2 f(t)\, dt + \int_{L_1} b_1 f(t)\, dt$$

$$= \int_{-b}^{0} [\Phi_1(t) + c_1\Phi_2(t)]dt + \frac{1+k}{1-k}\left[\int_0^b [\Phi_1(t) + c_1\Phi_2(t)]\, dt\right.$$

$$\left. + \int_b^1 [\Phi_1(t) + c_1\Phi_2(t)]\right]dt = 0 \cdot$$

Then c_1 can be solved from this compatibility equation as:

$$c_1 = -\frac{\displaystyle\int_{-b}^{0} \Phi_1(t)\, dt + \frac{1+k}{1-k}\left[\int_0^b \Phi_1(t)\, dt + \int_b^1 \Phi_1(t)\, dt\right]}{\displaystyle\int_{-b}^{0} \Phi_2(t)\, dt + \frac{1+k}{1-k}\left[\int_0^b \Phi_2(t)\, dt + \int_b^1 \Phi_2(t)\, dt\right]} \cdot \qquad \text{(V.2-23)}$$

Since $\Phi_1(t)$ and $\Phi_2(t)$ are known, the constant c_1 can be obtained by carrying out the numerical integrations in the above equation. Knowing the value of c_1, the complete solution of the distribution function is given by Eq. (V.2-20).

The same procedure is valid, for $b=1$ and $b > 1$. A typical dislocation distribution function of an elastic-plastic crack in a two-phase medium is shown in Fig. V-3.

For each value of the plastic zone length, b, the corresponding externally applied stress, σ_a, can be found from the constant c_1 by carrying out the above mentioned mathematical procedure. For a certain two-phase system, or a given k value, one can repeat this procedure for a set of b values. The corresponding values of applied stress needed to extend the plastic zone can then be obtained. Results of these calculations are summarized in Fig. V-4 for various ratios of rigidities of the two constituent phases. In plotting this figure, we have used the effective stress on dislocations, instead of the externally applied one. This effective stress, $\sigma_2 = \sigma_a(1+k)$, varies strongly with the ratio of rigidities of the two phases (Chapter II) and is the actual stress that drives dislocations in the yield zone.

The physical implication of Fig. V-4 is now examined. The extension of plastic zone is controlled by two factors, namely, the shear modulus and the friction stress of the second phase. In a certain composite, or for a given k value, the extension of plastic zone can be diminished by increasing the yield strength, σ_o, of the second phase. On the other hand, for a given effective applied stress on dislocations, the higher the shear modulus of the second phase is, the shorter the plastic zone will be.

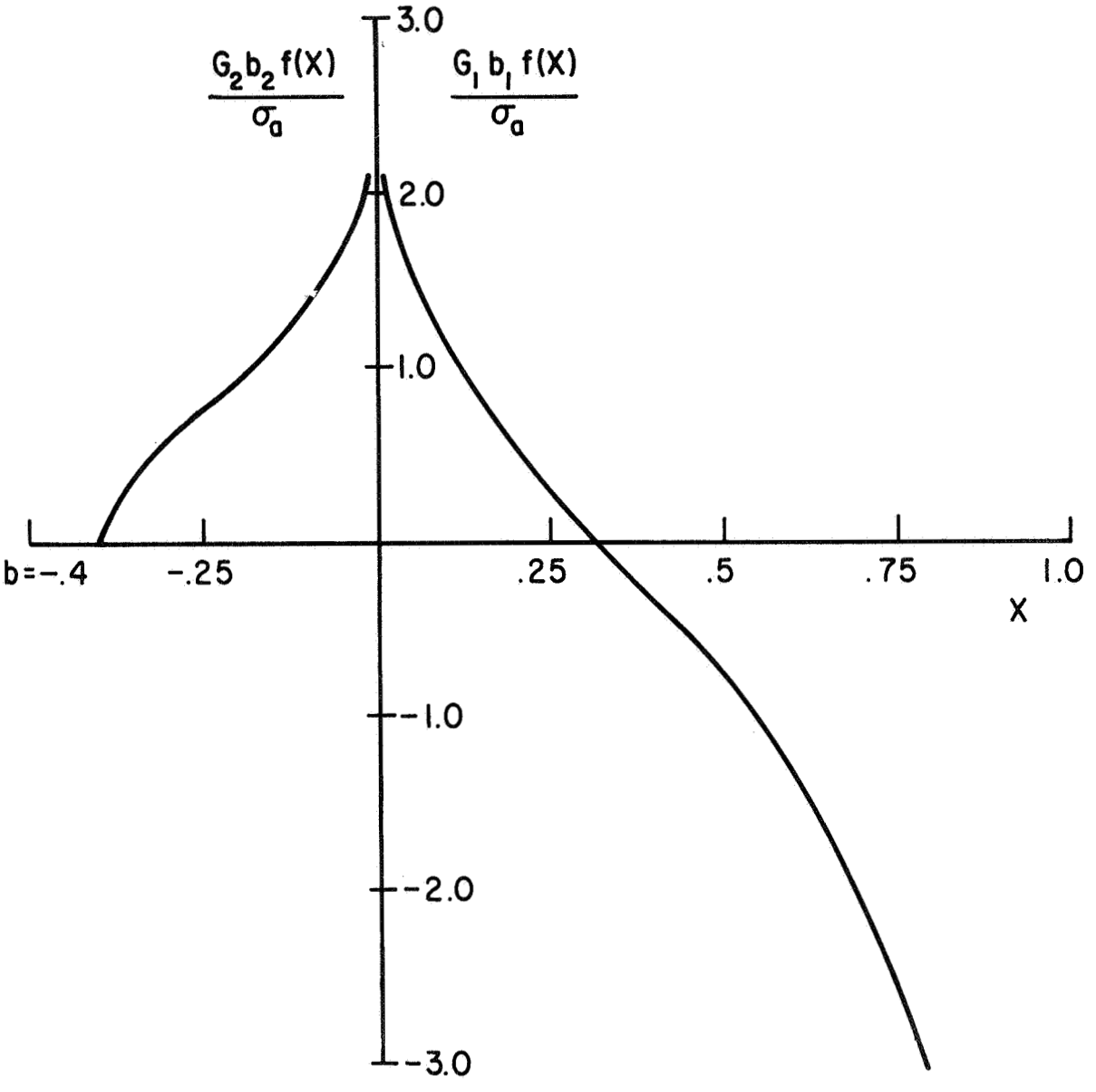

Fig. V-3. THE DISLOCATION DISTRIBUTION FUNCTION REPRESENTING THE ELASTIC-PLASTIC CRACK (k=-.6).

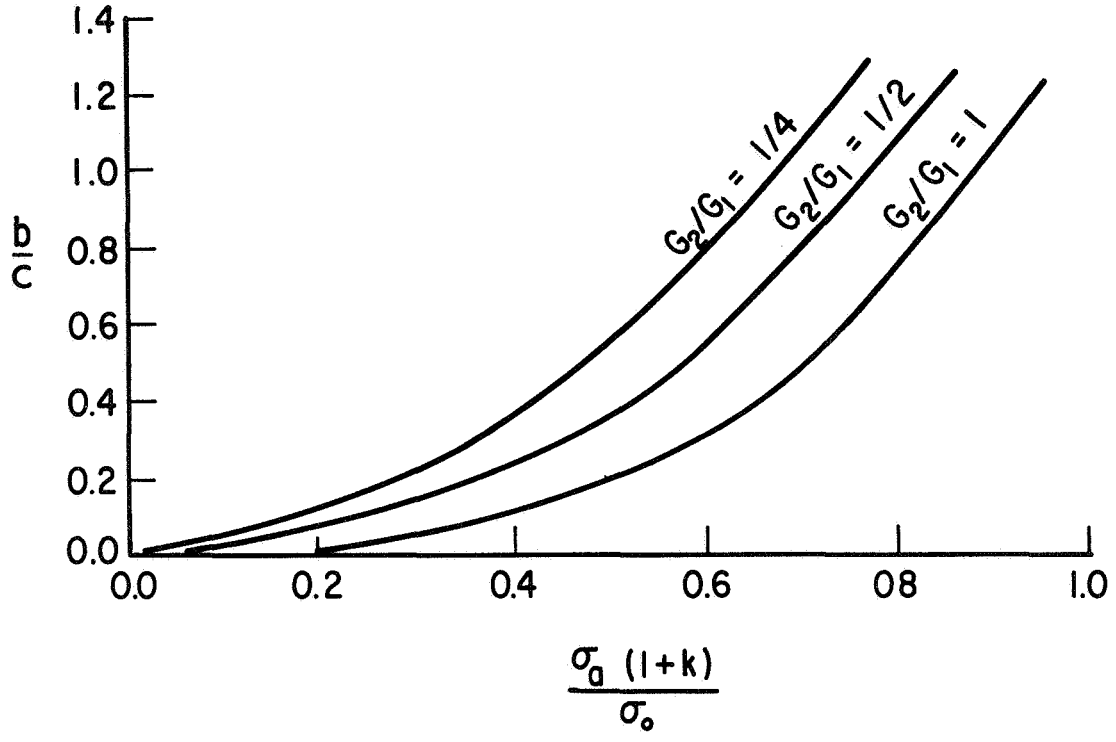

Fig. V-4. THE RELATIONSHIP BETWEEN APPLIED STRESSES AND PLASTIC ZONE LENGTHS.

Finally, the accuracy of the determination of applied stress for a given value of b needs to be examined. As can be seen from Fig. V-3, the ratio $\sigma_a(1+k)/\sigma_o$ becomes very large when b approaches unity. This in turn indicates that the constant $c_1 = \sigma_o/\sigma_a(1+k)$ becomes too small to be accurately determined by using Eq. (V.2-4). However, since the relation between the applied stress and the plastic zone length are expected to vary in a continuous manner, it is suggested that curves in Fig. V-4 for large values of b can be obtained by extrapolation.

3. Crack Opening Displacement

The crack opening displacement $\delta(x)$ at the crack tip is obtained by integrating the plastic displacement in the yield zone:

$$\delta(0) = \int_{-b}^{0} b_2 f(t)\, dt \ . \qquad (V.3\text{-}1)$$

Both $\delta(c)$ and b have the same unit as the crack length.

Numerical integration has been carried out for various systems of composites and for various sizes of plastic zones. The results are summarized in Fig. V-5 where the crack length is taken equal to unity such that $b/c = b$. This plot indicates that for a constant length of plastic zone, the crack opening displacement increases as the rigidity of the matrix phase decreases.

The plastic zone size, b, is determined by the effective applied stress on the plastic zone (Fig. V-4). As the yield zone extends, the plastic displacement at the crack tip accumulates. This will finally

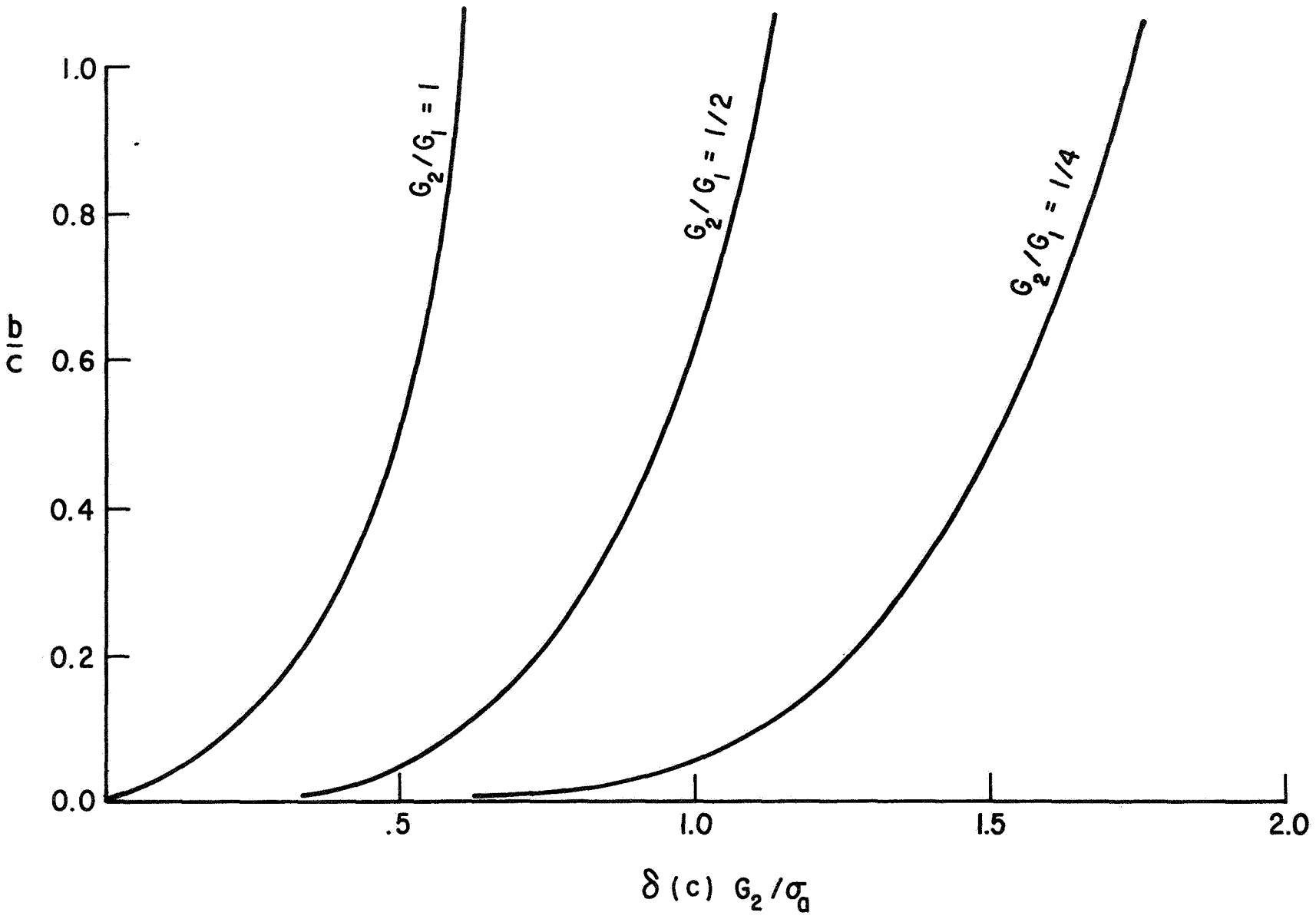

Fig. V-5. THE RELATIONSHIP BETWEEN PLASTIC ZONE LENGTHS AND CRACK OPENING DISPLACEMENTS.

lead to unstable crack propagation when a certain critical crack opening displacement, δ_c, is attained.

A thorough investigation of the relationship between fracture load and critical crack opening displacement is now discussed. In Fig. V-4 and Fig. V-5 we have plotted b/c vs. $\sigma_a(1+k)/\sigma_o$ and b/c vs. $\delta(c)G_2/\sigma_a$ respectively. By combining Fig. V-4 and Fig. V-5, a linear relationship between $\delta(c)G_2/\sigma_a$ and $\sigma_a(1+k)/\sigma_o$ is obtained as shown in Fig. V-6. In this case the parameter σ_a appears in both the abscessa and the ordinate. Both the intercept on the ordinate and the slope of the lines increase as the ratio G_2/G_1 decreases. By measuring the slopes and intercepts, linear equations can be written for these lines. Then by rearranging the parameters of these equations we can get a set of equations governing the variation of $\sigma(c)$ with σ_a/σ_o:

$$\delta(c) = \begin{cases} 0.67 \left(\frac{\sigma_a}{\sigma_o}\right)^2 & (k = 0) \\ 0.98 \left(\frac{\sigma_a}{\sigma_o}\right)^2 + \frac{0.375}{1+k} \frac{\sigma_a}{\sigma_o} & \left(k = \frac{-1}{3}\right) \\ 1.14 \left(\frac{\sigma_a}{\sigma_o}\right)^2 + \frac{0.97}{1+k} \frac{\sigma_a}{\sigma_o} . & (k = -0.6) \end{cases} \qquad \text{(V.3-2)}$$

These are depicted in Fig. V-7. Both linear and second order terms appear in the above equations. It is noted that at low applied stress the contribution of the second order term is small.

Now we proceed to consider several practical composite systems. The matrix phases where the plastic relaxation takes place are Aluminum

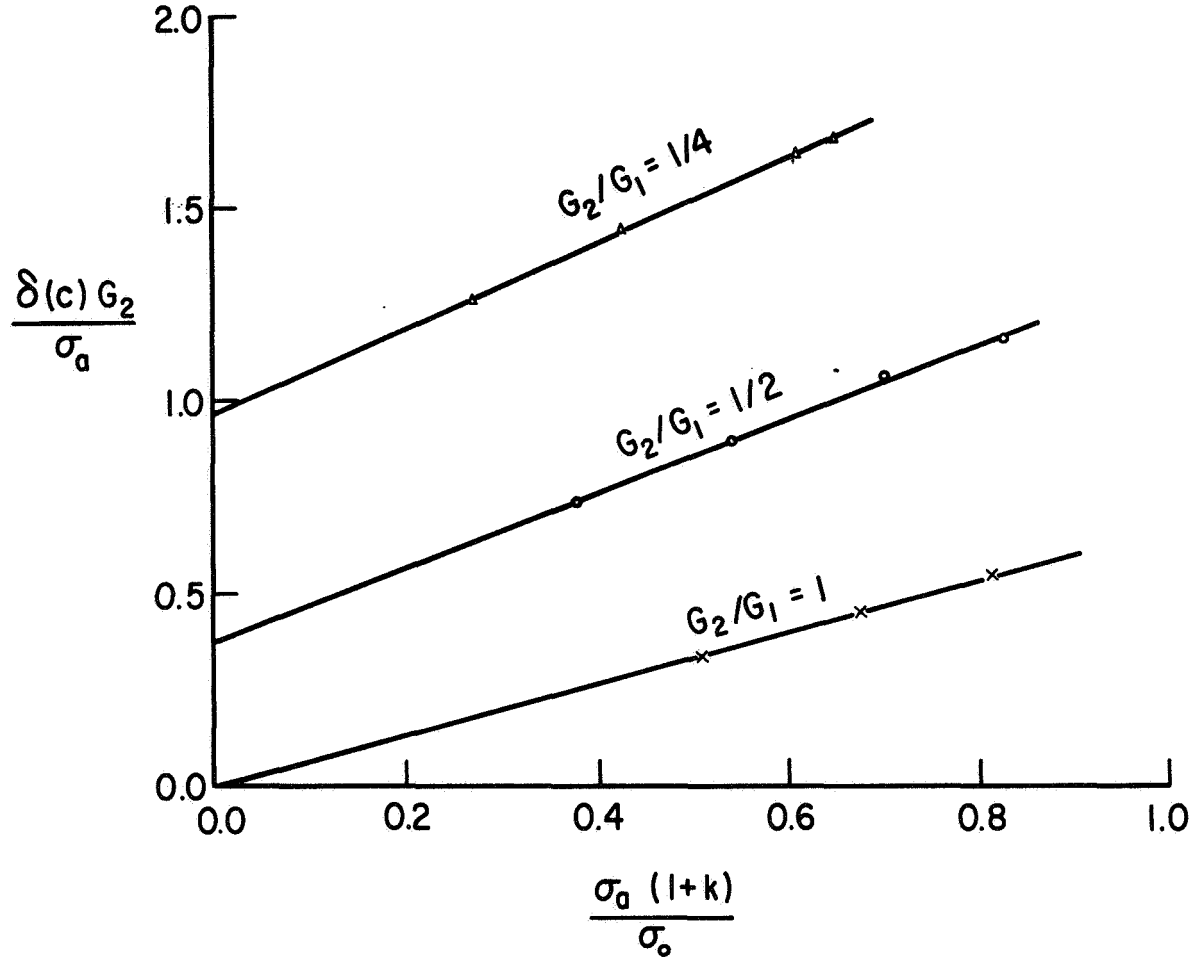

Fig. V-6. LINEAR RELATIONSHIPS BETWEEN $\delta(c)G_2/\sigma_a$ AND $\sigma_a(1+k)/\sigma_o$.

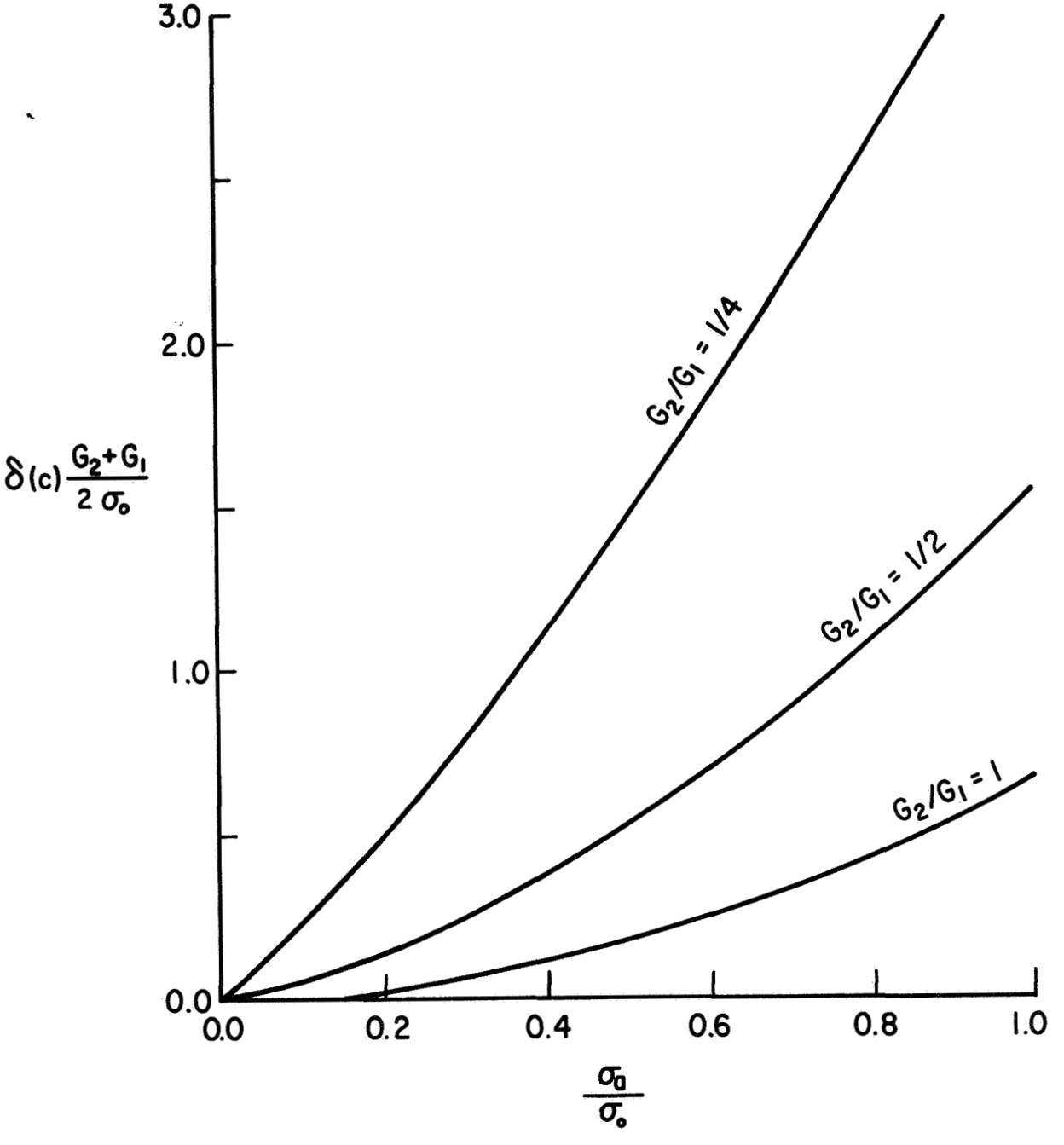

Fig. V-7. VARIATION OF $\delta(c)\,\frac{G_2 + G_1}{2\sigma_o}$ WITH σ_a/σ_o.

alloy 7075-T6 and 2024-T3. The elastic moduli and yield strength of these materials are given in the first four columns of Table V.1. The fracture toughness, G_{1c}, is calculated from the K_{1c} values and is shown in column 6. Knowing G_{1c}, the critical crack opening displacement, $\delta(c)$, can be approximated from the equation [50]:

$$G_{1c} = 2\sigma_Y \delta(c) \ . \qquad (V.3\text{-}3)$$

These are shown in the last column of Table V.1. Suppose that the reinforcements dispersed in the Aluminum alloy matrices are fibers or wires of Boron, Tungsten, Beryllium, Stainless Steel (18 Cr - 8 Ni) and Al_2O_3. The shear moduli of these materials are given in the second column of Table V.2. The ratio of rigidities of the hard and soft phases are shown in column 3. Notice that the matrix phases, Aluminum alloys 7075-T6 and 2024-T3, have the same rigidities. In columns 4 and 5 of Table V.2 the quantities $\delta(c)(G_2+G_1)/2\sigma_o$ of each composite system are evaluated for the two matrix phases using the values of $\delta(c)$ from Table V.1. From these values of $\delta(c)(G_2+G_1)/2\sigma_o$ the corresponding critical fracture load can be readily obtained from Fig. V-7 by extrapolation.

In Table V.3, the fracture stress of composites are listed for various crack lengths. We first consider the case where the crack length is one inch. For these hard phase materials under consideration, the critical fracture stresses range from 0.06 to 0.12 of the yield strength of the 7075-T6 Aluminum alloy and from 0.52 to 0.59 of the yield strength of the 2024-T3 Aluminum alloy. If the hard phase is of the same material as the matrix phase, larger fracture stresses are allowed as shown in the last two columns of Table V.3.

Table V.1

CRITICAL CRACK OPENING DISPLACEMENT OF THE MATRIX MATERIALS

Material	E_2 (ksi $\times 10^3$)	G_2 (ksi $\times 10^3$)	σ_y (ksi)	K_{1c} (ksi $-\sqrt{\text{in}}$)	G_{1c} (in-lb/in^2)	δ_c (10^{-3} in)
7075-T6	10.4	7.8	72	30 [46]	77	0.535
2024-T3	10.4	7.8	47	60 [47]	329	3.5

Table V.2

$\delta_c(G_2 + G_1)/2\sigma_o$ VALUES FOR DIFFERENT COMPOSITE SYSTEMS

Material	G_1 (10^6 psi)	G_2/G_1	$\delta_c \frac{G_2+G_1}{2\sigma_o}$ * (in)	$\delta_c \frac{G_2+G_1}{2\sigma_o}$ ** (in)
B	26.3 [48]	0.3	0.14	1.3
W	23.52	0.33	0.12	1.15
Be	20.45	0.38	0.11	1.05
Stainless Steel	22.5	0.34	0.11	1.12
Al_2O_3	34.7	0.225	0.16	1.6
7075-T6	7.8 [49]	1.0	0.06	
2024-T3	7.8 [49]	1.0		0.6

* δ_c and σ_o for Aluminum alloy 7075-T6

** δ_c and σ_o for Aluminum alloy 2024-T3

Table V.3

FRACTURE STRESSES OF COMPOSITES

Material	Reinforcements in Al Alloy Matrices					Pure Matrices	
	B	W	Be	Stainless Steel	Al_2O_3	7075-T6	2024-T3
σ_a/σ_o *	0.1	0.11	0.12	0.11	0.06	0.3	
σ_a/σ_o ***	0.58	0.56	0.59	0.55	0.52	0.94	
σ_a/σ_o **	0.54	0.54	0.58	0.54	0.52		0.94

* length of crack = 1" , matrix material : 7075-T6 Aluminum alloy

** length of crack = 1" , matrix material : 2024-T3 Aluminum alloy

*** length of crack = 1/10", matrix material : 7075-T6 Aluminum alloy

The case of a crack of length 0.1 inch in the 7075-T6 Aluminum alloy matrix is also described in the second row of Table V.3. These values are, as expected, considerably higher than those for the crack length of one inch. Note that the ratio σ_a/σ_o in the composite relative to the pure 7075-T6 alloy, increases as the crack length decreases. This indicates that the detrimental effect on fracture strength due to the introduction of second phase is less pronounced as the flaw size decreases. If the 2024-T3 Aluminum alloy is used as matrix material the ratio of σ_a/σ_o is higher than unity for a crack of 1/10 inch. Hence, the result is not shown here.

Several important conclusions concerning the fracture of composite materials have been reached in this and the last sections. These are summarized as follows:

(1) In a certain composite system, or for a given k value, the extension of plastic zone can be diminished by increasing the yield strength of the second phase material.

(2) For a given effective applied stress on dislocation, the higher the shear modulus of the second phase is, the shorter the plastic zone will be.

(3) For a constant length of plastic zone, the crack opening displacement increases as the rigidity of the matrix phase decreases.

(4) For a certain composite system, or a constant k value, the fracture stress at low applied loading can be increased by improving the toughness of the matrix phase. This is clearly seen in the first and third row of Table V.3.

(5) The bi-material system under consideration is an idealized situation. For fiber or laminated composites the critical crack opening displacement value, δ_c, is lower than the value used in the above calculation. The reasons are two-fold. First, the fracture toughness values of the matrix materials used here are those of homogeneous materials. In a composite, the plastic deformation of the matrix material is inevitably constrained by the neighboring hard fibers or laminas. This effect certainly lowers the toughness value. Secondly, in a practical composite system, the presence of a large volume fraction of hard phase materials tend to lower the ductility of the whole system. As a consequence, the composite tends to be brittle and $\delta(c)$ value is lowered.

4. Discussion

In the present analysis, it is assumed that the plastic zone is confined to a thin layer. The validity of this assumption is now examined. It is noted that in a homogeneous medium, the resultant shear stress at the tip of a mode III crack varies only with the radial distance from the tip. Analysis of an elastic-plastic crack in a homogeneous medium has been carried out by using both dislocation and classical plasticity theory [7,14]. In the dislocation theory, the plastic zone is assumed to be confined in a thin layer. The plastic zone considered by Hault and McClintock for a perfect-plastic solid is a circular region at the crack tip. Since the length of plastic zones deduced from both theories are in good agreement, it has been concluded that the length of plastic zone is insensitive to the shape in homogeneous medium (Chapter I).

There has been no solution obtained from classical plasticity theory for the problem considered in this chapter. Hence, there is no exact solution of the shape of plastic zone ahead of the crack in a two-phase medium. However, as far as the plastic zone length is concerned, it is not unrealistic to assume that the plastic zone is confined to a narrow region, coplanar with the crack. This is due to the fact that just as in the case of a homogeneous medium, the stress field induced in the neighboring phase due to a crack against an interface also varies only with the radial distance from the crack tip.

One further justification of the assumed plastic zone shape has been given by Cottrell [5]. The insensitivity of plastic zone length to the shape of zone is essentially because the interactions of distant dislocations are not greatly altered in magnitude by changing their relative coordinates from x to $(x + y)$, provided $x \cong y$. Further, the plastic displacement $\delta(c)$ at the tip is always of the order:

$$\delta(c) = 2b\epsilon_b = 2b \frac{\sigma_o}{G_2}$$

where ϵ_b is the strain in the plastic zone of length b.

CHAPTER VI

SUGGESTIONS FOR FUTURE WORK

The dislocation model of an elastic-plastic crack is very important in studying fracture of two-phase solids. Besides the problems discussed in the last five chapters of this dissertation, what needs further research is outlined as follows:

1. It is necessary to consider the cases where the second phases are of finite dimension. We have taken into account the cracking of a thin hard surface film with plastic deformation in the neighboring phase. This problem is equivalent to the situation of cracking a lamina of finite width and having plastic zones extended into the tough matrix. The width of the lamina will certainly affect the extension of plastic zones and the crack tip opening displacement.
2. It is believed that further investigation is necessary to consider the effect on the fracture behavior of a lamina due to neighboring laminas. In this model we have to consider at least three laminas while the central one is cracked. By changing the width of the laminas and the spacings in between, it is hopeful that we can optimize the volume fraction of the second phase material to get the most efficient service of the composite.
3. Problems of Modes I and II cracks are also of great practical importance. We have formulated mathematically the problem involving an elastic crack crossing a phase boundary. Further

investigation is needed to consider Mode I elastic crack in a lamina. As elastic-plastic cracks are concerned, it is necessary to take into consideration the spread of plasticity out of the crack plane.

REFERENCES

1. A. S. Tetelman and A. J. McEvily, Jr., Fracture of Structural Materials, John Wiley, New York (1967).

2. D. S. Dugdale, J. Mech. Phys. Solids, 8, 100 (1960).

3. N. I. Muskhelishvili, Some Basic Problems of the Mathematical Theory of Elasticity, P. Noordhoff, Ltd., Groningen, the Netherlands (1963).

4. F. A. Field, Ph.D. Dissertation, Stanford University (1962).

5. A. H. Cottrell, Proc. Roy. Soc., A 276, 1 (1963).

6. A. H. Cottrell, Proc. Roy. Soc., A 285, 10 (1965).

7. B. A. Bilby, A. H. Cottrell and K. H. Swinden, Proc. Roy. Soc., A 272, 304 (1963).

8. B. A. Bilby, A. H. Cottrell, E. Smith, and K. H. Swinden, Proc. Roy. Soc., A 279, 1 (1964).

9. B. A. Bilby and K. H. Swinden, Proc. Roy. Soc., A 285, 22 (1965).

10. J. D. Eshelby, Phil. Mag., 40, 903 (1949).

11. B. A. Bilby, R. Bullough and E. Smith, Proc. Roy. Soc., A 231, 263 (1955).

12. N. I. Muskhelishvili, Singular Integral Equations, P. Noordhoff, Ltd., Groningen, the Netherlands (1953).

13. K. H. Swinden, Ph.D. Dissertation, University of Sheffield (1964).

14. J. A. H. Hult and F. A. McClintock, 9th Int'l Congr. Appl. Mech., 8, 51 (1957).

15. E. Orowan, Rep. Progr. Phys., 12, 214 (1948).

16. G. R. Irwin, Trans. Amer. Soc. Metals, 40, 147 (1948).

17. A. K. Head, Aust. J. Phys., 13, 278 (1960).

18. Y. T. Chou, Acta Met., 13, 779 (1965).

19. E. Smith, Acta Met., 15, 249 (1967).

20. D. M. Barnett, Acta Met., 15, 589 (1967).

21. E. Smith, Int. J. Eng. Sci., 6, 129 (1968).

22. J. J. Hauser and B. Chalmers, Acta Met., 9, 802 (1961).

23. R. Z. Hook and J. P. Hirth, Acta Met., 15, 535 (1967).

24. J. P. Hirth, W. A. Tiller and G. M. Pound, A Critique on the Mathematical Theory of Spinodal Decomposition, to be published in Acta Met.

25. K. T. Sundara Raja Iyengar, Osterreichisches Ingenieur-Archiv, 16, H. 3, 185 (1962).

26. K. T. Sundara Raja Iyengar and R. S. Alwar, Zeitschrift fur Angewandte Mathematik und Physik, 14, 344 (1963).

27. Y. C. Fung, Fundamentals of Solid Mechanics, Prentice-Hall, Inc., New Jersey (1965).

28. E. G. Coker and L. N. G. Filon, A Treatise on Photo-Elasticity, 2nd ed., Cambridge University Press (1957).

29. J. W. Cahn, Acta Met., 9, 795 (1961).

30. J. G. Kuang and T. Mura, J. of Appl. Phys., 39, 109, (1968).

31. A. H. Cottrell, The Mechanical Properties of Matter, John Wiley, New York (1964).

32. B. Noble, Methods Based on the Wiener-Hopf Technique for the Solution of Partial Differential Equations, Pergamon Press (1958).

33. E. C. Titchmarsh, Introduction to the Theory of Fourier Integral, Oxford (1948).

34. G. F. Carrier, M. Krook and C. E. Pearson, Functions of a Complex Variable, McGraw-Hill, New York (1966).

35. J. Dundurs and G. P. Sendeckyj, J. Appl. Phys., 36, 10, 3353 (1965).

36. J. Dundurs and G. P. Sendeckyj, J. Mech. Phys. Solids, 13, 141 (1965).

37. J. B. Scarborough, Numerical Mathematical Analysis, Johns Hopkins Press (1958).

38. L. V. Kantorovich and V. I. Kroylov, Approximate Method of Higher Analysis, Gostekhizdat (1941).

39. S. G. Mikhlin, Integral Equations, Macmillan, New York (1957).

40. A. R. Zak and M. L. Williams, Trans. ASME, 142 (March, 1963).

41. P. C. Paris and G. C. M. Sih, Fracture Toughness Testing and Applications, 30, ASTM, Philadelphia (1965).

42. M. L. Williams, Bulletin, Seismological Soc. Am., 49, 199 (1959).

43. G. C. M. Sih and J. Rice, J. of Appl. Mech., 30 (1963).

44. F. Erdogan, J. of Appl. Mech., 30 (1963).

45. G. A. Cooper and A. Kelley, J. Mech. Phys. Solids, 15, 279 (1967).

46. J. G. Kaufman and H. Y. Hunsicker, "Fracture Toughness Testing at Alcoa Research Laboratories," Fracture Toughness Testing and its Applications, ASTM STP 381.

47. G. R. Irwin, "Fracture Mechanics," Structural Mechanics, edited by Goodier and Hoff, New York, Pergamon Press (1960).

48. H. L. Duengan, Lawrence Radiation Laboratory, Livermore, California, unpublished measurements.

49. Alcoa Aluminum Handbook, Aluminum Company of America, Pittsburg, Pa. (1967).

50. A. H. Cottrell, Proc. Roy. Soc., 282, 2 (1964).

Appendix A

INVERSION OF THE SINGULAR INTEGRAL EQUATION

Equation (I.4-1) can usually be reduced to the general form

$$\frac{1}{\pi i}\int_L \frac{G(t)}{t-t_o}\,dt = \phi(t_o)\ . \qquad \text{(A-1)}$$

L is any set of non-intersecting arcs in the complex plane. On L, $G(t)$ is unknown and $\phi(t)$ is a given complex function.

Singular integral equations with Cauchy type kernel have been studied in detail by Muskhelishvili [12]. The deduction of inversion formulas of the Cauchy integral taken over a union of arcs can be found in Chapter II of his book. The corresponding Hilbert problem is solved in §84 of that book. The underlying concepts of the analysis have been assembled in a concise form by Swinden [13]. It is introduced here.

Consider any complex function $F(x)$ sectionally holomorphic in the complex plane outside L. Let $F^+(t)$ and $F^-(t)$ be the limiting values of $F(z)$ as $z \to t$ from positive and negative sides of L respectively.

First consider the problem of finding $F(z)$ satisfying, on L, the relation

$$F^+(t_o) - F^-(t_o) = G(t_o) \qquad \text{(A-2)}$$

where $G(t_o)$ is assumed to be known. By using Cauchy theorem, it can be shown that the most general function satisfying (A-2) is

$$F(z) = \frac{1}{2\pi i} \int_L \frac{G(t)}{t-z}\, dt + R(z) \qquad \text{(A-3)}$$

where

$$R(z) = \sum_{i=1}^{\ell} \sum_{j\neq 0}^{i} a_{ij}(z-z_j)^{-m_j} + \sum_{i=0}^{m} a_i z^i \qquad \text{(A-4)}$$

is a function continuous over L and having a finite number of poles of orders $m_1, m_2, \ldots m_\ell$ and m at the points $z_1, z_2, \ldots z_\ell$ and ∞ not on L.

Now suppose that $G(t_o)$ is unknown and is a solution of (A-1). Also, $F(z)$ is sectionally holomorphic outside L and zero at infinity. Then the problem can be reformulated as the problem of finding a holomorphic function satisfying

$$F^+(t_o) + F^-(t_o) = \phi(t_o) \,. \qquad \text{(A-5)}$$

To do this the following definition is made:

$$\chi_p \equiv \prod_{k=1}^{n} (z-a_k)^{-\gamma} (z-b_k)^{\gamma-1} P_p(z) \qquad \text{(A-6)}$$

where a_k and b_k are the end points of the k^{th} arc comprising L and $P_p(z)$ is a polynominal of degree p with zeros on L. Also it can be

shown that $\gamma = \frac{1}{2}$ from limiting process. Relation (A-5) then becomes

$$f^{+}(t_o) - f^{-}(t_o) = g(t_o) \qquad \text{(A-7)}$$

in which $g(t_o)$ is a known function. The general solution of (A-7) is given by (A-3).

What remains to be done is to construct $\chi_p(z)$ with the property that in the finite plane, all zeros of $\chi_p(z)$ belong to L. Further, $F(z)$ is required holomorphic everywhere outside L. Consequently, $f(z)$ must be holomorphic except perhaps at infinity. This implies that in the solution of (A-7) the function $R(z)$ is no more than an arbitrary polynomial $Q_m(z)$ of degree m. From (A-7) it follows that

$$F(z) = [\chi_p(z)/2\pi i] \int_L [\phi(t)/\chi_p^{+}(t)(t-z)]\, dt + \chi_p(z)\, Q_m(z) . \qquad \text{(A-8)}$$

Suppose L is the union of n segments and $F(z)$ is bounded at a given set of end points $c_1, c_2, \ldots c_p$ and unbounded at the remaining points, then

$$P_p(z) = \prod_{k=1}^{p} (z - c_K) . \qquad \text{(A-9)}$$

Also define

$$R_1 \equiv \prod_{j=0}^{p} (z - c_j)$$

$$R_2 \equiv \prod_{j=p+1}^{2n} (z - c_j) . \qquad \text{(A-10)}$$

It follows from (A-6)

$$\chi_p(z) = \sqrt{R_1(z)/R_2(z)} . \qquad \text{(A-11)}$$

Also, we have:

$$\chi_p^+(t_o) = -\chi_p^-(t_o) = \sqrt{R_1(t_o)/R_2(t_o)} . \qquad \text{(A-12)}$$

Consequently, from (A-2), (A-8), (A-11) and (A-12) we obtain:

$$G(t_o) \equiv \frac{1}{\pi i}\left[\frac{R_1(t_o)}{R_2(t_o)}\right]^{1/2} \int_L \left[\frac{R_2(t)}{R_1(t)}\right]^{1/2} \frac{\phi(t)\, dt}{t - t_o}$$

$$+ \left[\frac{R_1(t_o)}{R_2(t_o)}\right]^{1/2} Q_m(t_o) . \qquad \text{(A-13)}$$

This is the general solution of (A-1) and R_1, R_2 are defined by (A-10) and Q_m is an arbitrary polynomial of degree m.

Finally, the requirement of finiteness of $F(z)$ at infinity leads to the following conditions. Define

$$A_k = \frac{1}{2\pi i} \int_L [-t^{k-1} \phi(t)/\chi_p^+(t)]\, dt , \qquad \text{(A-14)}$$

then if $p \geq n$, $Q_m(z) = 0$, $A_k = 0$ for $k = 1,2,..,p-n$ and for $p < n$, $m < n-p$.

APPENDIX B

THE WIENER-HOPF METHOD

There is an extensive array of important problems of which solution by Fourier or Mellin transform methods requires the use of an ingenious technique which was invented by Carlman and later developed by Wiener and Hopf.

Typically, in problems of differential equations with mixed boundary conditions on the line $y=0$, $-\infty < x < \infty$, or with boundary conditions on a half line, one is led via the Fourier and Mellin transform technique to the following functional relation:

$$A(\alpha)\,\Phi_+(\alpha) + B(\alpha)\Psi_-(\alpha) + c(\alpha) = 0 \qquad \text{(B-1)}$$

where the equation holds in a strip $\tau_- < \tau < \tau_+$, $-\infty < \sigma < \infty$ of the complex plane $\alpha = \sigma + i\tau$. $\Phi_+(\alpha)$ and $\Psi_-(\alpha)$ are regular in the half planes $\tau > \tau_-$ and $\tau < \tau_+$ respectively. The functions $A(\alpha)$, $B(\alpha)$ and $c(\alpha)$ are given functions of α regular and non-zero in the strip. τ_+ and τ_- are determined by the information regarding the behavior of these functions as α tends to infinity in appropriate half planes.

The fundamental step in the Winer-Hopf procedure for solution of this equation is to find $K_+(\alpha)$ regular and non-zero in $\tau > \tau_-$, $K_-(\alpha)$ regular and non-zero in $\tau < \tau_+$, such that

$$\frac{A(\alpha)}{B(\alpha)} = \frac{K_+(\alpha)}{K_-(\alpha)}\,. \qquad \text{(B-2)}$$

Use equation (B-2) to rearrange (B-1) as:

$$K_+(\alpha)\ \Phi_+(\alpha) + K_-(\alpha)\ \Psi_-(\alpha) + K_-(\alpha)\ c(\alpha)/B(\alpha) = 0\ . \qquad \text{(B-3)}$$

Decompose $K_-(\alpha)\ c(\alpha)/B(\alpha)$ in the form

$$K_-(\alpha)\ c(\alpha)/B(\alpha) = c_+(\alpha) + c_-(\alpha) \qquad \text{(B-4)}$$

where $c_+(\alpha)$ is regular in $\tau > \tau_-$, $c_-(\alpha)$ is regular in $\tau < \tau_+$. The decomposition involved in Eq. (B-4) is a procedure based upon the Cauchy's theorem. The decomposition in Eq. (B-2) as a quotient is equivalent to the decomposition of $\ell n(A(\alpha)/B(\alpha))$ as a sum. If decomposition involves an entire function, then it may be convenient to use an infinite-product expression for that entire function, so as to obtain at once its two appropriate factors.

Combine Eqs. (B-3) and (B-4) so as to define a function $J(\alpha)$ by

$$J(\alpha) = K_+(\alpha)\ \Phi_+(\alpha) + c_+(\alpha)$$

$$= -K_-(\alpha)\ \Psi_-(\alpha) - c_-(\alpha)\ . \qquad \text{(B-5)}$$

By analytical continuation, it is obvious that $J(\alpha)$ is an entire function on the α-plane. Now suppose that it can be shown that:

$$|K_+(\alpha)\ \Phi_+(\alpha) + c_+(\alpha)| < |\alpha|^p \qquad \text{as } \alpha \to \infty\ ,\quad \tau > \tau_-\ ;$$

$$|K_-(\alpha)\ \Psi_-(\alpha) + c_-(\alpha)| < |\alpha|^q \qquad \text{as } \alpha \to \infty\ ,\quad \tau < \tau_+\ . \qquad \text{(B-6)}$$

Then by Liouvill's theorem $J(\alpha)$ is a polynomial $P(\alpha)$ of degree less than or equal to the integral part of min(p.q), namely:

$$K_+(\alpha)\,\Phi_+(\alpha) + c_+(\alpha) = P(\alpha)$$

$$K_-(\alpha)\,\Psi_-(\alpha) + c_-(\alpha) = -P(\alpha)\ . \qquad \text{(B-7)}$$

These equations determine Φ_+ and $\Psi_-(\alpha)$ to within the arbitrary polynomial $P(\alpha)$, i.e., to within a finite number of arbitrary constants which must be determined otherwise. Equation (B-7) then determines $\Phi_+(\alpha)$ and $\Psi_-(\alpha)$.

It is noted that any partial-differential-equation boundary value problem which leads to a functional equation of the Weiner-Hopf type (B-1) can always be recast as an integral equation of the type

$$\int_0^\infty K(x-t)\,f(t)\,dt = f(x) \qquad (0 \leq x < \infty)\ . \qquad \text{(B-8)}$$

This can be achieved simply by taking the inverse transform of Eq. (B-1) and use the convolution theorem. Consequently, integral equations with kernel function of the type $K(x-t)$ can be solved by taking a Fourier or Mellin transform to recast it in the form of Eq. (B-1) and then proceed to solve in the same way as outlined above.

APPENDIX C

NUMERICAL SOLUTION OF LINEAR INTEGRAL EQUATIONS

Consider the type of integral equation

$$\Phi(x) = \lambda \int_a^b K(x,t)\, \Phi(t)\, dt + F(x) \,. \qquad \text{(C-1)}$$

The replacement of the given kernel by a degenerate one makes it possible to find the solution in the form of an expression which is valid for the whole interval $a \leq x \leq b$ and for arbitrary values of the parameter λ. A serious drawback of this method is the necessity of calculating the quadratures, which are sometimes rather complicated and quite numerous. This objection, moreover, applies also to the method of successive approximations. It is the present purpose to introduce a method for the approximate solution of integral equations which does not involve the calculation of quadratures [37,38,39].

This technique is based upon the modified method of Goursat and Nystrom. The method consists essentially of replacing the unknown function under the integral sign by a polynomial over an interval, and then evaluate the integral at certain specified points within interval of integration.

The first step in solving Eq. (C-1) is to approximate the definite integral on the right-hand side by a quadrature formula. The resulting formula has the general expression

$$\Phi(x) = F(x) + (b-a)\ [c_1 K(x,t_1)\ \Phi(t_1) + c_2 K(x,t_2)\ \Phi(t_2)$$

$$+ \ldots. + c_n K(x,t_n)\ \Phi(t_n)] \qquad \text{(C-2)}$$

where $t_1, t_2, \ldots t_n$ are subdivision points of the interval (a,b) and the c's are weighting coefficients. Both the number of subdivisions and the values of weighting coefficients depend on the type of quadrature formula used.

Let $x = t_i$ for $i = 1,2,\ldots n$ and denote $\Phi(t_i) = \Phi_i$ and $F(t_i) = F_i$. Hence from (C-2) we get n equations of the type

$$\Phi_i = F_i + (b-a)\ [c_1 K(t_i,t_1)\ \Phi_1 + c_2 K(t_i,t_2)\ \Phi_2 + \ldots$$

$$+ c_n K(t_i,t_n)\ \Phi_n] \qquad \text{(C-3)}$$

for $i = 1,2,\ldots n$.

This gives a system of n linear equations in the n unknowns $\Phi_1, \Phi_2, \ldots, \Phi_n$, which can be solved. Substitute these values into (C-2) then yields an approximate expression for $\Phi(x)$ in the whole interval.

When $n \to \infty$, the approximate expression for $\Phi(x)$ obtained by this method tends to the solution of the integral equation (C-1) as a limit, provided only that this solution exists and is unique. Proof of this may be found, for example, in the book by L. V. Kantorovich and V. I. Krylov [38].